

with it, as well as in cases of pathological pregnancy or of unsuccessful pregnancy.

See paragraph [0195] of the published application. The assertion is specific because it is directed to the specific subject matter disclosed in this application, and the assertion of utility is substantial because it asserts the use of the claimed subject matter in detecting, predicting, treating, and monitoring autoimmune diseases and their related pathologies, as well as pathological pregnancy or unsuccessful pregnancy. Thus, the specification asserts a specific and substantial utility for the claimed subject matter.

Paragraphs [0196] to [0203] discuss the links between retrovirus and autoimmune diseases and retrovirus and pregnancy disorders. Paragraph [0204] asserts, "All these observations make it possible to use and consider the above-described biological material as marker for an autoimmune disease or for pregnancy disorders." Here again, the specification asserts specific and substantial utility.

The question remains whether such assertions are credible. However, the Office Action fails to establish a *prima facie* case that the Applicants' assertions of utility are not credible. Indeed, the Office Action does not even recognize that the specification contains assertions of utility.

Case law directs that a statement of utility made by an applicant is presumed true. See *In re Langer*, 503 F.2d at 1391, 183 USPQ at 297; *In re Malachowski*, 530 F.2d 1402, 1404, 189 USPQ 432, 435 (CCPA 1976); *In re Brana*, 51 F.3d 1560, 34 USPQ2d 1436 (Fed. Cir. 1995); MPEP §2107.02(III)(A). MPEP §2107.02(III)(A) provides that when a statement of utility is evaluated by Office personnel, they should not begin by questioning the truth of the statement of utility but, instead, must start by asking if there is any reason to question the truth of the statement of utility. To overcome the presumption of truth, Office personnel must establish that it is more likely than not that one of ordinary skill in the art would doubt the

truth of the statement of utility. *Id.* Again, the Office Action is silent with respect to the credibility of the assertions of utility made in the specification.

The Office Action, page 6, asserts that there is a lack of evidence presented to indicate any association of the sequence to autoimmune diseases such as multiple sclerosis and rheumatoid arthritis and too unsuccessful pregnancy or pathological conditions a pregnancy. In response, Applicants submit herewith three articles that discuss the association of the HERV-W gene sequence and proteins it encodes with some of these conditions:

Ref 1: Antony et al., "Human endogenous retrovirus glycoprotein-mediated induction of redox reactants causes oligodendrocyte death and demyelination," *Nature Neuroscience*, 7(10):1088–1095 (2004);

Ref 2: Antony et al., "The Human Endogenous Retrovirus Envelope Glycoprotein, Syncytin-1, Regulates Neuronal Inflammation and its Receptor Expression in Multiple Sclerosis: A Role for Endoplasmic Reticulum Chaperones in Astrocytes," *Journal of Immunology*, 179:1210–1224 (2007);

Ref 3: Langbein et al., "Impaired Cytotrophoblast Cell-Cell Fusion Is Associated With Reduced Syncytin And Increased Apoptosis In Patients With Placental Dysfunction," *Molecular Reproduction and Development*, DOI 10.1002/mrd.207239, pp. 1–10, (2007).

Ref 1 reports that HERV-W encoded glycoprotein syncytin is upregulated in glial cells within acute demyelination lesions of multiple sclerosis patients. *See Abstract.* Syncytin expression induced the release of redox reactants that were cytotoxic to oligodendrocytes, which led to neuroinflammation and death of the oligodendrocytes, which was linked to neurobehavioral deficits. *Id.*

Ref 2 reports similar findings as those reported in Ref 1, and further investigates and reports the mechanisms by which Syncytin-1 mediated neuroimmune activation and oligodendrocyte damage in MS patients.

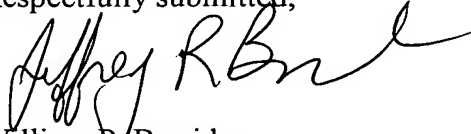
Ref 3 reports that the envelope gene of HERV-W is a key factor for mediating cell-cell fusion of cytotrophoblast, and discusses the link of Syncytin to patients with placental dysfunction.

These reference substantiate the Applicants' assertions of specific and substantial utility made in the specification. Reconsideration and withdrawal of the rejection are respectfully requested.

In view of the foregoing, it is respectfully submitted that this application is in condition for allowance. Favorable reconsideration and prompt allowance of the application are earnestly solicited.

Should the Examiner believe that anything further would be desirable in order to place this application in even better condition for allowance, the Examiner is invited to contact the undersigned at the telephone number set forth below.

Respectfully submitted,



William R. Berridge
Registration No. 30,024

Jeffrey R. Bousquet
Registration No. 57,771

WPB:JRB

Attachments:
Refs 1-3

Date: June 4, 2009

OLIFF & BERRIDGE, PLC
P.O. Box 320850
Alexandria, Virginia 22320-4850
Telephone: (703) 836-6400

DEPOSIT ACCOUNT USE AUTHORIZATION Please grant any extension necessary for entry; Charge any fee due to our Deposit Account No. 15-0461
--

Human endogenous retrovirus glycoprotein-mediated induction of redox reactants causes oligodendrocyte death and demyelination

Joseph M Antony¹, Guido van Marle¹, Wycliffe Opii², D Allan Butterfield², François Mallet³, Voon Wee Yong¹, John L Wallace⁴, Robert M Deacon⁵, Kenneth Warren⁶ & Christopher Power¹

Human endogenous retroviruses (HERVs) constitute 8% of the human genome and have been implicated in both health and disease. Increased HERV gene activity occurs in immunologically activated glia, although the consequences of HERV expression in the nervous system remain uncertain. Here, we report that the HERV-W encoded glycoprotein syncytin is upregulated in glial cells within acute demyelinating lesions of multiple sclerosis patients. Syncytin expression in astrocytes induced the release of redox reactants, which were cytotoxic to oligodendrocytes. Syncytin-mediated neuroinflammation and death of oligodendrocytes, with the ensuing neurobehavioral deficits, were prevented by the antioxidant ferulic acid in a mouse model of multiple sclerosis. Thus, syncytin's proinflammatory properties in the nervous system demonstrate a novel role for an endogenous retrovirus protein, which may be a target for therapeutic intervention.

As much as 8% of the human genome is derived from retrovirus-like elements, which are presumably remnants of retroviral infections that occurred during primate evolution^{1–3}. Many human endogenous retroviruses (HERVs) have retained functional promoter, enhancer and polyadenylation signals, and these regulatory sequences have the potential to modify the expression of adjacent genes^{4,5}. Despite the fact that most HERVs are unable to replicate because of mutations in structural retrovirus genes, specific open reading frames corresponding to HERV genes encode detectable proteins⁶.

An increase in the expression of HERV genes may be important in modulating host innate and adaptive immune responses with ensuing effects on the development of disease, although definitive proof of specific pathogenic effects linked to HERVs is lacking. Several human and animal exogenous retrovirus proteins, particularly the envelope proteins encoded by *env*, show a proclivity for causing neuropathogenic effects⁷. The precise functions of endogenous retrovirus proteins in the nervous system remain uncertain, despite the abundant expression of these proteins in many species including rodents, cats and non-human primates^{4,5,7}.

Studies have suggested that HERV expression in human brain is augmented in conditions of neuroinflammation⁸. The prototypic neuroinflammatory disease multiple sclerosis is characterized by infiltration of inflammatory cells, damage to and death of oligodendrocytes and demyelination, which result in physical and cognitive disabilities. Indeed, cytokines, arachidonic acid metabolites and redox reactants including nitric oxide are key determinants of pathogenicity

in multiple sclerosis^{9–11}, which is also influenced by the genetic susceptibility of an individual. The role of both exogenous and endogenous infectious pathogens in the pathogenesis of multiple sclerosis is unknown, but several viruses and bacteria have been implicated through specific mechanisms including transactivation of aberrant immune responses and molecular mimicry.

Here we have examined the effects of HERV expression on neural cell function and survival, focusing in particular on the HERV-W envelope glycoprotein syncytin and its pathogenic effects.

RESULTS

HERV-W *env* is upregulated in multiple sclerosis lesions

To investigate the expression of phylogenetically related HERV genes (Fig. 1a) in neuroinflammatory diseases, we examined the abundance of different HERV *env* mRNAs in brains from individuals diagnosed with multiple sclerosis or with other neurological diseases as controls. HERV-W *env* mRNA expression was selectively upregulated in brain tissue from individuals with multiple sclerosis as compared with controls, whereas other HERV *env* mRNAs were not (Fig. 1b). Sequencing of the resulting polymerase chain reaction (PCR) products confirmed that HERV-W *env* was overexpressed in the brain samples on the basis of comparisons with the HERV-W *env* sequence and other HERV *env* sequences in GenBank (<http://www.ncbi.nlm.nih.gov/genbank>). Western blotting indicated that syncytin (75 kDa), the protein encoded by HERV-W *env*, was also present in brain tissue from individuals with multiple sclerosis but showed limited

¹Department of Clinical Neurosciences, University of Calgary, Calgary, Alberta T2N 4N1, Canada. ²Department of Chemistry and Center of Membrane Sciences, University of Kentucky, Lexington, Kentucky 40506-0055, USA. ³UMR CNRS-bioMerieux, IFR128 BioSciences Lyon-Gerland, Ecole Normale Supérieure de Lyon, Lyon 69364, France. ⁴Department of Pharmacology & Therapeutics, University of Calgary, Calgary, Alberta T2N 4N1, Canada. ⁵Department of Experimental Psychology, University of Oxford, Oxford OX1 3UD, UK. ⁶Department of Medicine, University of Alberta, Edmonton, Alberta T6G 2B7, Canada. Correspondence should be addressed to C.P. (power@ucalgary.ca).

Published online 26 September 2004; doi:10.1038/nn1319

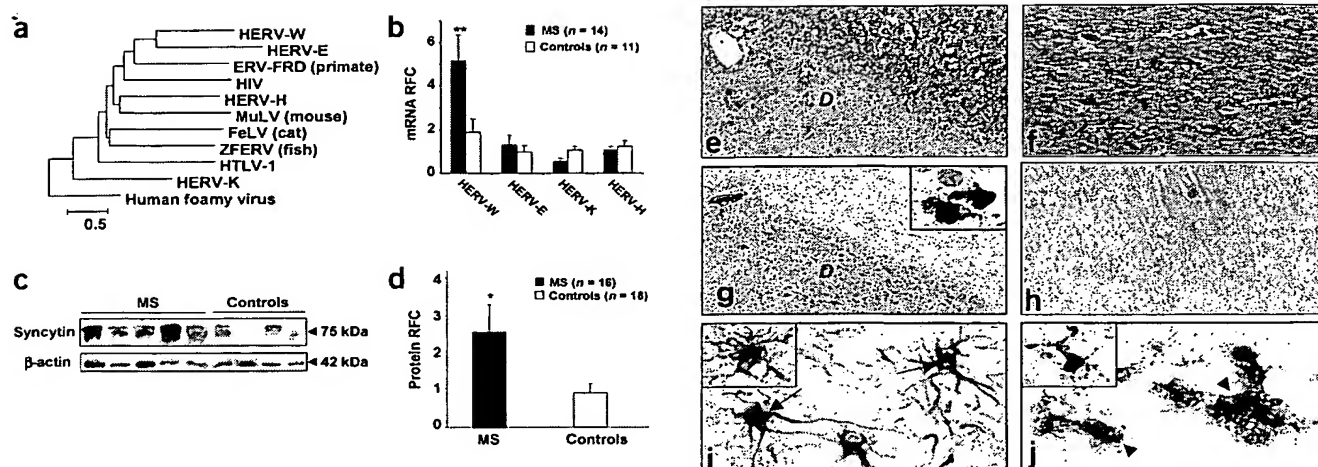


Figure 1 *In vivo* expression of HERV *env*. (a) Phylogenetic tree showing the evolutionary relationship between different endogenous (ERV-FRD, MuLV, ZFERV, HERV-W, -E, -H, -K) and exogenous (HIV, HTLV-1) retrovirus *env* genes in mice, fish, cats, non-human primates and humans including those studied here. (b) Real-time RT-PCR analysis, showing a significant (threefold) increase in the mRNA of HERV-W *env* in individuals with multiple sclerosis (MS) relative to other HERVs and to control individuals affected with other neurological diseases. (c) Representative western blot of brain tissue lysates from individuals with MS, showing an increase in syncytin immunoreactivity as compared with controls. (d) Quantification of western blots, showing an increase in syncytin immunoreactivity in MS brain as compared with controls. (e–j) Active lesions from MS brain show an increase in syncytin expression. (e,f) Active demyelinating (D) lesion from frontal lobe sections of a MS brain, showing myelin debris in macrophages (e) as compared with normal myelin (f). Sections were stained with Luxol fast blue and hematoxylin and eosin. (g,h) Serial sections from the same active lesion, showing an increase in syncytin expression in an area of active demyelination (g) that is absent in control sections (h). iNOS immunoreactivity (dark blue) is colocalized with syncytin (brown) in glia (g, inset). (i) Double-label immunohistochemical assessment of acute lesions in MS brain, showing that syncytin expression (blue) in activated astrocytes colocalizes (arrows) with GFAP immunoreactivity (brown). Inset, GFAP-immunoreactive astrocyte. (j) As i, but showing that syncytin expression (brown) in microglia and macrophages colocalizes (arrowheads) with Iba-1 immunoreactivity (blue). Inset, Iba-1-immunoreactive microglia. Original magnification, $\times 50$ (e–h); $\times 400$ (i,j); $\times 1,000$ (g,i,j, insets). Values are the mean \pm s.e.m. * $P < 0.05$, ** $P < 0.01$.

expression in controls (Fig. 1c). Comparison of syncytin immunoreactivity in brain showed a roughly 3.0-fold increase in the multiple sclerosis group relative to controls (Fig. 1d).

In the multiple sclerosis group, acute lesions containing active demyelination with numerous lipid- or myelin-filled macrophages and hypertrophied astrocytes (Fig. 1e) showed syncytin immunoreactivity (Fig. 1g) in cells resembling activated glia, which also contained inducible nitric oxide synthase (iNOS) immunoreactivity (Fig. 1g, inset). Lipid vacuole-filled syncytin-immunopositive cells

resembling phagocytic macrophages were evident at the margins and the cores (Supplementary Fig. 1 online) of both acute and chronic demyelinating lesions (Table 1). Syncytin-positive cells were not detected in control brain sections (Fig. 1h), however, which showed normal myelination (Fig. 1f).

Because astrocytes¹² and microglia¹³ are important modulators of neuroinflammation, we determined whether syncytin expression was selectively upregulated in these immunologically active cells. Double-label immunohistochemical assessment detected enhanced expression of syncytin in the astrocytes (Fig. 1i) and microglia (Fig. 1j) of brain sections (frontal white matter) from individuals with multiple sclerosis, but not in other neural cells including neurons and myelin-forming oligodendrocytes (data not shown).

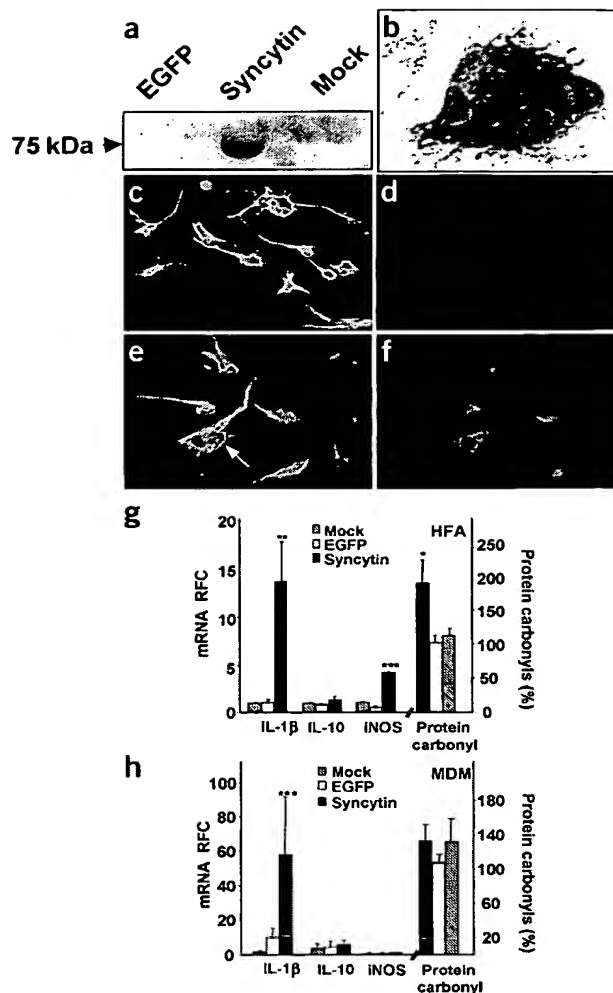
To examine the relative expression of different HERV *env* mRNAs in specific types of cell that have been implicated in neuroinflammation, we studied human cell lines with and without cellular activation. In monocytoid (U937) cells treated with phorbol-12-myristate-13-acetate (PMA), peak mean HERV expression was detected at 4 h, along with a significant increase in HERV-W *env* mRNA as compared with other HERV mRNAs (Supplementary Fig. 2 online). In PMA-treated astrocytic (U373) cells, the most highly expressed HERV was HERV-H *env* mRNA at 24 h, but there was also a significant

Table 1 Clinical and neuropathological features of individuals with multiple sclerosis showing syncytin immunoreactivity in demyelinating lesions

Section ID	1			2					3								
Age at death (yr)	65			71					38								
Gender	F			F					M								
MS type ^a	SP			SP					RR								
Duration of MS (yr)	>10			>10					8								
Pattern of syncytin immunoreactivity ^b																	
Lesion type ^c	SA	C	C	SA	SA	C	C	C	SA	SA	SA	A	A	A	C	C	C
Lesion edge	3+	1+	0	2+	1+	2+	1+	0	3+	4+	3+	4+	4+	4+	3+	2+	3+
Lesion core	4+	2+	1+	4+	3+	3+	2+	1+	2+	2+	2+	4+	4+	0	1+	1+	0
Periplaque white matter	1+	0	0	1+	1+	1+	1+	0	0	1+	2+	0	1+	0	0	1+	0
Normal-appearing white matter	1+	0	0	1+	1+	1+	1+	0	0	0	0	0	0	1+	0	0	0

^aClinical course: SP, secondary progressive; RR, relapsing remitting. ^bScoring pattern: 0, no cells; 1+, 1–10 cells per high-power field (hpf, $\times 200$); 2+, 10–50 cells/hpf; 3+, 50–100 cells/hpf; 4+, 100–500 cells/hpf. ^cLesion type: SA, subacute; A, acute; C, chronic.

Figure 2 Syncytin induces proinflammatory molecules in glial cells. (a,b) Analysis of BHK cells transfected with SINrep5-syncytin. Syncytin immunoreactivity by western blotting (a) and syncytia formation (b) were detected in cells transfected with SINrep5-syncytin, but not in mock-infected cells or cells transfected with SINrep5-EGFP. (c–f) Confocal microscopy of uninfected HFAs immunostained for GFAP (c) and syncytin (d), and astrocytes infected with SINrep5-syncytin (MOI 1.0) immunostained for GFAP (e) and syncytin (f). (g) HFAs infected with SINrep5-syncytin showed a significant increase in IL-1 β and iNOS mRNA expression and an increase in protein carbonyl levels relative to cells infected with SINrep5-EGFP and mock-infected cells, but showed similar expression of IL-10 mRNA. (h) Expression of IL-1 β mRNA was increased in MDMs relative to controls after SINrep5-syncytin infection, whereas that of IL-10 and iNOS mRNA and levels of protein carbonyls did not differ. Original magnification, $\times 1,000$ (b); $\times 600$ (c–f); ** $P < 0.01$, *** $P < 0.001$.



increase in HERV-W *env*. By contrast, PMA stimulation did not induce HERV *env* expression in peripheral blood lymphocytes (PBLs), although expression of interleukin-1 β (IL-1 β) was significantly increased (Supplementary Fig. 2 online), similar to our findings in monocytoïd and astrocytic cells (data not shown). In fact, we observed suppression of HERV *env* mRNA when PBLs were stimulated with PMA.

Taken together, these studies indicate that in individuals affected with multiple sclerosis, syncytin is upregulated in active demyelinating lesions and shows selective expression in cells that mediate neuroinflammation.

Syncytin activates proinflammatory molecules in glia

Because syncytin was abundantly expressed *in vivo* in brain tissue from individuals with multiple sclerosis (Fig. 1b–d,g,i,j), we constructed a SINrep5-based vector that efficiently expressed the HERV-W *env* open reading frame encoding syncytin (Fig. 2a) and that also mediated syncytia formation in baby hamster kidney (BHK) cells (Fig. 2b). The SINrep5-syncytin virus infected human fetal astrocytes (HFAs; Fig. 2f) which expressed glial fibrillary acidic protein (GFAP; Fig. 2c–e) and macrophages, but not oligodendrocytes (data not shown). We examined the syncytin-mediated induction of genes related to neuroinflammation 24 h after infection, which showed that the proinflammatory cytokine IL-1 β was significantly increased in both HFAs (Fig. 2g) and monocyte-derived macrophages (MDMs; Fig. 2h) infected with SINrep5-syncytin, as compared with control cells including cells infected with SINrep5 expressing enhanced green fluorescent protein (EGFP) and mock-infected cells. In addition, the mean expression of iNOS was enhanced in HFAs (Fig. 2g), but not in MDMs (Fig. 2h), after infection with SINrep5-syncytin. The anti-inflammatory cytokine IL-10, however, was not induced in either cell type, suggesting that syncytin expression selectively induces proinflammatory responses.

As compared with controls, a marked increase in mean protein carbonyl levels was also observed in the conditioned medium from HFAs infected with SINrep5-syncytin (Fig. 2g), but not in that derived from MDMs (Fig. 2h). Conversely, there was no significant difference in the mean quantities of malondialdehyde (a product of lipid peroxidation)¹⁴ in conditioned medium from SINrep5-syncytin infected HFAs or MDMs as compared with controls (Supplementary Fig. 3 online). These observations indicated that syncytin induces a proinflammatory molecular profile in astrocytes that includes an increase in the oxidation of cellular proteins.

Syncytin causes oligodendrocyte damage and death

Because oligodendrocytes are the principal cell type that is susceptible to injury associated with neuroinflammation and demyelination,

we examined their morphology and survival after treatment with conditioned medium from HFAs and MDMs infected with SINrep5-syncytin. Conditioned medium from HFAs infected with SINrep5-syncytin was highly cytotoxic to human oligodendrocytes as compared with that derived from control HFAs that were either infected with SINrep5-EGFP or mock infected (Fig. 3a). Notably, conditioned medium from HFAs infected with SINrep5-syncytin also induced a higher mean amount of oligodendrocyte death than did that from MDMs infected with SINrep5-syncytin (Fig. 3b). In addition, human oligodendrocytes treated with medium from HFAs infected with SINrep5-syncytin also showed a significant retraction of cellular processes as compared with controls ($P < 0.001$; Fig. 3c).

We confirmed these results in rat oligodendrocytes using the same cytotoxicity protocol, which showed that conditioned medium from HFAs infected with SINrep5-syncytin similarly caused a significantly higher mean amount of cell death than did that from MDMs infected with SINrep5-syncytin (Fig. 3d). In addition to cell loss, rat oligodendrocytes treated with conditioned medium from HFAs infected with SINrep5-syncytin showed marked process retraction as compared with controls (Supplementary Fig. 4 online).

As a control, the envelope protein from another neurotropic retrovirus HIV-JRFL, obtained from an individual with HIV-associated dementia, was expressed in HFAs using the same vector (SINrep5), and

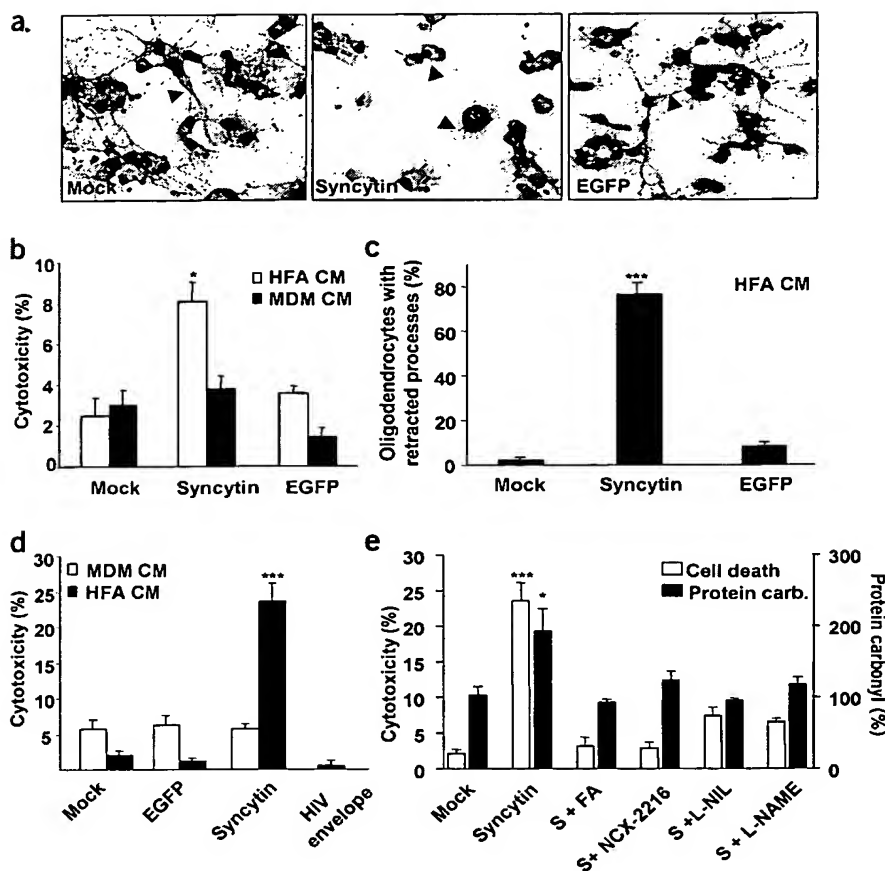


Figure 3 Synctin causes oligodendrocyte damage and death. (a) Human oligodendrocytes (hOLs) treated with conditioned medium (CM) from HFAs infected with SINrep5-synctin showed retracted cellular processes (arrowhead) with cell loss, whereas SINrep5-EGFP-infected and mock-infected controls showed abundant cell numbers and intact processes (arrowhead). (b) hOLs treated for 24 h with CM from HFAs infected with SINrep5-synctin showed significantly higher cytotoxicity than did controls. CM from MDMs infected with SINrep5-synctin was not toxic to hOLs. (c) hOLs treated for 24 h with CM from HFAs infected with SINrep5-synctin showed significantly more cells with retracted processes than did controls. (d) CM from HFAs infected with SINrep5-synctin, but not with a SINrep5-expressed HIV envelope protein, induced significant cytotoxicity in rat OLs. (e) Synctin (S)-induced OL cytotoxicity and protein carbonyl abundance in the CM of HFAs were reduced when HFAs were treated with the antioxidants ferulic acid (FA; 50 μ M), NCX-2216 (6 μ M), L-NIL (0.5 μ M) and L-NAME (5.0 μ M). Original magnification, $\times 400$. * $P < 0.05$; *** $P < 0.001$.

was found not to cause oligodendrocyte cytotoxicity (Fig. 3d). Conditioned medium from HFAs and MDMs infected with SINrep5-synctin was not cytotoxic to human neurons under similar conditions, whereas the envelope protein from HIV-JRFL was highly cytotoxic to neurons (Supplementary Fig. 5 online). Thus, soluble factors released from astrocytes that are selectively induced by synctin cause cellular injury and death in oligodendrocytes.

Antioxidants prevent synctin-induced oligodendrocyte injury

Because protein carbonyl formation is mediated by redox reactants such as nitric oxide and its metabolite peroxynitrite¹⁴, we considered that compounds that scavenge redox reactants might reduce oligodendrocyte death. HFAs infected with SINrep5-synctin were treated with a polyphenolic antioxidant, ferulic acid¹⁵; a non-steroidal anti-inflammatory-based antioxidant, NCX-2216; and two iNOS inhibitors, *N*⁶-(1-iminoethyl)-lysine, hydrochloride (L-NIL; 0.5 μ M) and *N*^ω-nitro-L-arginine methyl ester (L-NAME; 5.0 μ M). Oligodendrocytes treated with the conditioned medium from these astrocytes showed a marked reduction in both mean oligodendrocyte cytotoxicity and protein carbonyl levels, as compared with oligodendrocytes not treated with either drug (Fig. 3e).

Indeed, protection of oligodendrocytes by ferulic acid and NCX-2216 against synctin-mediated toxicity was found to be dependent on dose (Supplementary Fig. 6 online). Treatment with ferulic acid did not affect infection or expression by SINrep5-synctin (data not shown). Conversely, treatment with other established neuroprotectants including MK801, an *N*-methyl-D-aspartate (NMDA) receptor antagonist, NBQX, an α -amino-3-hydroxy-5-methyl-4-isoxazolepropionate

Ferulic acid inhibits synctin-induced neurological deficits

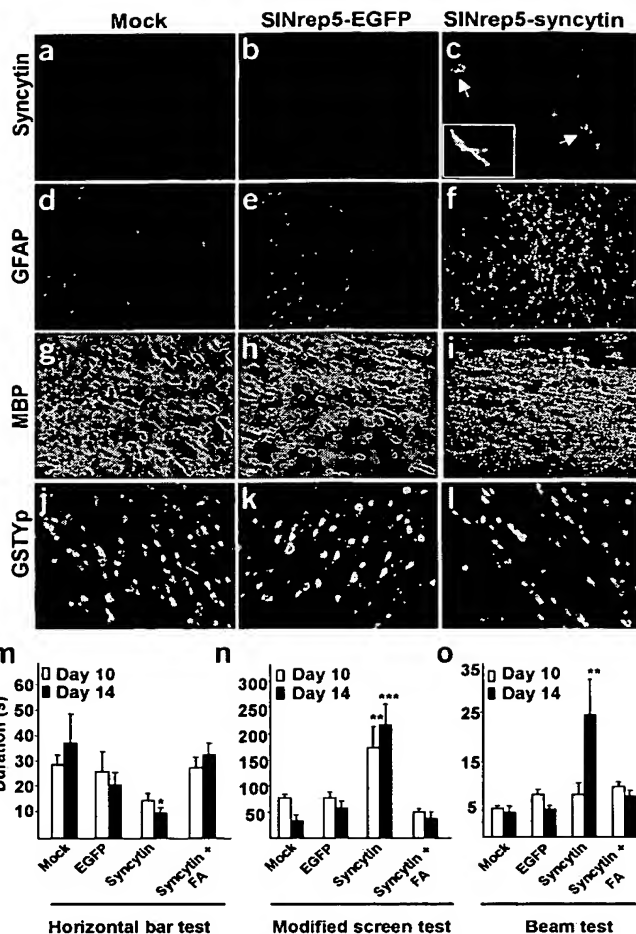
As synctin caused a significant increase in oligodendrocyte cytotoxicity, we examined the *in vivo* effects of synctin after stereotaxic implantation of the SINrep5-synctin virus into the corpus callosum of CD-1 mice. This brain region was selected because it is abundant in myelin, oligodendrocytes and astrocytes and is specifically injured in demyelinating diseases such as multiple sclerosis, resulting in motor and cognitive abnormalities (Fig. 4).

After the implantation of SINrep5-synctin, synctin was detected near the implantation site (Fig. 4c), and synctin-expressing astrocytes were visible in the corpus callosum (Fig. 4c, inset). Serial tissue sections showed increased numbers of hypertrophied astrocytes (Fig. 4f,m) and microglia (Supplementary Fig. 8 online) in the corpus callosum of mice implanted with SINrep5-synctin as compared with mice implanted with SINrep5-EGFP (Fig. 4e) or control conditioned medium (Fig. 4d). In addition, myelin in the corpus callosum of mice implanted with SINrep5-synctin showed a vacuolar appearance after immunostaining for myelin basic protein (MBP; Fig. 4i) as compared with controls (Fig. 4g,h). There were substantially fewer immunoreactive oligodendrocytes (GSTYp positive) in mice that received the synctin-expressing virus (Fig. 4l) than in controls (Fig. 4j,k).

To verify the latter observation, we carried out stereological cell counts of immunoreactive oligodendrocytes, which showed a significant reduction in mean cell numbers in mice implanted with SINrep5-synctin as compared with controls (Table 2). By contrast, astrocyte counts in the same mice indicated that there was a significant increase in activated astrocytes. The decrease in oligodendrocyte numbers and

(AMPA) receptor antagonist, interferon- β (IFN- β) and glatiramer acetate did not reduce synctin-related oligodendrocyte death (Supplementary Fig. 7 online). Thus, synctin-induced oligodendrocyte cytotoxicity is probably mediated by the pathogenic effects of redox reactants in this *in vitro* system.

Figure 4 Syncytin induces neuroinflammation and neurobehavioral abnormalities in mice. (a–c) Syncytin immunoreactivity was detected in the corpus callosum for up to 14 d in mice implanted with SINrep5-syncytin (c) but not in mock-implanted (a) or SINrep5-EGFP-implanted (b) mice. (d–f) Astrogliosis indicated by intense GFAP immunoreactivity was observed in the corpus callosum of mice implanted with SINrep5-syncytin (f), whereas normal astrocytes were observed in controls (d,e). (g–i) White matter of mice implanted with SINrep5-syncytin showed a vacuolar appearance (i), whereas healthy myelin was seen in controls (g,h). GSTYp-immunopositive oligodendrocytes were decreased in the white matter of mice implanted with SINrep5-syncytin (l) as compared with controls (j,k). (m–o) Ferulic acid (FA) abrogates syncytin-induced neurobehavioral changes in mice. Mice implanted with SINrep5-syncytin showed a significantly reduced ability to grasp a horizontal rod (m), a significantly diminished ability to grasp and to escape from an inverted screen (n) and delays in the time taken to cross a cantilevered beam, as compared with SINrep5-EGFP-implanted and mock-implanted controls ($n = 6$ mice per group in each test). Treatment of mice implanted with SINrep5-syncytin with FA (20 mg/kg administered daily by oral gavage) increased ability to grasp the bar (m), improved ability to grasp and to escape from the inverted screen (n) and reduced the time taken to cross the cantilevered beam (o). Original magnification, $\times 400$ (a–c); $\times 1,000$ (d–f); $\times 200$ (g–i); $\times 200$ (j–l). Values are the mean \pm s.e.m.; * $P < 0.05$, ** $P < 0.005$, *** $P < 0.0001$.



increase in hypertrophied astrocytes caused by syncytin expression were reversed by daily treatment with ferulic acid (Table 2).

We confirmed the above neuropathological findings by neurobehavioral testing of mice receiving SINrep5-EGFP, mock-implanted control conditioned medium and SINrep5-syncytin with and without concurrent ferulic acid treatments. At days 3 and 7, there were no differences in performance among the different groups (Supplementary Fig. 9 online). At days 10 and 14 after implantation, however, mice implanted with SINrep5-syncytin grasped the horizontal rod for significantly less time than did the control mice ($P < 0.05$; Fig. 4m). In addition, although mice implanted with SINrep5-syncytin retained some ability to hold on to the screen, they were slower to reach the screen edge (Fig. 4n), whereas mice implanted with SINrep5-EGFP or control conditioned medium were more curious and reached the edges of the inverted screen more quickly ($P < 0.0001$).

Mice implanted with SINrep5-syncytin showed mean delays in the time taken to cross a cantilevered beam as compared with mice implanted with SINrep5-EGFP or control conditioned medium ($P < 0.005$; Fig. 4o), suggesting that the SINrep5-syncytin implanted mice showed diminished motor activity and exploratory behavior. When mice implanted with SINrep5-syncytin were treated with ferulic acid for 14 d, the neurobehavioral outcomes in the horizontal bar test (Fig. 4m), modified screen test (Fig. 4n) and beam test (Fig. 4o) were significantly improved. Striatal implantation of SINrep5-syncytin in mice did not result in neuronal damage, as assessed by neurobehavioral studies¹⁶ (Supplementary Fig. 5 online).

Table 2 Cell counts of immunoreactive astrocytes and oligodendrocytes in corpus callosum^a

	Mock	SINrep5-EGFP	SINrep5-syncytin	SINrep5-syncytin plus ferulic acid
Oligodendrocytes	653.97 (0.05)	760.53 (0.06)	356.32 (0.07)†	731.99 (0.04)
Astrocytes	130.50 (0.12)	198.98 (0.14)	402.49 (0.09)†	177.08 (0.17)

^aGSTYp-immunopositive (oligodendrocytes) and GFAP-immunopositive (astrocytes) cells were counted by stereological methods in the corpus callosum of mice implanted with SINrep5-syncytin, SINrep5-EGFP or control conditioned medium (mock). One group of SINrep5-syncytin-implanted mice was treated daily with ferulic acid. Mean results are shown, with the coefficient of error in parentheses. † $P < 0.0001$.

In accordance with our *in vitro* observations, these *in vivo* studies indicate that syncytin induces neuroinflammation, oligodendrocyte and myelin damage, and neurobehavioral abnormalities that are abrogated by the antioxidant ferulic acid.

DISCUSSION

We have shown that expression of both the mRNA and protein (syncytin) encoded by the HERV-W *env* gene is increased in the brains of individuals with multiple sclerosis and in specific cell types involved in neuroinflammation in demyelinating and demyelinated lesions. In addition, we have shown that *in vitro* syncytin mediates the production of proinflammatory molecules such as iNOS, IL-1 β and redox reactants that at high levels are damaging to the brain^{9,14,17}. An

explicit function for syncytin is unknown in the brain in contrast to the placenta, where it seems to be important for placental development^{18–21}. However, our findings, including increased levels of iNOS and redox reactants, are consistent with the neuroinflammatory profile of astrocytes associated with multiple sclerosis^{22–24}. In addition to the proinflammatory effects of syncytin in glial cells, soluble factors derived from syncytin-expressing astrocytes are toxic to oligodendrocytes but not to neurons, implying that syncytin uses a

select mechanism for killing and/or targeting individual cell types—a possibility that is congruent with studies showing that astrocytes may influence oligodendrocyte survival^{25–27}.

We did not detect syncytin in supernatants from astrocytes infected with SINrep5-syncytin, precluding the possibility that a direct interaction between syncytin and target cells leads to cytotoxicity. Nonetheless, syncytin expression in astrocytes resulted in cellular stress, manifested by the induction of IL-1 β , iNOS and redox reactants. Notably, syncytin expression was evident in glia at both the margin and the core of acute demyelination (Fig. 1f), emphasizing its role in cellular stress. Of interest, polymorphisms in retrovirus-encoded envelope proteins from HIV²⁸ and murine leukemia virus²⁹ that alter intracellular envelope expression in glial cells have been associated with pathogenic effects in the nervous system. These effects may occur through misfolding of the envelope protein or protein accumulation in the endoplasmic reticulum, resulting in a stress response by the cell and the subsequent release of neurotoxic molecules including redox reactants³⁰.

Given that iNOS was induced in astrocytes, probable redox stress products include nitric oxide, reactive nitrogen-oxygen species, peroxynitrite and superoxide anions, which are capable of damaging target tissues, particularly the brain^{14,22}, and are also toxic to oligodendrocytes³¹. By contrast, we did not observe an increase in the *in vitro* generation of lipid peroxidation products, in agreement with studies on the pathogenesis of multiple sclerosis³². Although the precise pathway by which oxidation of a protein released by astrocytes mediates oligodendrocyte toxicity remains to be determined, a potential mechanism might involve oxidation of a released matrix metalloproteinase³³.

We have also shown that by inducing proinflammatory molecules and redox reactants, ultimately resulting in oligodendrocyte death, syncytin modulates neurobehavioral changes in a mouse model that shows pathology similar to other animal models of multiple sclerosis. The present neurobehavioral changes are also reminiscent of those seen in individuals with multiple sclerosis including weakness, gait unsteadiness and altered executive functions^{34,35}. In addition, our studies have shown that ferulic acid, the plant-derived phenolcarboxylic acid that acts as an antioxidant^{15,36}, ameliorates oligodendrocyte death *in vitro* and *in vivo* and significantly improves neurobehavioral outcomes.

In summary, our study indicates that syncytin may be involved in the pathogenesis of active demyelination, principally by evoking redox reactant-mediated cellular damage in the brain. Alternatively, given its persistent expression in lesion cores, the syncytin-mediated glial stress reaction might antagonize remyelination. In this regard, ferulic acid and equivalent compounds might be considered in trials designed to evaluate their efficacy for reducing demyelination or enhancing remyelination, similar to the protective effects of ferulic acid in neurons¹⁵. In addition, because HERVs represent a substantial proportion of the human genome and often express proteins, the potential pathogenic (or reparative) effects of other HERV proteins expressed in the nervous system warrant further investigation.

METHODS

Cell cultures. Human and rat oligodendrocytes³⁷, HFAs³⁸, human LAN-2 neuronal cells¹⁶, human MDMs⁸ and PBLs³⁹, U373 astrocytoma⁴⁰ and U937 monocytoid cells⁸ (American Type Culture Collection) were cultured as described. To assess the effect of astrocyte and monocyte stimulation on HERV expression, we treated U373, PBL and U937 cells with 50 ng/ml of PMA (Sigma) for 4–72 h, collected them and isolated RNA as described⁸.

Real-time PCR with reverse transcription (RT-PCR). Total RNA and cDNA were prepared from brain tissue or cells as described⁴⁰. Primers for GAPDH,

IL-1 β and iNOS have been described⁴⁰. We also used primers for IL-10 (5'-CCTCTCACCGTCTTGTTC-3' and 5'-GCAGAGTTGCTTGTCTCC-3'), HERV-W *env* (5'-TGCCCCATCGTATAGAGTCT-3' and 5'-CATGTACCCGGGTGAGTTGG-3'), HERV-H *env* (5'-TTACCCCATCATCAGTCCCCAT-3' and 5'-GAGCTCTTCGGTCCCATTTG-3'), HERV-E *env* (5'-TCGCCAAAGCCAGAGTT-3' and 5'-AAGGGGAAATGAGGA-3') and HERV-K (II) *env* (5'-TTTATGGGGCCGAGACTTGTTA-3' and 5'-AGCGGCTACTGATTTACCATAC-3'). Semiquantitative real-time RT-PCR analysis was done by monitoring in real-time the increase of fluorescence of SYBR-green dye on a Bio-Rad i-Cycler. Data were normalized to the GAPDH mRNA level and are expressed as the relative fold change (RFC) in mRNA as described⁴⁰.

Human brain tissue samples. Brain tissue (frontal white matter) was collected with informed consent at autopsy, as described⁸. Control subjects included 18 individuals (mean age 56 \pm 16.4 yr), who were diagnosed with Alzheimer's disease (n = 6), HIV infection (encephalitis, n = 4; gliosis, n = 4), cerebral arteriosclerosis (n = 2), anoxic encephalopathy (n = 1) or normal brain pathology (n = 1). The multiple sclerosis group included 16 individuals (age 63.3 \pm 13.4 yr) who had been classified with primary progressive (n = 4), secondary progressive (n = 10) or relapsing-remitting (n = 2) multiple sclerosis and had an estimated disability status scale score of 7–10 before death. Frozen brain tissue from individuals with multiple sclerosis was obtained from the Multiple Sclerosis Patient Care and Research Clinic, Edmonton, Alberta, Canada. Brain tissue sections from chronic demyelinated plaques from individuals with multiple sclerosis were used for histochemical and immunohistochemical studies.

Immunohistochemistry and histochemistry. Paraffin-embedded sections were immunostained with antibodies to Iba-1 (1.0 μ g/ml; ref. 40) for macrophage and microglia detection, GFAP (diluted 1:2,000; DAKO) for astrocyte detection, iNOS (1:500; Santa Cruz Biotech), GSTYp (1:600; Biotrin) and adenomatous polyposis coli (APC, 1:500; Ab-7, Oncogene Research Products) for oligodendrocyte detection, and syncytin (1:1,000; 6A2B2)¹⁹ as reported¹⁶. To double label both microglia and astrocytes with cell-type-specific markers and syncytin, sections were probed with antibodies to Iba-1 and GFAP respectively, followed by incubation with biotinylated goat anti-rabbit IgG (H+L) (1:500; Vector Laboratories) and subsequently with Elite ABC reagent (Vector Laboratories) or peroxidase-conjugated Affinipure goat anti-rabbit IgG (H+L) (1:500; Jackson ImmunoResearch), and then developed by diaminobenzidine (DAB) treatment for peroxidase or bromochloroindolyl phosphate (BCIP) and nitro blue tetrazolium (NBT) for alkaline phosphatase activity.

Immunofluorescence and confocal laser scanning microscopy. Paraffin-embedded sections from mice were immunostained with mouse anti-MBP (diluted 1:1,000; Sternberger Monoclonals), rabbit anti-mouse GSTYp (1:600; Biotrin) and anti-APC (1:500; Ab-7, Oncogene Research Products). Slides were examined on an Olympus FV300 confocal laser-scanning microscope. Cultured oligodendrocytes derived from adult human and rat brains were stained with a monoclonal antibody (O1) that recognizes galactocerebroside (Gal-C), a marker for mature oligodendrocytes⁴¹. The total number of cells and the number with processes at 24 h were counted per well (10 fields at \times 400 magnification) after treatment with conditioned medium from HFAs or MDMs infected with SINrep5-syncytin or SINrep5-EGFP. APC-positive oligodendrocytes and GFAP-positive astrocytes in the vicinity of the implantation site were counted (five fields at \times 400; expressed as total number of GSTYp-positive cells in an area of 2,376 μ m²).

We used three serial sections (5 μ m) from six mice per treatment group to quantify numbers of GFAP-positive astrocytes and GSTYp-positive oligodendrocytes by a stereological method⁴². In brief, a systematic random sample of three sections that spanned the corpus callosum was selected for analysis. Sections were selected at equal intervals in the series comprising a known fraction of the section series (ssf). The labeled astrocytes and oligodendrocytes were counted (Σ Q) under a known fraction of the section area (asf). The height of the optical disectors (h) positioned in the central part of the section thickness (t) was used to determine the ratio h/t (tsf). The total number (N) of astrocytes or oligodendrocytes were estimated as $N = \Sigma Q \times 1/ssf \times 1/asf \times 1/tsf$. The coefficient of error was determined by the formula $CE(\Sigma Q) = s.e.m./mean$.

Western blot analysis. Protein extracts were prepared from various brain tissue and cell samples with lysis buffer and concentrations were determined by BCA assay (Pierce). We separated proteins by 10% SDS-PAGE, transferred them to nitrocellulose membranes and probed them with antibodies to syn- cytin and β -actin as reported⁸. The 75-kDa band was analyzed by densitome- try, and the mean results are expressed as the RFC in the density of the band in the multiple sclerosis group as compared with controls.

Construction of SINrep5 virus. The Sindbis virus-based (SIN) vector sys- tem used in this study has been described²⁸. In brief, the 1.832-kbp *env* open reading frame from pHCMVenvpH74 (ref. 19) was cloned into pSINrep5 to obtain pSINrep5-syn- cytin. Virus stocks were prepared as described²⁸. On average, 10^6 to 10^7 infectious virus particles per ml were obtained for SINrep5-syn- cytin and SINrep5-EGFP, respectively. All infections were done with the same number of virus particles (multiplicity of infection (MOI) 1.0). HFAs and MDMs (5×10^4 per well) were seeded in 16-well chamber slides and infected with SINrep5-syn- cytin or SINrep5-EGFP (MOI 1.0 each) or mock-infected with conditioned medium.

Cell survival assay. To determine whether oligodendrocyte cytotoxicity can be inhibited, HFAs were treated with NBQX (30 μ M; Sigma), MK-801 (30 μ M; Sigma), glatiramer acetate (25 μ g/ml; Teva), IFN- β (100 U/ml; Serono), ferulic acid (0.005, 0.5, 5, 50 or 250 μ M; Sigma), NCX-2216 (60 nM, 600 nM and 6 μ M; a gift of NicOx S.A.), L-NIL (0.5 μ M, Sigma) and L-NAME (5.0 μ M, Sigma) followed by infection with SINrep5-syn- cytin overnight at 37 °C. Adult rat brain-derived oligodendrocytes were treated subsequently with either con- ditioned medium (diluted 1:1 with AIM-V medium) from drug-treated or SINrep5-syn- cytin-infected HFA for 24 h. Conditioned media for toxicity assays were obtained from HFA and MDM infected with SINrep5-syn- cytin or SINrep5-EGFP. We prepared LAN-2 neurons as described¹⁶. All experiments were repeated at least three times. To measure cellular injury, oligodendrocytes were immunostained with antibody to Gal-C and cells with and without processes were counted. To quantify cell death, the trypan-blue exclusion method was used as described²⁸.

Protein carbonyl and 4-hydroxynonenol (HNE) assays. Protein oxidation was determined¹⁴ by an oxidized protein detection kit (Oxyblot, ONCOR). Samples were incubated for 20 min with 12% SDS and 2,4-dinitrophenylhy- drazine (DNPH) in 10% trifluoroacetic acid with vortexing every 5 min, and then neutralized with Oxyblot Neutralization solution. We blotted 600 ng of protein onto nitrocellulose paper by the slot blotting technique. Membranes were incubated with blocking buffer for 30 min at 24 °C, incubated with rabbit antibodies to DNPH (diluted 1:150) for 90 min, and then by anti-rabbit IgG coupled to alkaline phosphatase (1:15,000) for 2 h at 24 °C. After being washed and developed with SigmaFast chromogen (Sigma), blots were analyzed by computer-assisted imaging software (Scion Imaging). Samples for HNE detec- tion were similarly analyzed by the slot blotting technique except that a rabbit antibody to HNE (1:4,000; Calbiochem) was used as a primary antibody as described¹⁴. Results are expressed as the RFC as compared with values obtained in AIM-V medium.

In vivo implantation of viruses and drug treatment. SINrep5-EGFP or SINrep5-syn- cytin virus (0.5×10^6 particles/ml in 3 μ l) was stereotactically implanted bilaterally into the corpus callosum of CD-1 mice aged 10 weeks ($n = 6$ for each treatment). Control mice ($n = 6$) were implanted with con- ditioned medium from mock-infected cultures (1-mm anterior, 2.0-mm lateral and 1.5-mm deep relative to bregma). In addition, the right striatum of CD-1 mice aged 10 weeks ($n = 4$ for each treatment) were stereotactically implanted with SINrep5-EGFP and SINrep5-syn- cytin (0.5×10^6 particles/ml) as described²⁸. Similarly, for treatment with ferulic acid, mice ($n = 6$) were implanted with SINrep5-syn- cytin and subjected by daily oral gavage with ferulic acid (20 mg per kg (body weight) on a daily basis) for 14 d. Mice were killed on day 14 and intracardially perfused with saline, followed by 4% paraformaldehyde (PFA). All mouse experiments were done in accordance with Canadian Council on Animal Care guidelines.

Neurobehavioral studies. Behavioral tests were conducted in mice that had been implanted with the SINrep5-syn- cytin or SINrep5-EGFP virus or con-

trol conditioned medium (mock-implanted) on days 3, 7, 10 and 14 after implantation. The horizontal bar test involved a test of coordination and forelimb strength using a horizontal bar (0.2 cm thick, 38 cm long) held 49 cm above a bench⁴³. The static rod test involved a test of coordination using five rods (60 cm long) of varying thickness (diameters: 35 mm, rod 1; 28 mm, rod 2; 22 mm, rod 3; 15 mm, rod 4; 9 mm, rod 5). These rods were bolted to the edge of a bench so that the rods protruded their full 60-cm length horizontally into space. We placed a mouse at the exposed end of the widest rod and measured the time that it took to orient 180° from the start- ing position and to travel to the other end⁴³. Muscle strength and seeking behavior were determined by using an inverted screen test. The invertable screen was a 43-cm square wire mesh consisting of 12-mm squares of 1-mm diameter wire surrounded by a 4-cm deep wooden beading⁴³. We modified the inverted screen test by placing the mouse at a point that was equidistant from the edges of the screen. We started the stop-clock once the screen was inverted and noted the time that the mouse took to reach the edge of the inverted screen as a measure of curiosity and seeking behavior. The rotary behavior of the mice with implants in the striatum was analyzed at 3, 7, 10 and 14 d after implantation, as described²⁸.

Statistical analysis. Because multiple treatments were used in all experiments, a one-way analysis of variance (ANOVA) with Tukey-Kramer multiple com- parisons test was used for analysis. Data were analyzed using GraphPad InStat version 3.01 for Windows 95 (GraphPad Software).

Note: Supplementary information is available on the Nature Neuroscience website.

ACKNOWLEDGMENTS

We thank P. Kubes, C. Hao and A. Clark for discussion; and C. Silva, A. Sullivan and A. Hood for technical assistance. J.M.A. holds a studentship from the Multiple Sclerosis Society of Canada (MSSC); G.v.M. is a Canadian Institutes of Health Research (CIHR)/Alberta Heritage Foundation for Medical Research (AHFMR) Fellow; V.W.Y. holds a Canada Research Chair (Tier 1) in neuroimmunology; J.L.W. is an AHFMR Scientist and C.P. is an AHFMR Scholar/CIHR Investigator. These studies were supported by the MSSC and CIHR Interdisciplinary Health Research Team (IHRT).

COMPETING INTERESTS STATEMENT

The authors declare that they have no competing financial interests.

Received 8 April; accepted 30 August 2004

Published online at <http://www.nature.com/natureneuroscience/>

1. Lander, E.S. *et al.* Initial sequencing and analysis of the human genome. *Nature* **409**, 860–921 (2001).
2. Costas, J. Characterization of the intragenomic spread of the human endogenous retrovirus family HERV-W. *Mol. Biol. Evol.* **19**, 526–533 (2002).
3. Hughes, J.F. & Coffin, J.M. Evidence for genomic rearrangements mediated by human endogenous retroviruses during primate evolution. *Nat. Genet.* **29**, 487–489 (2001).
4. van de Lagemaat, L.N., Landry, J.R., Mager, D.L. & Medstrand, P. Transposable ele- ments in mammals promote regulatory variation and diversification of genes with specialized functions. *Trends Genet.* **19**, 530–536 (2003).
5. Sverdlov, E.D. Retroviruses and primate evolution. *BioEssays* **22**, 161–171 (2000).
6. Bock, M. & Stoye, J.P. Endogenous retroviruses and the human germline. *Curr. Opin. Genet. Dev.* **10**, 651–655 (2000).
7. Power, C. Retroviral diseases of the nervous system: pathogenic host response or viral gene-mediated neurovirulence? *Trends Neurosci.* **24**, 162–169 (2001).
8. Johnston, J.B. *et al.* Monocyte activation and differentiation augment human endogenous retrovirus expression: implications for inflammatory brain diseases. *Ann. Neurol.* **50**, 434–442 (2001).
9. Calabrese, V. *et al.* Nitric oxide synthase is present in the cerebrospinal fluid of patients with active multiple sclerosis and is associated with increases in cere- brospinal fluid protein nitrotyrosine and S-nitrosothiols and with changes in glu- tathione levels. *J. Neurosci. Res.* **70**, 580–587 (2002).
10. Lu, F. *et al.* Oxidative damage to mitochondrial DNA and activity of mitochondrial enzymes in chronic active lesions of multiple sclerosis. *J. Neurol. Sci.* **177**, 95–103 (2000).
11. Bo, L. *et al.* Induction of nitric oxide synthase in demyelinating regions of multiple sclerosis brains. *Ann. Neurol.* **36**, 778–786 (1994).
12. John, G.R. *et al.* Multiple sclerosis: re-expression of a developmental pathway that restricts oligodendrocyte maturation. *Nat. Med.* **8**, 1115–1121 (2002).
13. Carson, M.J. Microglia as liaisons between the immune and central nervous sys- tems: functional implications for multiple sclerosis. *Glia* **40**, 218–231 (2002).
14. Butterfield, D.A. & Lauderback, C.M. Lipid peroxidation and protein oxidation in

- Alzheimer's disease brain: potential causes and consequences involving amyloid β -peptide-associated free radical oxidative stress. *Free Radic. Biol. Med.* **32**, 1050–1060 (2002).
15. Kanski, J., Aksenova, M., Stoyanova, A. & Butterfield, D.A. Ferulic acid antioxidant protection against hydroxyl and peroxy radical oxidation in synaptosomal and neuronal cell culture systems *in vitro*: structure-activity studies. *J. Nutr. Biochem.* **13**, 273–281 (2002).
 16. Zhang, K. *et al.* HIV-induced metalloproteinase processing of the chemokine stromal cell derived factor-1 causes neurodegeneration. *Nat. Neurosci.* **6**, 1064–1071 (2003).
 17. Hua, L.L., Kim, M.O., Brosnan, C.F. & Lee, S.C. Modulation of astrocyte inducible nitric oxide synthase and cytokine expression by interferon β is associated with induction and inhibition of interferon gamma-activated sequence binding activity. *J. Neurochem.* **83**, 1120–1128 (2002).
 18. Blond, J.L. *et al.* Molecular characterization and placental expression of HERV-W, a new human endogenous retrovirus family. *J. Virol.* **73**, 1175–1185 (1999).
 19. Blond, J.L. *et al.* An envelope glycoprotein of the human endogenous retrovirus HERV-W is expressed in the human placenta and fuses cells expressing the type D mammalian retrovirus receptor. *J. Virol.* **74**, 3321–3329 (2000).
 20. Frendo, J.L. *et al.* Direct involvement of HERV-W env glycoprotein in human trophoblast cell fusion and differentiation. *Mol. Cell. Biol.* **23**, 3566–3574 (2003).
 21. Mi, S. *et al.* Syncytin is a captive retroviral envelope protein involved in human placental morphogenesis. *Nature* **403**, 785–789 (2000).
 22. Calabrese, V. *et al.* Disruption of thiol homeostasis and nitrosative stress in the cerebrospinal fluid of patients with active multiple sclerosis: evidence for a protective role of acetylcarnitine. *Neurochem. Res.* **28**, 1321–1328 (2003).
 23. Smith, K.J. & Lassmann, H. The role of nitric oxide in multiple sclerosis. *Lancet Neurol.* **1**, 232–241 (2002).
 24. Danilov, A.I. *et al.* Nitric oxide metabolite determinations reveal continuous inflammation in multiple sclerosis. *J. Neuroimmunol.* **136**, 112–118 (2003).
 25. Lieberman, A.P., Pitha, P.M., Shin, H.S. & Shin, M.L. Production of tumor necrosis factor and other cytokines by astrocytes stimulated with lipopolysaccharide or a neurotropic virus. *Proc. Natl. Acad. Sci. USA* **86**, 6348–6352 (1989).
 26. Rosen, C.L., Bunge, R.P., Ard, M.D. & Wood, P.M. Type 1 astrocytes inhibit myelination by adult rat oligodendrocytes *in vitro*. *J. Neurosci.* **9**, 3371–3379 (1989).
 27. Takahashi, J.L., Giuliani, F., Power, C., Imai, Y. & Yong, V.W. Interleukin- 1β promotes oligodendrocyte death through glutamate excitotoxicity. *Ann. Neurol.* **53**, 588–595 (2003).
 28. van Marle, G., Ethier, J., Silva, C., Mac Vicar, B.A. & Power, C. Human immunodeficiency virus type 1 envelope-mediated neuropathogenesis: targeted gene delivery by a Sindbis virus expression vector. *Virology* **309**, 61–74 (2003).
 29. Lynch, W.P. & Sharpe, A.H. Differential glycosylation of the Cas-Br-E env protein is associated with retrovirus-induced spongiform neurodegeneration. *J. Virol.* **74**, 1558–1565 (2000).
 30. Wesselingh, S.L. & Thompson, K.A. Immunopathogenesis of HIV-associated dementia. *Curr. Opin. Neurol.* **14**, 375–379 (2001).
 31. Scott, G.S., Virag, L., Szabo, C. & Hooper, D.C. Peroxynitrite-induced oligodendrocyte toxicity is not dependent on poly(ADP-ribose) polymerase activation. *Glia* **41**, 105–116 (2003).
 32. Ravikumar, A., Arun, P., Devi, K.V., Augustine, J. & Kurup, P.A. Isoprenoid pathway and free radical generation and damage in neuropsychiatric disorders. *Indian J. Exp. Biol.* **38**, 438–446 (2000).
 33. Gu, Z. *et al.* S-nitrosylation of matrix metalloproteinases: signaling pathway to neuronal cell death. *Science* **297**, 1186–1190 (2002).
 34. Paty, D.W., Noseworthy, J.H. & Ebers, G.C. Diagnosis of multiple sclerosis. in *Multiple Sclerosis* (eds. Paty, D.E. & Ebers, G.C.) 68–75 (F.A. Davis Company, Philadelphia, 1998).
 35. Anlar, O., Tombul, T. & Kisli, M. Peripheral sensory and motor abnormalities in patients with multiple sclerosis. *Electromyogr. Clin. Neurophysiol.* **43**, 349–351 (2003).
 36. Ogiwara, T. *et al.* Inhibition of NO production by activated macrophages by phenol-carboxylic acid monomers and polymers with radical scavenging activity. *Anticancer Res.* **23**, 1317–1323 (2003).
 37. Yong, V.W. & Antel, J.P. Culture of glial cells from human brain biopsies. in *Protocols for Neural Cell Culture* (eds. Fedoroff, S. & Richardson, A.) 81–96 (Humana, Totowa, NJ, 1997).
 38. Power, C. *et al.* Neuronal death induced by brain-derived human immunodeficiency virus type 1 envelope genes differs between demented and nondemented AIDS patients. *J. Virol.* **72**, 9045–9053 (1998).
 39. Bar-Or, A. *et al.* Analyses of all matrix metalloproteinase members in leukocytes emphasize monocytes as major inflammatory mediators in multiple sclerosis. *Brain* **126**, 2738–2749 (2003).
 40. Power, C. *et al.* Intracerebral hemorrhage induces macrophage activation and matrix metalloproteinases. *Ann. Neurol.* **53**, 731–742 (2003).
 41. Bansal, R., Warrington, A.E., Gard, A.L., Ranscht, B. & Pfeiffer, S.E. Multiple and novel specificities of monoclonal antibodies O1, O4, and R-mAb used in the analysis of oligodendrocyte development. *J. Neurosci. Res.* **24**, 548–557 (1989).
 42. West, M.J., Ostergaard, K., Andreassen, O.A. & Finsen, B. Estimation of the number of somatostatin neurons in the striatum: an *in situ* hybridization study using the optical fractionator method. *J. Comp. Neurol.* **370**, 11–22 (1996).
 43. Guenther, K., Deacon, R.M., Perry, V.H. & Rawlins, J.N. Early behavioural changes in scrapie-affected mice and the influence of dapsone. *Eur. J. Neurosci.* **14**, 401–409 (2001).

The Human Endogenous Retrovirus Envelope Glycoprotein, Syncytin-1, Regulates Neuroinflammation and Its Receptor Expression in Multiple Sclerosis: A Role for Endoplasmic Reticulum Chaperones in Astrocytes¹

Joseph M. Antony,* Kristofor K. Ellestad,[†] Robert Hammond,[†] Kazunori Imaizumi,[‡] François Mallet,[§] Kenneth G. Warren,[¶] and Christopher Power^{2*¶}

Retroviral envelopes are pathogenic glycoproteins which cause neuroinflammation, neurodegeneration, and endoplasmic reticulum stress responses. The human endogenous retrovirus (HERV-W) envelope protein, Syncytin-1, is highly expressed in CNS glia of individuals with multiple sclerosis (MS). In this study, we investigated the mechanisms by which Syncytin-1 mediated neuroimmune activation and oligodendrocytes damage. In brain tissue from individuals with MS, ASCT1, a receptor for Syncytin-1 and a neutral amino acid transporter, was selectively suppressed in astrocytes ($p < 0.05$). Syncytin-1 induced the expression of the endoplasmic reticulum stress sensor, old astrocyte specifically induced substance (OASIS), in cultured astrocytes, similar to findings in MS brains. Overexpression of OASIS in astrocytes increased inducible NO synthase expression but concurrently down-regulated ASCT1 ($p < 0.01$). Treatment of astrocytes with a NO donor enhanced expression of early growth response 1, with an ensuing reduction in ASCT1 expression ($p < 0.05$). Small-interfering RNA molecules targeting Syncytin-1 selectively down-regulated its expression, preventing the suppression of ASCT1 and the release of oligodendrocyte cytotoxins by astrocytes. A Syncytin-1-transgenic mouse expressing Syncytin-1 under the glial fibrillary acidic protein promoter demonstrated neuroinflammation, ASCT1 suppression, and diminished levels of myelin proteins in the corpus callosum, consistent with observations in CNS tissues from MS patients together with neurobehavioral abnormalities compared with wild-type littermates ($p < 0.05$). Thus, Syncytin-1 initiated an OASIS-mediated suppression of ASCT1 in astrocytes through the induction of inducible NO synthase with ensuing oligodendrocyte injury. These studies provide new insights into the role of HERV-mediated neuroinflammation and its contribution to an autoimmune disease. *The Journal of Immunology*, 2007, 179: 1210–1224.

Multiple sclerosis (MS)³ is a demyelinating disease of the CNS defined by inflammatory destruction of myelin and ensuing axonal damage (1). Although MS is widely assumed to be an adaptive T cell-mediated autoim-

mune disease, increasing evidence points to the pathogenic involvement of resident CNS cells including microglia/macrophages and astrocytes in MS pathogenesis, which participate in innate immune processes (2). Inflammatory responses mediated by glia-derived cytokines and chemokines in neurodegenerative diseases regulate levels of several amino acid transporters, which impact on the progression of disease (3). Interestingly, several transporters also function as receptors for different neurotropic retroviruses (4). The human endogenous retrovirus (HERV-W) envelope glycoprotein, Syncytin-1, binds to two receptors including the sodium-dependent transporters of polar neutral amino acids, alanine, serine, cysteine, and threonine (ASCT1 and ASCT2) (4), which are localized on both neurons and glia (5) and are known to modulate both neurotrophic (6) and neurotoxic (7) effects in the CNS.

Syncytin-1 is a complex human endogenous retroviral protein that is largely beneficial to the host in terms of facilitating placental development (8). However, in the brains of MS patients, Syncytin-1 modulates an inflammatory cascade when its expression is increased by various factors including exogenous viruses (9). Recent studies indicate that Syncytin-1 transcript levels are quantitatively increased in the brains of MS patients compared with other inflammatory neurological disease controls (10). Interestingly, TNF- α , an inflammatory molecule in the brains of MS patients, was found to enhance Syncytin-1 expression in astrocytes (11), which consequently results in production of free radicals and cytokines (12) that could affect expression of ASCT1 and ASCT2, given that free radicals influence expression of membrane proteins (13, 14). Free radicals are also produced when cells undergo

*Department of Clinical Neurosciences, University of Calgary, Calgary, Alberta, Canada; [†]Department of Pathology, London Health Sciences Centre and University of Western Ontario, London, Ontario, Canada; [‡]Department of Anatomy, Faculty of Medicine, University of Miyazaki, Japan; [§]Unité Mixte de Recherche, Centre National de la Recherche Scientifique-bioMérieux, l'Institut Fédératif de Recherche 128 BioSciences Lyon-Gerland, Ecole Normale Supérieure de Lyon, Lyon, France; and [¶]Department of Medicine, University of Alberta, Edmonton, Alberta, Canada

Received for publication December 18, 2006. Accepted for publication May 1, 2007.

The costs of publication of this article were defrayed in part by the payment of page charges. This article must therefore be hereby marked *advertisement* in accordance with 18 U.S.C. Section 1734 solely to indicate this fact.

¹J.M.A. was supported by a Studentship from the Alberta Heritage Foundation for Medical Research (AHFMR) and Multiple Sclerosis Society of Canada (MSSC). C.P. holds a Canada Research Chair (Tier 1) in Neurological Infection and Immunity and an AHFMR Senior Scholarship. The MSSC and Canadian Institutes for Health Research supported these studies.

²Address correspondence and reprint requests to Dr. Christopher Power, Departments of Medicine, Medical Microbiology, and Immunology, 611 Heritage Medical Research Center, University of Alberta, Edmonton, Alberta, T6G 2S2 Canada. E-mail address: chris.power@ualberta.ca

³Abbreviations used in this paper: MS, multiple sclerosis; ER, endoplasmic reticulum; MuLV, murine leukemia virus; MoMuLV, Moloney MuLV; iNOS, inducible NO synthase; BiP, IgH chain-binding protein; OASIS, old astrocyte specifically induced substance; Egr1, early growth response 1; Iba, ionized calcium-binding adaptor protein; GFAP, glial fibrillary acidic protein; siRNA, small-interfering RNA; CNP, 2', 3'-cyclic nucleotide 3'-phosphodiesterase; Tg, transgenic; Wt, wild type; EGFP, enhanced GFP; MDM, monocyte-derived macrophage; YFP, yellow fluorescent protein; SNP, sodium nitroprusside; CGT, ceramide galactosyltransferase.

Copyright © 2007 by The American Association of Immunologists, Inc. 0022-1767/07/\$2.00

persistent endoplasmic reticulum (ER) stress (15), a constellation of host responses, which maintain cellular homeostasis, termed the unfolded protein response (16). Accumulation of misfolded proteins contribute to disruption of ER function, resulting in the unfolded protein response (17). Induction of ER stress molecules including activating transcription factor-4 has been previously demonstrated in MS lesions (18). Furthermore, accumulation of proteins such as MHC class I in the ER (15) or ER stress induction by IL-1 β or NO impairs oligodendrocyte repair (19). Several retroviral envelope proteins induce ER stress, together with suppressing the cognate viral receptor (20). For example, infection by murine leukemia virus (MuLV) down-modulates expression of its cell surface receptor, mCAT-1 (21). Several lines of evidence implicate glia in retrovirus-induced ER stress and neuropathogenesis (22). Infection of astrocytes with Moloney MuLV (MoMuLV)-*ts1*, leads to an ER stress response defined by neuroinflammation and neurodegeneration. In fact, envelope proteins from both the retroviruses, MoMuLV-*ts1* and FrCas^E, mediate ER stress in the brain (22–25) and directly affect oligodendrocyte viability by inducing the proapoptotic ER stress gene, *GADD153/CHOP* (26).

Up-regulation of HERVs has been observed in the context of neuroinflammation (27) and cytokine treatment (28). Earlier studies showed induction of both Syncytin-1 and inducible NO synthase (iNOS) in glial cells in the brains of MS patients, particularly in astrocytes (12, 29). Importantly, iNOS induced mitochondrial calcium flux thereby activating ATF-6 (30). The transcription factor, old astrocyte specifically induced substance (OASIS), is activated in response to ER stress by modulating expression of the Ig H chain-binding protein (BiP), thereby protecting astrocytes from ER stress (31). We hypothesized that in an inflammatory milieu mediated by increased Syncytin-1 levels in astrocytes, the expression of its receptors ASCT1 and ASCT2 might be modulated, possibly through ER stress-related mechanisms. The present studies revealed that Syncytin-1 induced several ER stress-associated molecules including OASIS and *GADD153/CHOP*, which in turn augmented iNOS expression in astrocytes. In this study, we describe a novel pathway for oligodendrocyte injury in which Syncytin-1 induced OASIS expression in astrocytes accompanied by production of NO and the transcription factor, early growth response 1 (Egr1), leading to the suppression of ASCT1 in astrocytes with ensuing adverse effects on oligodendrocyte proteins involved in myelin formation.

Materials and Methods

Human brain tissue and immunohistochemistry

Brain tissue (frontal white matter) was collected at autopsy as described previously (27). Control subjects included 19 patients: Alzheimer's disease ($n = 6$); HIV infection with encephalitis ($n = 4$) or gliosis ($n = 4$); cerebral arteriosclerosis ($n = 2$); anoxic encephalopathy ($n = 1$); normal brain pathology ($n = 2$). MS patients included 20 patients who had been classified as primary progressive ($n = 6$), secondary progressive ($n = 10$), and relapsing-remitting ($n = 4$) and had Estimated Disability Status Scale scores ranging from 7 to 9 before death. Frozen brain tissue from MS patients was obtained from the Multiple Sclerosis Patient Care and Research Clinic (Edmonton, Alberta, Canada) and the Neurovirology Laboratory Brain Bank (University of Calgary, Calgary, Alberta, Canada), as previously described (12, 32, 33). Histological sections of brain tissue with clear evidence of acute lesion formation and normal appearing white matter were used. Within limits of assessment, care was taken to isolate tissue that might have lesions. Paraffin-embedded sections from the above tissues were immunostained with Abs to ionized calcium-binding adaptor protein 1 (Iba-1; 1.0 μ g/ml; Wako), glial fibrillary acidic protein (GFAP; 1/2000; DakoCytomation), Syncytin-1 (8) (6A2B2; 1/1000), ASCT1 and ASCT2 (1/40; U.S. Biologicals), mouse anti-myelin basic protein (MBP; 1/1000; Sternberger Monoclonals), 2', 3'-cyclic nucleotide 3'-phosphodiesterase (CNP) (1/500; Chemicon International), iNOS, Egr1, *GADD153/CHOP*, BiP, and ERp57 (1/100; Santa Cruz Biotechnology), as previously described (33–35). All slides were examined with a Zeiss Axioskop 2 upright microscope and the Spot system (Diagnostic Instruments) to provide digital images.

Cell culture and reagents

Cell cultures (U937, HFA, U373, HEK293T) were maintained, as described (12). Oligodendrocytes were harvested and prepared from adult Sprague-Dawley rats. Briefly, brains from 6-mo-old rats were harvested and pooled. Cells were dissociated by trypsin digestion and isolated by Percoll gradient centrifugation as described (36). Cell isolates, consisting of oligodendrocytes, astrocytes, and microglia, were plated onto uncoated 25-cm² flasks. In contrast to astrocytes and microglia, adult oligodendrocytes are poorly adherent on uncoated substrate; floating cells were collected the following day and, when subjected to another round of differential adhesion, resulted in oligodendrocyte cultures of >95% purity. Purified oligodendrocytes were then plated onto Lab-Tek 16-well chamber slides (Nunc) or glass coverslips coated with 10 μ g/ml poly-L-ornithine (Sigma-Aldrich). Oligodendrocytes were cultured in MEM supplemented with 10% FBS, 20 μ g/ml gentamicin, and 0.1% dextrose. Mouse bone marrow-derived macrophages were prepared as described (37). Cells were treated with human or murine TNF- α , IL-1 β , IL-10 (R&D Systems), sodium nitroprusside (SNP; 100 nM; Axxora Life Science), benzylserine (Bachem), L-NAME (5.0 μ M; Sigma-Aldrich), or 50 ng/ml PMA (Sigma-Aldrich).

Pseudotyped viral infections

Pseudotyped virions expressing Syncytin-1 were generated by cotransfecting 293T cells with plasmids expressing firefly luciferase within an envelope-inactivated HIV-1 clone (pNL-Luc-E⁺) and the expression vector containing the full-length Syncytin-1 sequence (pCDNA-Syncytin-1) or pCDNA3.1 alone (8, 38). As a control, HIV-JRFL envelope (38) was used for pseudotype formation. Transduction of target cells by pseudotyped virus led to expression of luciferase, which was quantified in cells, lysed 48 h following infection, using the Luciferase Assay kit (BD Pharmingen). For experiments described in the study, 100- μ l supernatants were used for infection of target cells.

Small-interfering RNA (siRNA) and quantitative PCR

Human *Syncytin-1* gene (GenBank Accession ID: NM_014590) was amplified using the primers 5'-ATCTAAAGCTTGCCACCATGGCCCTCCCTTATC-3' and 5'-TGAGTACCGCGGACTGCTTCCTGCTGAA-3' and the PCR product was cloned into the *HindIII* and *SacII* sites (underlined) of pYFP-N1 (BD Clontech) to obtain Syncytin-1-yellow fluorescent protein (YFP) fusion construct (2.5 μ g), which was transfected into HEK293T cells with or without siRNA (200 pM). siRNA duplexes were synthesized by Invitrogen Life Technologies ("Stealth siRNA"). The sequences of the duplexes used were as follows: enhanced YFP sense, ACG GCA AGC UGA CCC UGA AGU UCA U; enhanced YFP antisense, AUG AAC UUC AGG GUC AGC UUG CCG U; Syncytin-1 sense, GCU AGG UGC ACU AGG UAC UGG CAU U; Syncytin-1 antisense, AAU GCC AGU ACC UAG UGC ACC UAG C. Semiquantitative real-time RT-PCR was performed by monitoring in real time the increase of fluorescence of the SYBR Green dye (Molecular Probes) on the iCycler (Bio-Rad) with normalization to GAPDH or β -actin (33) using primers described in Table 1.

Transgenic (Tg) mice and genotyping

(5'-AAGGAATAAAGCGGCCGCATGGCCCTCCCTTATCATATCTTT C-3') and (5'-AAAAGGAAAAGCGGCCGCCTAACTGCTTCCTGCTG-3') primers with *NotI* tags (underlined) and a silent mismatch (C, italicized) in the sense sequence were used to PCR amplify Syncytin-1 from pHCM-Vph74 (8), resulting in a 1.6-kb PCR product, which along with a pFGH vector bearing the *GFAP* promoter (39) were digested with *NotI*. The PCR product was cloned into pFGH to obtain pFGH-Syncytin-1, which was digested with *EcoRI* to produce a fragment of 5 kbp that was used for pronuclear microinjection. PCR genotyping from tail biopsies was performed to detect the transgene (267 bp) using Syncytin-1 primers 5'-AC CCATACCTCAAACCTCACCTG-3' and 5'-CTTTTGTTCGGGGCTT AGATA-3'. For the purposes of the present study, 12-wk-old F₅ Tg mice with wild-type (Wt) littermate controls ($n = 6$ /group) were used. All studies and procedures adopted University of Calgary Animal Care Committee guidelines.

Western blot analysis

Ten micrograms of protein was separated by 10% SDS-polyacrylamide at 120 V for 2 h. Proteins were transferred overnight at 4°C onto nitrocellulose membranes, followed by blocking with 10% skimmed milk to prevent nonspecific binding. Western blot analysis was performed using the mAb 6A2B2, which detects Syncytin-1 (8, 12), OASIS (31), actin-HRP, and iNOS (1/100; Santa Cruz Biotechnology); *GADD153/CHOP* and BiP were detected by Abs, mentioned above.

Table 1. List of oligonucleotide PCR primers used in the study

Primer	Sequence
PLP	5'-CTTCCCTGGTGGCCACTGGATTGT-3' and 5'-CCGCAGATGGTGGTCTTGTAGTCG-3'
MOG	5'-CCTCTCCCTTCTCCTCCTTC-3' and 5'-AGAGTCAGCACACCGGGGTT-3'
CNPase	5'-CTACCCTCCACGAGTGCAAGACGCT-3' and 5'-AGTCTAGTCGCCACGCTGTCTTGGG-3'
OASIS	5'-CAACGCACCCCACTCACAGACACC-3' and 5'-GGAGCAGCAAAGCCCGCACTAACT
GADD153	5'-AACCAGCAGAGGTCACAAGC-3' and 5'-AGCCGTTCATTCTCTTCAGC-3'
CGT	5'-TTATCGGAAATTCACAAGGAT-3' and 5'-TGGCGAAGAATGTAGTCTATC-3'
IFN- α	5'-GTGATCTCCTGAGACCCAC-3' and 5'-GGTAGAGTTCGGTGCAGAAT
PERK	5'-AAGTAGATGACTGCAATTACGCTATCAA-3' and 5'-TTTAACCTTCCCGATTACCTTCTC-3'
ERp57	5'-TCAAGGGTTTCTCATCTACTTC-3' and 5'-TTAATTCACGGCCACCTTCAT-3'
BiP	5'-TCATCGGACGCACTTGGAA-3' and 5'-CAACCACCTTGAATGGCAAGA-3'
hASCT1	5'-TCCCATAGGCACTGAGATAGAAG-3' and 5'-CAAGGAACATGATCCACAGGTA-3'
hASCT2	5'-CCTGCTGGGGGTGCTCTTTGGACA-3' and 5'-TTGAGTTGGGGACATGAGTGAGAA-3'
mASCT1	5'-CCTGGCTTGATGATGAACGC-3' and 5'-CTGGTGTGCTCACCCTGTC-3'
mASCT2	5'-CCATCGGCGCCACGGTCAACAT-3' and 5'-GTGGCGAGGGGAGTGGATTGAGA-3'
Egr1	5'-AGCAGCACCTTCAACCCTCA-3' and 5'-CAGCACCTTCTCGTTGTTTCA-3'
Egr3	5'-TTGGGAAAGTTCGCCTTCG-3' and 5'-ATGATGTTGCTCCTGGCACC-3'
Egr4	5'-CCCCGCTGGATGCCCTTTTC-3' and 5'-ACTCTCCGCGTCCGCTACTCC-3'
Syncyntin-1	5'-TGCCCCATCGTATAGGAGTCT-3' and 5'-CATGTACCCGGGTGAGTTGG-3'
iNOS	5'-CAAAGGCTGTGAGTCTGCAC-3' and 5'-ACTTTGATCAGAAGCTGTCCC-3'

Transfection

Five micrograms of the constructs OASIS-FLAG (31) and pVGW427 (40) were transfected into HFA or HEK293T cells using Transfectin Lipid reagent (Bio-Rad) or Lipofectamine 2000 (Invitrogen Life Technologies), respectively.

Syncyntin-1 overexpression and microarray analysis

Astrocytes were infected with a Sindbis virus-derived vector expressing Syncyntin-1 (SINrep5-Syncyntin-1), enhanced GFP (EGFP; SINrep5-EGFP), or mock infected as described (12) and immunostained for Syncyntin-1 expression using 6A2B2. Total cellular RNA from infected astrocytes was hybridized using Affymetrix Human Genome U133 Plus 2 arrays. Expression values were calculated using GeneChip Operating Software (Affymetrix). The experimental approach and data acquisition were performed in accordance with Minimum Information about a Microarray Experiment requirements.

Quantitative immunofluorescence

After fixation in 4% paraformaldehyde, cells were permeabilized by PBS containing 0.1% Triton X-100. Cells were then blocked with Li-Cor Odyssey blocking buffer and primary Abs were added at a concentration of 1/500 and incubated overnight at 4°C. Following washes with PBS containing 0.1% Tween 20, secondary Abs (IRDye 800 conjugated or Alexa Fluor conjugated) were added at a concentration of 1/200 and incubated 1 h at room temperature, after which cells were washed. The plate was then scanned using the Odyssey Infrared Imaging System (600 and 700 nm, 169 μ m resolution, 2 mm offset, and intensity setting of 5 for both channels). Label intensity was measured by densitometric analysis of the wells.

Cell counts

Fluorescently (Alexa 488; Molecular Probes/Invitrogen Life Technologies)-labeled cells were counted (10 fields) from a total area of 23,760 μ m²

using a $\times 10$ objective on a Zeiss Axioskop microscope and expressed as a percentage.

Neurobehavioral studies

Behavioral tests were conducted as described (41). The horizontal bar test involved a test of coordination and forelimb strength using a horizontal bar that was 0.2 cm thick, 38 cm long, held 49 cm above a bench (41). The static rod test involved a test of coordination using five rods each 60 cm long and of varying thickness (diameter) (rod 1: 35 mm; rod 2: 28 mm; rod 3: 22 mm; rod 4: 15 mm; and rod 5: 9 mm). These rods were bolted to the edge of a bench such that the rods horizontally protruded their full 60-cm length into space. A mouse was placed at the exposed end of the widest rod and the time taken to orient 180 degrees from the starting position and the time taken to travel to the other end were noted (41). A test of muscle strength and seeking behavior were determined using the inverted screen test. The inverted screen was a 43-cm square inch of wire mesh consisting of 12-mm squares of 1-mm diameter wire and surrounded by a 4-cm deep wooden beading (41). We modified the inverted screen test by placing the mouse at a point that was equidistant from the edges of the screen and the stop clock was started once the screen was inverted and measured the time taken to reach the edge of the inverted screen, as a measure of curiosity and seeking behavior.

Statistical analyses

Statistical tests were performed using GraphPad InStat version 3.01 software including the Mann-Whitney *U* or unpaired *t* tests and, when multiple treatments were used, a one-way ANOVA with the Tukey-Kramer multiple comparisons test.

Results

ASCT1 expression is selectively diminished in MS brain tissue

Loss of amino acid transporter expression from astrocytes in neurodegenerative diseases results in glutamate-mediated excitotoxic damage and death of neurons (42). Indeed, decreased levels of glutamate transporters have also been described in MS lesions (5). To investigate the expression of other amino acid transporter proteins serving as Syncyntin-1 receptors in the nervous system, we examined ASCT1 and ASCT2 expression. We analyzed tissue sections from MS and non-MS control brains. Demyelinated (D) lesions from MS patient brains (Fig. 1*Aii*) stained less intensely with Luxol fast blue and H&E compared with a non-MS control brain section (Fig. 1*Ai*). Serial sections of demyelinated regions in the brains of MS patients demonstrated a marked increase in Syncyntin-1 immunoreactivity (Fig. 1*Aiv*), particularly in astrocytes expressing GFAP (Fig. 1*Aiii*; Syncyntin-1: blue; astrocytes: brown; *inset*, GFAP-positive astrocyte). Similar sections revealed intense ASCT1 immunoreactivity in the white matter of non-MS brain sections (Fig. 1*Av*) on glial cells including both astrocytic (Fig. 1*A*, *inset*, arrow) and monocytoic cells (data not shown) but conversely, ASCT1 expression was reduced in MS sections (Fig. 1*Avi*, arrow indicates an ASCT1-positive cell). Expression of ASCT2, however, revealed no differences in immunoreactivity between the white matter of non-MS (Fig. 1*Avii*) and MS patients (Fig. 1*Aviii*). ASCT2 expression was predominantly expressed on activated microglia (Fig. 1*Aviii*, arrow). Corroborating these findings was the observation that ASCT1 transcript levels were significantly diminished in MS brain white matter relative to non-MS brains (Fig. 1*B*). Conversely, ASCT2 transcript levels did not differ in white matter between clinical groups. ASCT1 transcript levels did not differ in (frontal) cortex between non-MS and MS patients, while ASCT2 was not detected in the cortex (Fig. 1*B*). Thus, ASCT1 was selectively down-regulated in astrocytes of white matter tissue from MS patients in conjunction with increased expression of Syncyntin-1.

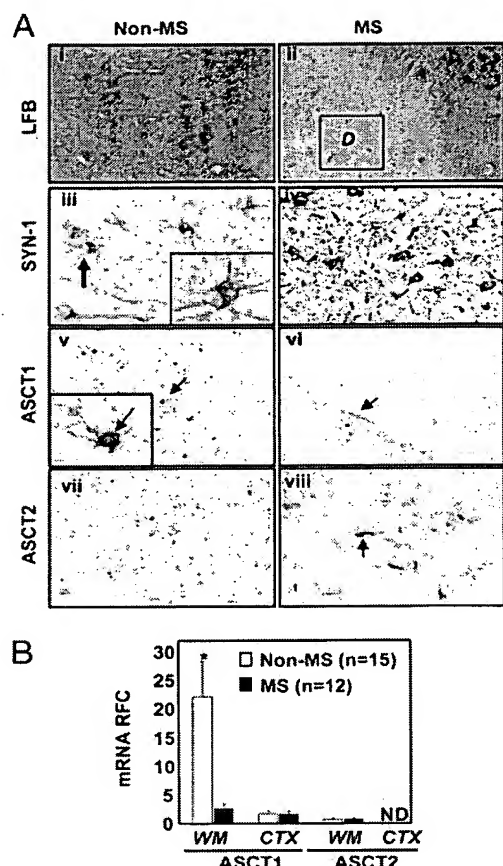


FIGURE 1. ASCT1 expression is suppressed in MS. *A*, Demyelinated (D) lesions from chronic MS patient brains (*ii*) stained less intensely with Luxol fast blue, H&E compared with non-MS controls (*i*). MS brains showed marked increase in Syncytin-1 immunoreactivity (*iv*), particularly in GFAP-positive astrocytes (*iii*, inset). ASCT1 expression was detected in non-MS brains (*v*), particularly in astrocytes (*v*, inset) compared with minimal immunoreactivity in acute MS white matter (*vi*). ASCT2 expression did not differ between MS (*viii*) and non-MS controls (*vii*). MS brains showed diminished ASCT1 mRNA in white matter (WM) but not in the frontal cortex (CTX) compared with non-MS controls. ASCT2 mRNA was undetectable in the CTX and did not differ between groups in the WM (*B*). (Original magnification, $\times 50$ (*A*, *i* and *ii*); $\times 400$ (*A*, *iii*–*viii*) (inset, $\times 1000$)) (***, $p < 0.001$; *, $p < 0.05$).

Inflammation increases Syncytin-1 expression while Syncytin-1 diminishes ASCT1 levels in astrocytes

The envelope proteins of the HERV-W family induce several proinflammatory molecules (12, 43). We have also demonstrated previously that Syncytin-1 expression in brain-derived cells is induced by different mitogens (12). Because *HERV-R* gene expression is induced by TNF- α and IL-1 β (28), we determined whether inflammation might induce Syncytin-1. Examination of Syncytin-1 mRNA in astrocytes treated with proinflammatory molecules revealed its induction by TNF- α in a concentration-dependent manner (Fig. 2*A*). Because ASCT1 down-regulation was observed in astrocytes of MS lesions, which also exhibited enhanced Syncytin-1 expression, we confirmed this in vivo result in an ex vivo system and determined the mechanism by which Syncytin-1-mediated suppression of its receptors in astrocytes. Cell cultures of purified brain-derived astrocytes, neurons, and monocyte-derived macrophages (MDM) were established. Expression of ASCT2 has been previously demonstrated in human fetal astrocytes (44) and

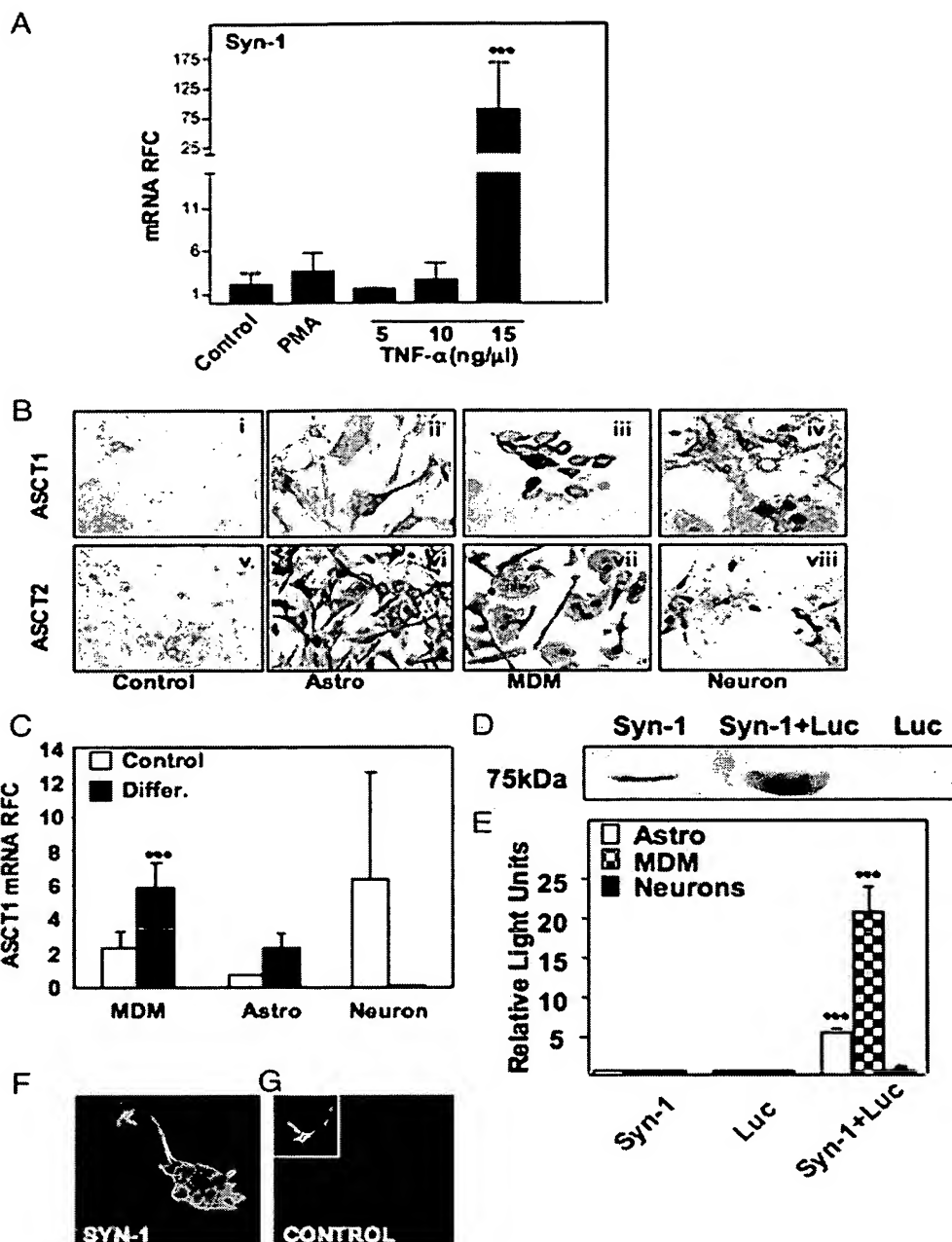
placenta (45). However, the evidence for ASCT1 and ASCT2 protein expression in the brain-derived cells is sparse. Indeed, immunocytochemical detection of ASCT1 and ASCT2 revealed abundant expression in cultured human fetal astrocytes (Astro, Fig. 2*B*, *ii* and *vi*), MDM (Fig. 2*B*, *iii* and *vii*), and neurons (Fig. 2*B*, *iv* and *viii*) compared with the controls (Fig. 2*B*, *i* and *v*) suggesting ubiquitous expression in these brain-derived cells. To investigate the effects of mitogen/cellular differentiation on individual receptor expression, we examined transcript levels of each gene in primary human fetal astrocytes, MDMs, and neuronal (LAN-2) cells. PMA treatment disclosed significantly increased ASCT1 mRNA expression in MDMs (Fig. 2*C*), whereas no changes were seen with respect to ASCT1 and ASCT2 in other cell types (Fig. 2*C* and data not shown).

Syncytin-1 is able to form pseudotyped virus particles (4, 46, 47), but its cell tropism in the nervous system was unknown. We investigated whether Syncytin-1 was functional in the above cell types by using a pseudotyped virus assay. Supernatants from cells transfected with only pCDNA-Syncytin-1 or cotransfected with pNL-Luc-E⁺R⁺ exhibited Syncytin-1 immunoreactivity suggesting that Syncytin-1-pseudotyped virions were released into the culture medium (Fig. 2*D*). Infection with the pseudotyped viruses revealed that human MDMs and astrocytes but not human neurons were permissive to infection (Fig. 2*E*). Moreover, a feline lymphocyte line (MYA-1) was not permissive to the pseudotyped viruses (data not shown). Because Syncytin-1 was functional in these latter studies, we overexpressed Syncytin-1 in human fetal astrocytes by transduction of a Syncytin-1-expressing Sindbis virus (12), which revealed syncytia formation in astrocytes (Fig. 2*F*), confirmed by glial fibrillary acidic protein (GFAP) positivity (Fig. 2*G*, inset). cDNA microarray analysis was subsequently performed of astrocytic cells transduced with the Sindbis virus-derived vector expressing Syncytin-1. The cDNA expression profile revealed several genes that were also affected in acute lesions from brains of MS patients in an earlier study (48) (Table II). Importantly, the two receptors for Syncytin-1, ASCT1 and ASCT2, were markedly suppressed in astrocytes overexpressing Syncytin-1 (Table III). Moreover, several genes involved in MS, particularly an MS lesion-specific transcript and a disintegrin and metalloproteinase (ADAM)-10 in addition to multiple genes involved in ER stress, myelin synthesis, and immune response, previously uncharacterized in MS lesions, were modulated in astrocytes expressing Syncytin-1 (Table III). These results suggested that TNF- α induces Syncytin-1 expression in astrocytes, whose enhanced levels contribute to diminished expression of its receptors in astrocytes. Nonetheless, the mechanism(s) by which Syncytin-1 contributed to suppression of its receptors remained uncertain.

ER chaperones are up-regulated in astrocytes overexpressing Syncytin-1

As several retroviral proteins cause neuropathogenic effects through aberrant protein expression (24, 26, 49), we investigated whether the increased levels of Syncytin-1 in the brains of MS patients (12) contributed to an integrated response leading to cellular pathology. Human fetal astrocytes, which overexpressed Syncytin-1, demonstrated significantly increased transcript levels of GADD153/CHOP, BiP, PERK, ERp57, and OASIS (Fig. 3*A*), but not in astrocytes transduced by an EGFP-expressing virus (control) ($p < 0.05$). However, ER chaperone genes were not induced in MDMs overexpressing Syncytin-1 relative to EGFP-expressing MDMs (Fig. 3*B*). Indeed, astrocytes transduced with an HIV-1 envelope-expressing construct also did not show induction of the same ER chaperone genes (data not shown). To determine the

FIGURE 2. Inflammation drives Syncytin-1 expression. Syncytin-1 expression was significantly induced in astrocytes treated with 15 ng/ml TNF- α compared with untreated control (A). B, Immunostaining of human fetal astrocytes (ii and vi), macrophages (iii and vii), and primary neurons (iv and viii) revealed the expression of ASCT1 and ASCT2, compared with control cells for which the primary Abs were omitted (i and v). Relative quantification of ASCT1 and ASCT2 was performed using cDNA prepared from MDM, astrocytes (U373), and neurons (LAN-2). ASCT1 mRNA expression was significantly increased in differentiated MDMs (C). However, there were no significant differences in the levels of ASCT2 expression among the cell lines examined. Syncytin-1 immunoreactivity in supernatants from HEK293T cells transfected with pCDNA-Syncytin-1 (Syn-1) was enhanced by cotransfection with pNL-Luc-E⁻R⁻ (Luc) compared with pNL-Luc-E⁻R⁻ alone (D). MDMs and astrocytes but not neurons were permissive to infection by the pseudotyped virus (E). Syncytin-1 (SYN-1) expressing human fetal astrocytes (F) but not controls (G) exhibit syncytia formation ((inset, GFAP-positive astrocytes) (original magnification, $\times 200$ (B, F and G)) (***, $p < 0.001$).



comparative transcript levels of ER chaperone genes in Syncytin-1-expressing astrocytes and brains of MS patients, we examined ER chaperone gene induction in brain white matter from MS ($n = 15$) and non-MS controls ($n = 12$). The expression profile of ER chaperones observed in Syncytin-1-expressing astrocytes closely resembled transcript abundance in brain white matter tissue of MS patients relative to non-MS controls (Fig. 3C). In particular, the induction of OASIS was highly significant ($p < 0.001$) in MS brains compared with non-MS controls. To determine the cell types expressing ER chaperones, we analyzed tissue sections from MS and non-MS control brain sections. Serial sections from the same lesions showed increased GADD153/CHOP (Fig. 3Dii) and BiP (Fig. 3Div) expression compared with non-MS control brain (Fig. 3D, i and iii, respectively). GADD153/CHOP expression was increased in several cell types, but most prominently in astrocytes, colocalized with

GFAP immunoreactivity (Fig. 3Dii, inset) (GADD153/CHOP: blue; GFAP: brown) in brains of MS patients. BiP expression was found in several cell types including astrocytes (Fig. 3Div, arrow) and macrophages (Fig. 3Div, arrowhead) in the white matter of MS demyelinating lesions compared with non-MS controls (Fig. 3Diii), whereas ERp57 (data not shown) was minimally expressed. However, PERK, a key component of the ER stress pathway, was not detected by immunohistochemistry, which might be a limitation of the Ab used in this study, rather than its absence, as transcript levels were detected (Fig. 3C). Considering the recent evidence showing ER stress in oligodendrocytes (15) and induction of GADD153/CHOP by retroviral infections leading to oligodendropathy (26), we expected to see ER stress proteins in these myelin-producing cells. However, the acute demyelinating lesions examined in the present study did not reveal any GADD153/CHOP-immunopositive

Table II. Genes increased and decreased in Syncytin-1-expressing astrocytes, showing a similar profile in lesions from MS patients

	Gene Name	Function	Fold Change	GenBank ID
Increased	<i>CEBPG</i>	CCAAT/enhancer-binding protein (C/EBP), γ	2.75	BE622659
	<i>TNFRSF6</i>	Tumor necrosis factor receptor superfamily, member 6	2.433333	NM_000043
	<i>RCN1</i>	Reticulocalbin 1, EF-hand calcium-binding domain	1.607143	NM_002901
Decreased	<i>GAD2</i>	Glutamate decarboxylase 2 (pancreatic islets and brain, 65 kDa)	0.961538	BQ128302
	<i>SPOCK2</i>	Sparc/osteonectin, cwcv and kazal-like domains proteoglycan (testican) 2	0.955752	NM_014767
	<i>SST</i>	Somatostatin	0.913462	NM_001048
	<i>NEUROD2</i>	Neurogenic differentiation 2	0.875	AB021742
	<i>PVALB</i>	Parvalbumin	0.869565	NM_002854
	<i>CCNI</i>	Cyclin 1	0.854701	BG530368
	<i>SCD</i>	Stearoyl-CoA desaturase (δ -9-desaturase)	0.842105	BC005807
	<i>RPS4Y1</i>	Ribosomal protein S4, Y-linked 1	0.827586	NM_001008
	<i>RAB5B</i>	RAB5B, member RAS oncogene family	0.820896	AF267863
	<i>PEG3</i>	Paternally expressed 3	0.817308	AF208967
	<i>HTR7</i>	5-Hydroxytryptamine (serotonin) receptor 7 (adenylate cyclase-coupled)	0.706767	NM_019859
	<i>ACAT2</i>	Acetyl-coenzyme A acetyltransferase 2 (acetoacetyl coenzyme A thiolase)	0.704403	BC000408
	<i>HSPA6</i>	Heat shock 70-kDa protein 6 (HSP70B')	0.7	NM_002155
	<i>AQP11</i>	Aquaporin 11	0.680272	AI886656
	<i>MAP1D</i>	Methionine aminopeptidase 1D	0.675676	AA779679
	<i>KIF5A</i>	Kinesin family member 5A	0.666667	AF063608
	<i>CNP</i>	2',3'-Cyclic nucleotide 3' phosphodiesterase	0.619792	AK098048
	<i>EXTL3</i>	Exostos (multiple)-like3	0.619355	BC006363

oligodendrocytes. Thus, multiple ER chaperones including OASIS and GADD153/CHOP were overexpressed in brain glia of MS patients, suggesting a role for ER stress in the pathogenesis of MS.

OASIS contributes to inflammation and diminished ASCT1 expression in astrocytes

As several retroviral proteins, including Syncytin-1, induce free radicals in glia (12), we hypothesized that Syncytin-1 might influence expression and function of its putative receptors, ASCT1 and ASCT2, in the brain (50), perhaps through regulation by free radical produc-

tion and removal, similar to the related transporter, xCT (13, 51, 52), whose expression in microglia potentiates neuronal injury in Alzheimer's disease (53). Corresponding to increased transcript levels of OASIS in MS brain lesions (Fig. 3C), Western blot analysis (Fig. 4A, inset) of non-MS ($n = 6$) and MS ($n = 6$) patient brain lysates revealed a significant increase in OASIS immunoreactivity in the brain (Fig. 4A). Because OASIS induces the transcription of target genes by acting on the ER stress responsive element and cAMP responsive element (54), we hypothesized that OASIS might trigger iNOS, perhaps through the cAMP responsive element within the iNOS

Table III. Gene profile in Syncytin-1-expressing astrocytes showing up-regulation and down-regulation of immune response, myelin-related, and ER stress genes

	Gene Name	Function	Fold Change	GenBank ID
ER stress response				
	<i>STCH</i>	Stress 70 protein chaperone, microsome-associated, 60 kDa	8.3	AI718418
	<i>HSPH1</i>	Heat shock 105-kDa/110-kDa protein 1	5.285714	NM_006644
	<i>LONP</i>	Peroxisomal lon protease	3.32	AV700132
	<i>FLJ23560</i>	Hypothetical protein FLJ23560	2.564103	NM_024685
	<i>FLJ14281</i>	Hypothetical protein FLJ14281	2.375	NM_024920
	<i>HSPD1</i>	Heat shock 60-kDa protein 1 (chaperonin)	2.236842	NM_002156
	<i>SERP1</i>	Stress-associated endoplasmic reticulum protein 1	2.261905	AL136807
	<i>HERPUD1</i>	Homocysteine-inducible, endoplasmic reticulum stress-inducible, ubiquitin-like domain member 1	0.735294	BC015447
	<i>HSPA5BP1</i>	Heat shock 70-kDa protein 5 (glucose-regulated protein, 78 kDa) binding protein 1	0.710692	AB046803
	<i>GADD45B</i>	Growth arrest and DNA-damage-inducible, β	0.702899	AV658684
Syncytin-1		HERV-W envelope glycoprotein	3.114286	AC000064
<i>SLC1A4 (ASCT1)</i>		Solute carrier family 1 (glutamate/neutral amino acid transporter), member 4	0.677632	W72527
<i>SLC1A5 (ASCT2)</i>		Solute carrier family 1 (neutral amino acid transporter), member 5	0.693431	AF105230
MS related				
	<i>ADAM10</i>	A disintegrin and metalloproteinase domain 10	8.25	N51370
<i>MS lesion</i>		MS lesion transcript	6.818182	N73682
	<i>CMT4B2</i>	Charcot-Marie-Tooth neuropathy 4B2 (autosomal recessive, with myelin outfolding)	4.478261	AK022478
	<i>MBP</i>	Myelin basic protein	0.734266	NM_002385
	<i>MAG</i>	Myelin-associated glycoprotein	0.685039	X98405
Immune response				
	<i>SOC5</i>	Suppressor of cytokine signaling 5	5.375	NM_014011
	<i>STAT1</i>	Signal transducer and activator of transcription 1, 91 kDa	2.121951	NM_007315
	<i>TLR4</i>	Toll-like receptor 4	2.05	NM_003266
	<i>TLR9</i>	Toll-like receptor 9	0.731707	AB045180
	<i>IL23A</i>	Interleukin 23, α subunit p19	0.724138	NM_016584
	<i>OLIG1</i>	Oligodendrocyte transcription factor 1	0.722222	AL355743
	<i>TLR8</i>	Toll-like receptor 8	0.606838	NM_016610
	<i>OAS1</i>	2',5'-oligoadenylate synthetase 1, 40/46 kDa	0.413408	NM_002534

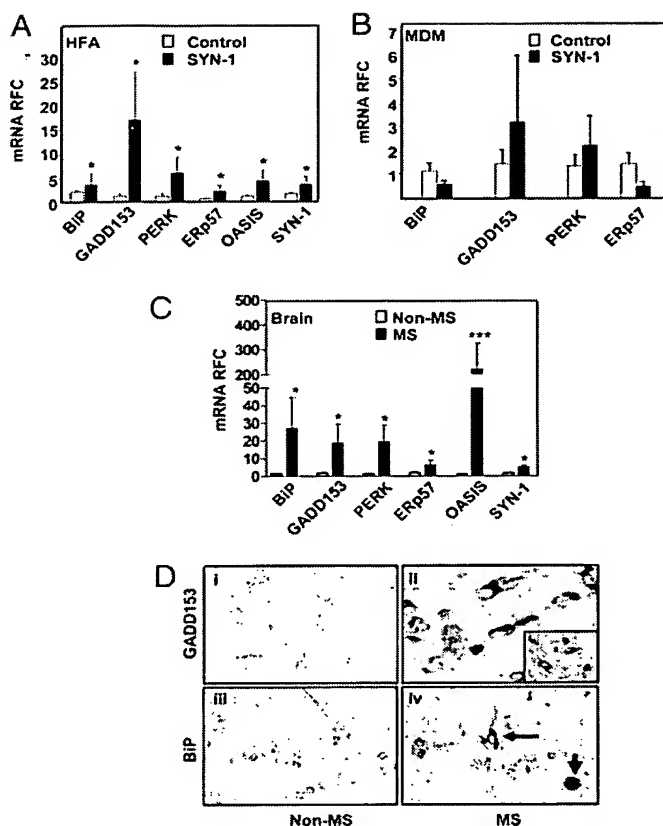


FIGURE 3. ER chaperones are up-regulated in astrocytes overexpressing Syncytin-1. Syncytin-1 (SYN-1) expressing human fetal astrocytes (HFA) but not controls exhibit increase in mRNA relative fold change (RFC) in mRNA of Syncytin-1 and ER chaperone genes, BiP, GADD153/CHOP, PERK, ERp57, and OASIS compared with controls (A). MDMs expressing Syncytin-1 did not show any increase in the transcript levels of ER chaperone genes (B). Increased transcript levels of Syncytin-1, BiP, GADD153/CHOP, PERK, ERp57, and OASIS were evident in the white matter tissue of MS ($n = 12$) brains relative to non-MS controls ($n = 11$) (C). D, MS brains showed marked increase in GADD153/CHOP immunoreactivity (ii), particularly in GFAP-positive astrocytes (ii, inset) and BiP (iv) expression compared with non-MS controls (i and iii). (Original magnification, $\times 400$ (i–iv); inset, $\times 1000$) (***, $p < 0.001$; *, $p < 0.05$).

promoter (55). Indeed, increased expression of iNOS in OASIS-transfected astrocytes was evident compared with the control (empty vector) (Fig. 4B). Based on these results, we transfected astrocytes with an OASIS expression vector. Overexpression of OASIS resulted in down-regulation of Syncytin-1 receptor, ASCT1, but not ASCT2, with the latter gene demonstrating increased expression (Fig. 4C). Interestingly, soluble Syncytin-1 also induced OASIS transcription in astrocytes, which was inhibited by a mAb to Syncytin-1 (data not shown). Thus, Syncytin-1-induced OASIS expression, resulting in iNOS induction, which was associated with down-regulation of ASCT1 expression, but not ASCT2, thereby recapitulating the present observations in MS brain lesions.

Syncytin-1 directly contributes to ASCT1 suppression

Retroviral envelope glycoproteins including Syncytin-1 mediate immune responses (12, 43) and receptor expression (45). To examine whether the down-regulation of ASCT1 in our model was directly due to enhanced Syncytin-1 expression, we constructed a vector that expressed Syncytin-1-YFP fusion protein. Syncytin-1 was cloned into the pYFP vector for subsequent expression in

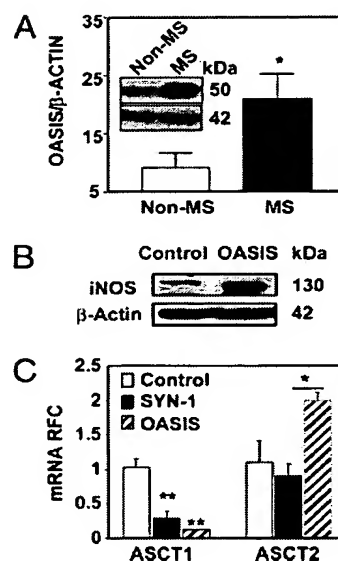


FIGURE 4. OASIS contributes to inflammation and diminished ASCT1 expression in astrocytes. OASIS immunoreactivity (50 kDa) was increased in MS brains compared with non-MS controls (A, inset). Graphic analysis of OASIS immunoreactivity relative to β -actin revealed a significant increase in MS brains (B). iNOS immunoreactivity was increased in astrocytes overexpressing OASIS relative to the empty vector (Control) (C). Astrocytes overexpressing OASIS or Syncytin-1 (SYN-1) down-regulated ASCT1, but not ASCT2 compared with empty pcDNA 3.1 vector (Control) (C) (**, $p < 0.01$; *, $p < 0.05$).

various target cells. Transfected cells expressed the fusion protein with minimal cell death for at least 72 h (Fig. 5A, i and ii). Human fetal astrocytes, which expressed Syncytin-1-YFP (Fig. 5Ai), were transfected with siRNAs directed to the surface unit of Syncytin-1 (Fig. 5Aiii) and expression of YFP was monitored as an indication of Syncytin-1 knockdown. Cells transfected with Syncytin-1-YFP, with (Fig. 5A, iii and iv) or without (Fig. 5A, i and ii) siRNA treatment, were viable but siRNA treatment abrogated Syncytin-1 expression, indicated by absence of YFP expression (Fig. 5Aiii). Having confirmed knockdown of Syncytin-1 by monitoring expression of YFP by confocal microscopy of live cells (Fig. 5A, i and iii) and preserved cellular viability by bright field microscopy (Fig. 5A, ii and iv) for 72 h, we proceeded to confirm whether Syncytin-1 transcripts were similarly inhibited by siRNA against Syncytin-1. Syncytin-1-YFP expression was correlated with high transcript levels of Syncytin-1 in astrocytes relative to mock-transfected control cells (Fig. 5B). siRNA directed to Syncytin-1 suppressed transcript levels of Syncytin-1 in HFA (Fig. 5B) and HEK293T cells (data not shown). Because siRNA-mediated knockdown of Syncytin-1 was optimized, we tested whether Syncytin-1 influenced the expression of its cognate receptors. Indeed, astrocytes that expressed Syncytin-1 displayed significantly lower levels of ASCT1 but not that of another amino acid transporter, EAAT1 (Fig. 5C). However, when these cells were subsequently treated with siRNA to block Syncytin-1, the transcript level of ASCT1 was restored (Fig. 5C). These results indicated that the down-regulation of ASCT1 in astrocytes is a consequence of enhanced Syncytin-1 expression, which was consistent with observations made in the white matter lesions of MS patients.

Syncytin-1 impairs expression of myelin proteins

Oligodendrocyte injury and death might represent an early neuropathological feature of MS, in advance of infiltrating inflammatory

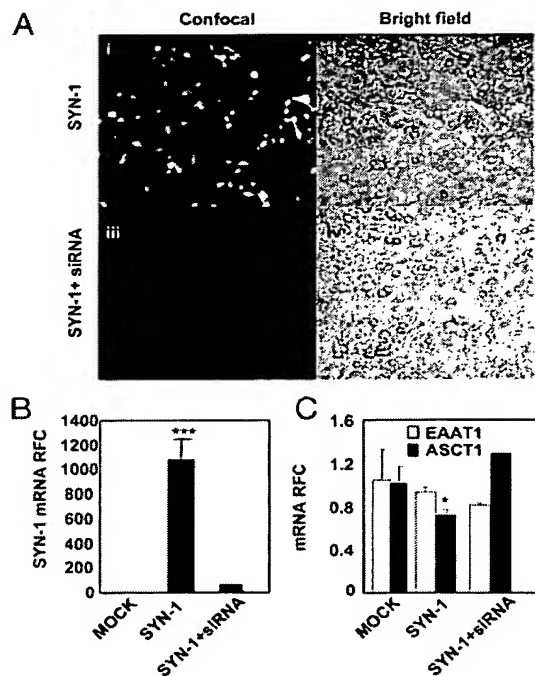


FIGURE 5. Synctin-1 down-regulates ASCT1. *A*, Confocal (*i* and *iii*) and bright-field microscopy (*ii* and *iv*) images of cells expressing Synctin-1 (SYN-1) (*i*) together with siRNA against Synctin-1 (SYN-1 + siRNA) showed reduced expression of Synctin-1 (*iii*). RT-PCR confirmed Synctin-1 knockdown by Synctin-1-directed siRNA (*B*). Synctin-1 expression reduced the ASCT1 transcript level, which was significantly reversed by siRNA-mediated knockdown of Synctin-1 (*C*). Under similar conditions, expression of another amino acid transporter, EAAT1 was not altered (*C*) (***, $p < 0.001$; *, $p < 0.05$).

cells (56), but it is also a cardinal feature of established MS lesions (57). In our earlier study, we used other oligodendrocyte markers such as adenomatous polyposis coli and GSTpi, revealing that Synctin-1 mediated cell death through an uncertain mechanism (12). To determine whether a direct cause-and-effect relationship existed between expression of Synctin-1 in astrocytes and expression of myelin proteins, we examined the effects of supernatants from astrocytes overexpressing Synctin-1 on an early myelination marker, CNP, and a late myelination marker, MBP, both of which are present in the present oligodendrocyte cultures. The cell culture protocol was a modification of procedures adopted to isolate mouse oligodendrocytes and we have been successful in using this culture system in earlier studies (12, 58). Supernatants from Synctin-1-transfected astrocytes reduced the number of CNP-positive oligodendrocytes (Fig. 6*Aii*). However, siRNA-mediated knockdown of Synctin-1 in astrocytes markedly reversed these adverse effects, restoring CNP immunoreactivity (Fig. 6*Aiii*) to control levels (Fig. 6*Ai*). siRNA-mediated inhibition of Synctin-1 expression restored the total number of CNP-positive oligodendrocytes, which was reduced by Synctin-1 expression in astrocytes (Fig. 6*B*). Immunofluorescence levels of CNP-expressing oligodendrocytes (Fig. 6*C*), which were reduced by Synctin-1-mediated toxicity, were also rescued by siRNA-mediated inhibition of Synctin-1 expression in astrocytes but there was no effect of Synctin-1 on MBP immunofluorescence (Fig. 6*C*). Because our observations indicated a reduction in expression of ASCT1 in MS brain white matter (Fig. 1) and in astrocytes overexpressing Synctin-1 (Fig. 4 and Table III), we hypothesized that inhibition of ASCT transporters may adversely affect astrocyte function. Supernatants from astrocytes treated with benzylserine, an inhibitor of ASCT transporters (59), were found to activate caspase-3 in rat oligodendrocytes in a concentration-dependent manner (Fig. 6*D*). Indeed, similar

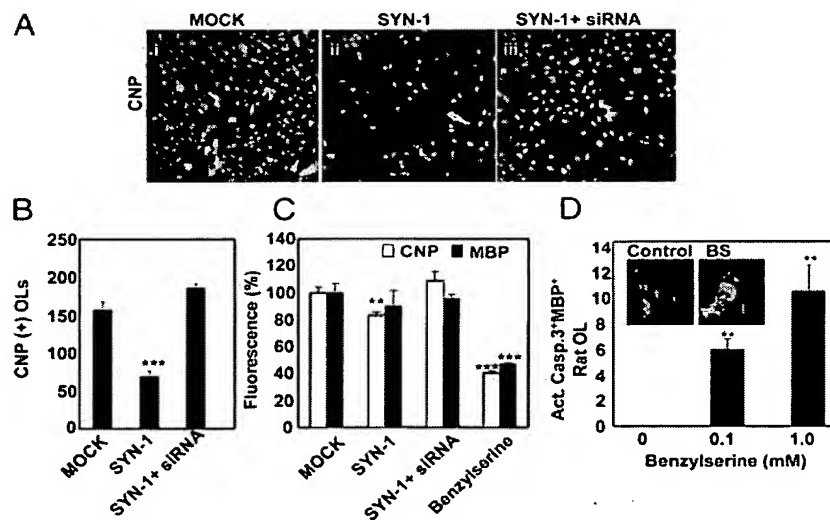


FIGURE 6. Synctin-1 diminishes oligodendrocyte viability. *A*, Oligodendrocytes treated with supernatants from mock (*i*), Synctin-1 (SYN-1) overexpressing (*ii*), and Synctin-1 overexpressing with anti-Synctin-1 siRNA transduction (*iii*) human fetal astrocytes revealed that the supernatants from Synctin-1-overexpressing astrocytes were cytotoxic to oligodendrocytes (*ii*). Spontaneous death of oligodendrocytes in cultures ranged from 1.2 to 2.5%. siRNA-mediated knockdown of Synctin-1 reversed the toxic effects of Synctin-1-expressing astrocyte supernatants as shown by counts of the number of CNP-positive oligodendrocytes (*B*) as well as quantitative analysis of immunofluorescence depicted as a percent of CNP immunoreactivity (*C*). Immunoreactivity of MBP was not affected by various treatments (*C*). Supernatants from human fetal astrocytes treated with 1 mM benzylserine decreased oligodendrocyte viability as demonstrated by significantly low levels of CNP and MBP immunoreactivity (*C*). Human fetal astrocytes (HFA) were treated with benzylserine dissolved in DMSO or medium containing similar amounts of DMSO. A total of 100 μ l of supernatant from HFA was added to rat oligodendrocytes cultured on a chamber slide and incubated for 24 h at 37°C. Oligodendrocytes were immunostained for MBP (red) and activated caspase-3 (green). The number of activated caspase-3 and MBP-positive oligodendrocytes was counted per field and expressed as a ratio of positive cells in benzylserine (BS) containing supernatant to that of DMSO containing supernatant from astrocytes. Results indicate a concentration-dependent increase in oligodendrocyte damage and injury with benzylserine treatment (*D*). (Original magnification, $\times 400$ (*A*)) (***, $p < 0.001$; **, $p < 0.01$).

treatment of oligodendrocytes reduced immunofluorescence levels of both CNP and MBP (Fig. 6C), more so than astrocytes expressing Syncytin-1 ($p < 0.01$). Thus, Syncytin-1 expression and inhibition of ASCT reduced oligodendrocyte viability, as evidenced by suppression of myelin protein and cell death.

iNOS and Egr1 suppress ASCT1 in astrocytes

Brains of MS patients display increased expression of iNOS (12, 60) and Egr1 (18), a transcriptional repressor of ASCT1 (61). Given that OASIS induced iNOS in astrocytes, we examined the contributions of iNOS and Egr1 to the expression of ASCT1. Transfection of astrocytes with a vector expressing Syncytin-1 revealed significant induction of Egr1, but not Egr3 and Egr4 ($p < 0.05$; Fig. 7A). Treatment of astrocytes with the NO donor, SNP, reduced ASCT1 mRNA ($p < 0.05$; Fig. 7B). Expression of Egr1 was also significantly increased by SNP in keeping with earlier studies showing that NO enhanced Egr1 expression (62) ($p < 0.001$; Fig. 7B). Our observations were confirmed by quantitative immunofluorescence analysis of Egr1 expression, which was increased in astrocytes after SNP or Syncytin-1 treatment ($p < 0.05$; Fig. 7C). SNP treatment decreased ASCT1 expression in a dose-dependent manner in astrocytes ($p < 0.05$; Fig. 7D), confirming our PCR results (Fig. 7B). The suppression of ASCT1 transcripts observed in Syncytin-1-overexpressing astrocytes was significantly reversed by treatment of cells with a nonspecific NOS inhibitor, L-NAME (Fig. 7E). ASCT1 suppression was independent of regulation by cytokines, as both IL-10 and IL-1 β significantly increased the transcription of ASCT1 (Fig. 7F). Enhanced expression of Egr1 was also observed in MS brain white matter lesions (Fig. 7H) compared with non-MS controls (Fig. 7G). Egr1 was localized predominantly in the cytoplasm of astrocytes in the white matter (GFAP-positive astrocytes: blue; Egr1: brown) (Fig. 7H, inset). Thus, these observations indicated that diminished ASCT1 expression on astrocytes was induced by Syncytin-1 and modulated by NO and Egr1.

Syncytin-1-Tg mice exhibit neuroinflammation and induction of ER chaperones

We have previously reported up-regulation of Syncytin-1 in the brains of MS patients relative to age-matched controls (12). To extend the ex vivo data obtained above, we generated Tg mice expressing Syncytin-1, under the control of the GFAP promoter (39) in CD-1 mice (Fig. 8A). Transgene detection was performed by PCR assay using tail-derived genomic DNA (Fig. 8B). As Syncytin-1 Tg mice displayed no disease phenotype, we used a model of MS in which TNF- α was stereotactically implanted into the corpus callosum (12), an anatomical region frequently exhibiting demyelination in MS patients (63). TNF- α activates GFAP (64) and also enhanced Syncytin-1 expression in astrocytes (Fig. 2A). Because Syncytin-1 Tg and Wt littermates stereotactically implanted with PBS did not demonstrate Syncytin-1 expression (Fig. 8C), subsequent comparisons were made between Tg and Wt animals implanted with TNF- α , which significantly induced Syncytin-1 mRNA (Fig. 8D) and protein (Fig. 8E) expression in brains of Tg mice. To determine whether Syncytin-1 expression in the brain provoked an inflammatory response in mice, we examined TNF- α -implanted Syncytin-1-Tg and Wt littermates, which showed that the inflammatory genes TNF- α and IFN- α were increased in the implanted Tg mice brains relative to implanted Wt animals (Fig. 8F). Induction of proinflammatory molecules was specific to the brain, because treatment of macrophages from Syncytin-1-Tg mice with TNF- α did not induce proinflammatory gene expression differentially compared with Wt-derived macrophages (data not shown). Interestingly, expression of CNP and another

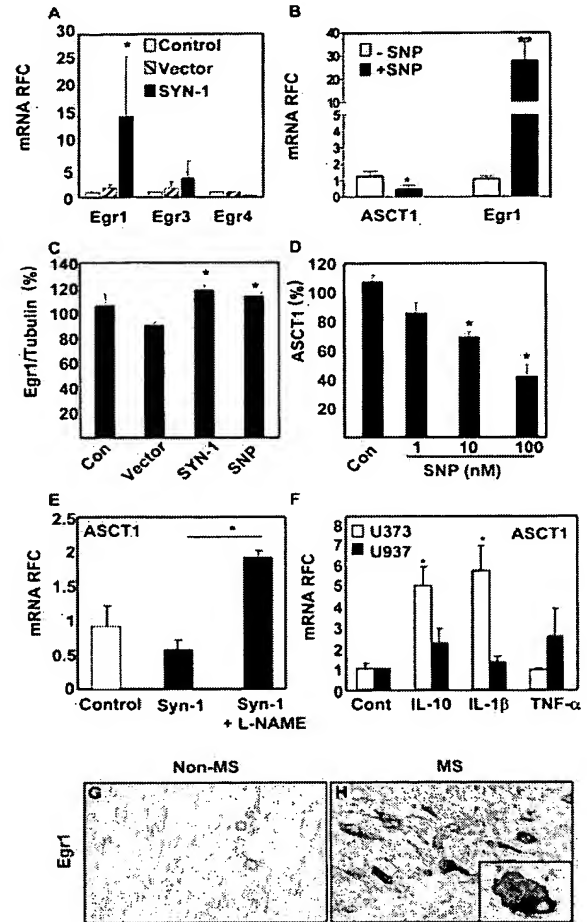
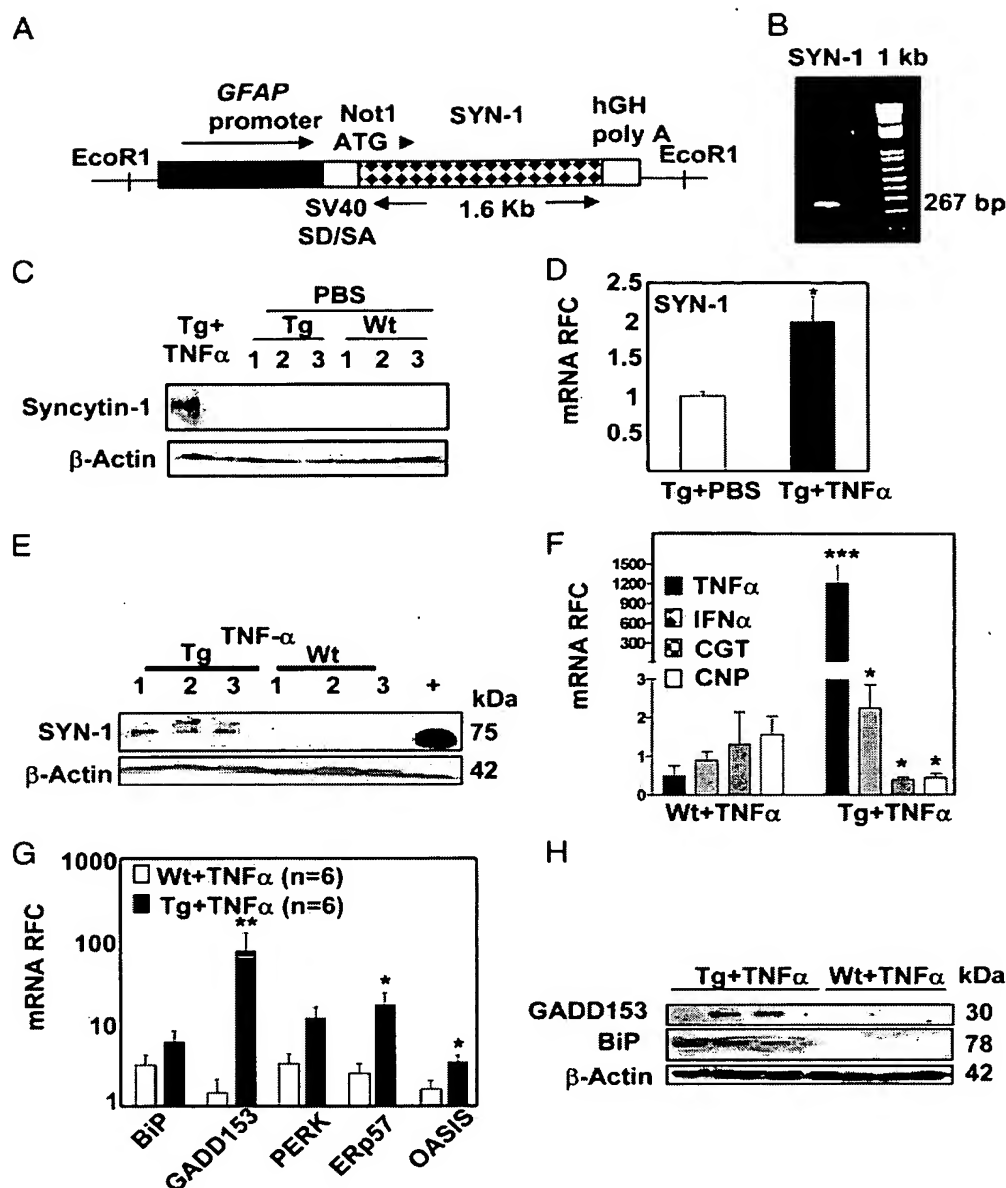


FIGURE 7. iNOS and Egr1 suppress ASCT1 abundance. Expression of Syncytin-1 (SYN-1) in astrocytes induced the expression of the repressive transcription factor Egr1, but not Egr3 and Egr4, (A) compared with mock (Control) or empty vector (Vector) transfected cells. Treatment of astrocytes with the NO donor, SNP (+SNP) significantly decreased ASCT1 expression, concurrently increasing the expression of Egr1 compared with untreated cells (-SNP) (B). Quantitative immunofluorescence of Egr1 showed significant induction in astrocytes treated with soluble Syncytin-1 (SYN-1) or SNP relative to supernatants from empty vector (Vector) or mock (Control) transfected HEK293T cells (C). SNP dose-dependently suppressed ASCT1 in astrocytes, measured by quantitative immunofluorescence analysis (D). The suppression of ASCT1 in astrocytes expressing Syncytin-1 was reversed when cells were treated with the nonselective NOS inhibitor, L-NAME (5 μ M) (E). Astrocytes (U373) and monocytoid cells (U937) were treated with IL-10, IL-1 β , and TNF- α (10 ng/ml) for 24 h and expression of ASCT1 was examined by real-time RT-PCR, which revealed a significant increase with IL-10 and IL-1 β , but not with TNF- α treatment, in astrocytes but not monocytoid cells (F). MS brains (H) revealed increased expression of Egr1 in astrocytes in the white matter compared with non-MS controls (G). (Original magnification, $\times 400$ (G and H); inset H, $\times 1000$) (**, $p < 0.01$; *, $p < 0.05$).

marker of oligodendrocyte/myelination, ceramide galactosyltransferase (CGT), were significantly reduced in Tg mice (Fig. 8F). Brain tissue from TNF- α -implanted Tg mice also revealed significant induction of ER chaperone gene transcripts, ERp57, OASIS, and GADD153/CHOP, compared with Wt littermates (Fig. 8G), while both BiP and PERK showed a trend toward increased transcript levels. OASIS, which is induced during astrocytic ER stress (31) (Fig. 3A) and in acute lesions of MS patients (Fig. 4A), was also increased in the brain of Syncytin-1-Tg mice (Fig. 8G). Expression of BiP and GADD153/CHOP proteins was increased in

FIGURE 8. Syncytin-1-Tg mice show neuroinflammation and ER stress. The *Syncytin-1* gene was cloned into pFGH vector containing the GFAP promoter (A). Transgene integration was confirmed by genotyping revealing a 267-bp product (SYN-1) (B). Implantation of PBS into the corpus callosum of Syncytin-1-Tg mice did not induce Syncytin-1 expression compared with implantation with TNF- α , where the Syncytin-1 immunoreactive band is seen in lane 1 (C). TNF- α implantation induced Syncytin-1 transcript levels in Tg mice compared with PBS-implanted Tg mice (D). TNF- α implantation induced Syncytin-1 immunoreactivity on Western blot in Tg mice brains but not in Wt littermates (E). TNF- α implantation also enhanced levels of the proinflammatory genes, *TNF- α* and *IFN- α* , and decreased levels of the oligodendrocyte markers, CGT and CNP, in Syncytin-1-Tg mice relative to Wt littermates (F). TNF- α implantation significantly enhanced levels of ER chaperone genes, particularly *GADD153/CHOP*, *Erp57*, and *OASIS*, in the brains of Syncytin-1-Tg mice relative to Wt littermates (G). These latter results were also confirmed by Western blot analysis, which revealed induction of *GADD153/CHOP* and BiP in Syncytin-1-Tg mice brains (H). (***, $p < 0.001$; **, $p < 0.01$; *, $p < 0.05$).



brains of Syncytin-1-Tg mice (Fig. 8H). Thus, the Syncytin-1-Tg mice exhibited neuroinflammation with induction of several ER chaperones, similar to observations in MS brains.

Syncytin-1-Tg animals show diminished myelin proteins and neurobehavioral deficits

The brains of TNF- α -implanted Syncytin-1-Tg mice revealed astrogliosis, demonstrated by increased GFAP immunoreactivity and astrocyte hypertrophy (Fig. 9A, *i* and *ii*). Iba-1 immunoreactivity on monocytoic cells was also augmented in the brains of Tg mice compared with Wt littermates (Fig. 9A, *iii* and *iv*). Brains of Tg mice displayed increased numbers of infiltrating CD3-positive T cells relative to controls (Fig. 9A, *v* and *vi*). Importantly, Syncytin-1-positive astrocytes (Fig. 9A*viii*, *inset*) in brains of Tg mice demonstrated increased iNOS immunoreactivity (Fig. 9A*viii*), relative to Wt littermates (Fig. 9A*vii*), which supported the notion that iNOS and ER stress induction are closely coupled (65). Analysis of CNP immunoreactivity in the corpus callosum demonstrated a marked reduction in Syncytin-1-Tg mice (Fig. 9A*x*) compared with

Wt littermates implanted with TNF- α (Fig. 9A*ix*), confirming earlier observations (12). The Syncytin-1-Tg mice, thus, did not possess a hypomyelination phenotype, but rather a specific demyelination because CNP immunostaining in the corpus callosum was unaffected in sites remote from TNF- α implantation. Expression of the ER chaperone, BiP, was observed in both groups (Fig. 9A, *xi* and *xii*), while GADD153/CHOP expression was prominently expressed in oligodendrocytes in brains of Syncytin-1-Tg mice (Fig. 9A, *xiv* and *xiii*, *inset*) compared with Wt littermates implanted with TNF- α (Fig. 9A*xiii*). Expression of the ER stress protein, GADD153/CHOP, in oligodendrocytes corroborates recent observations in murine retrovirus-induced oligodendropathy (26). Complementing these findings, Syncytin-1-Tg mice implanted with TNF- α displayed significantly lower ASCT1 transcript levels but ASCT2 did not differ between groups. This finding corresponded to higher iNOS mRNA levels in the Tg mice (Fig. 9B), emphasizing our immunohistochemical analysis. This effect appeared to be specific to iNOS because transcript levels of neuronal NOS did not differ between Wt and Tg mice implanted with TNF- α (data

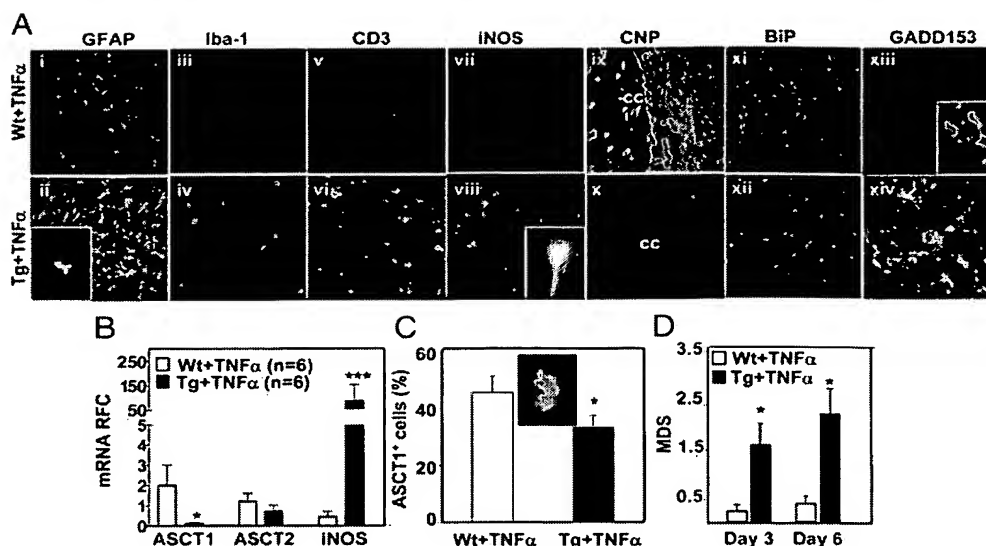


FIGURE 9. Syncytin-1-Tg mice display neuroinflammation, oligodendrocyte loss and neurobehavioral abnormalities. **A**, Syncytin-1-Tg mice implanted with TNF- α revealed astrocytosis (GFAP immunoreactivity) (ii, inset), microgliosis (Iba-1 immunoreactivity) (iv), infiltrating CD3-positive T cells (Avi), and iNOS immunoreactivity in Syncytin-1-positive cells (viii, inset) compared with Wt littermates (i, iii, v, and vii). CNP expression was reduced in the corpus callosum (CC) of Syncytin-1-Tg mice implanted with TNF- α (x) compared with Wt littermates (ix). BiP expression was observed in Wt and Tg mice (xi and xii), while GADD153/CHOP expression was prominently expressed in oligodendrocytes in brains of Syncytin-1-Tg mice (xiv and xiii, inset) compared with Wt littermates implanted with TNF- α (xiii). TNF- α implantation induced iNOS but reduced ASCT1 expression, but not ASCT2, in Syncytin-1-Tg mice relative to Wt littermates (**B**). Analysis of ASCT1-immunopositive cells in the corpus callosum (**C**, inset) revealed significantly lower numbers in TNF- α -implanted brains of Syncytin-1-Tg mice compared with Wt littermates (**C**). Mean deficit scores (MDS) revealed significantly high MDS scores for Syncytin-1-Tg mice implanted with TNF- α compared with Wt littermates (**D**). (***, $p < 0.001$; *, $p < 0.05$) (Original magnification, $\times 400$ (**A**); inset (**A** and **C**), $\times 1000$).

not shown). Furthermore, the number of ASCT1-positive cells was reduced in Syncytin-1-Tg mice implanted with TNF- α compared with Wt littermates (Fig. 9C). Stereotaxic implantation of TNF- α into the corpus callosum of Syncytin-1-Tg animals resulted in significant neurobehavioral deficits compared with TNF- α -implanted Wt littermates at days 3 and 6 postimplantation (Fig. 9D). The mean deficit scores were obtained from a combination of three behavioral tests described previously (41). TNF- α -implanted Tg mice grasped a horizontal rod for a significantly shorter length of time compared with the Wt littermates. In addition, Tg mice were sufficiently impaired that they could not hold on to an inverted screen and reach the screen edge, while Wt littermates reached the edges of the inverted screen more quickly. Lastly, Tg mice implanted with TNF- α exhibited mean delays in the time taken to cross a cantilevered beam, compared with Wt littermates, suggesting that the Tg mice showed diminished motor activity and exploratory behavior. Thus, in vivo Syncytin-1 overexpression resulted in neuroinflammation characterized by induction of iNOS and activation of ER chaperones, particularly OASIS and subsequent down-regulation of the Syncytin-1 receptor, ASCT1, resulting in suppression of myelin proteins and neurobehavioral abnormalities.

Discussion

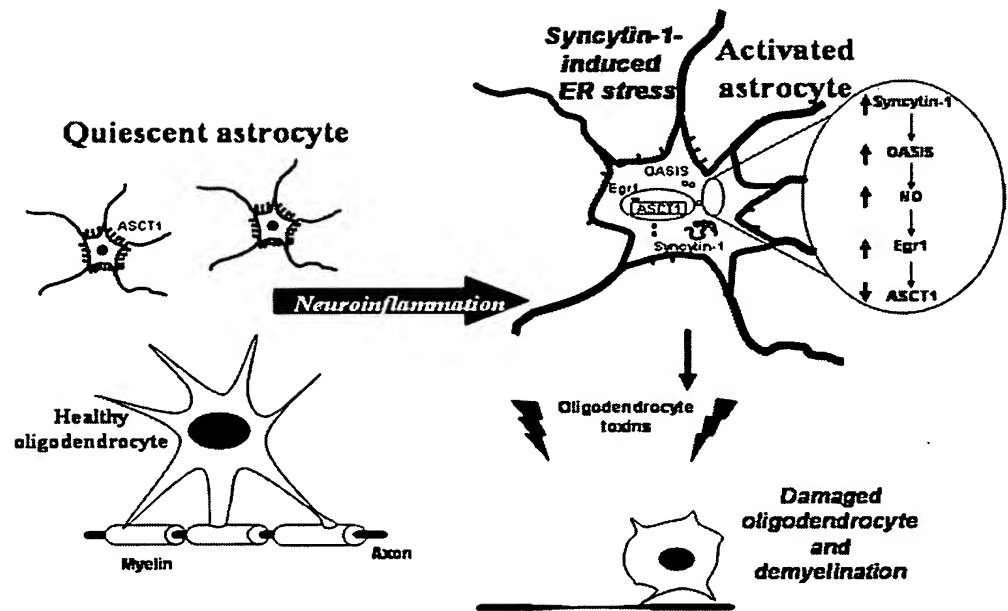
Sustained activation of the innate immune cells within the CNS in concert with persistent adaptive immune responses promotes neural injury during MS, independent of the roles of infiltrating T and B cells (66, 67). Herein, overexpression of a human endogenous retrovirus envelope protein, Syncytin-1, in astrocytes exerted neuropathogenic effects by inducing the ER chaperone, OASIS, with ensuing down-regulation of the Syncytin-1 receptor, ASCT1, accompanied by the release of oligodendrocyte cytotoxins (Fig. 10). Activation of OASIS-induced iNOS and

the transcriptional repressor Egr1 in astrocytes contributed to diminished ASCT1 expression (Fig. 10) observed in clinical samples, cell culture models, and a new Tg mouse model of MS. Given that HERVs represent 8% of the human genome and are able to express biologically active proteins (40), the present studies underscore the potential impact of *HERV* gene expression on disease mechanisms.

Previous studies have demonstrated that Syncytin-1 expression in astrocytes increases proinflammatory molecules (12). However, Syncytin-1 expression in astrocytes is also induced by an inflammatory milieu, highlighting a vicious cycle with deleterious implications for oligodendrocytes. Moreover, excessive or chronic ER stresses result in apoptotic cell death (31), which is a feature of MS, including mounting evidence for the role of ER stress in affecting oligodendrocyte viability (26). The current studies implicate astrocytes in the pathogenesis of MS, which is plausible assuming the pivotal role of astrocytes in maintaining homeostasis in the CNS through regulation of neuroinflammatory, neurotrophic, and neurotoxic factors (68). Because ER stress responses can regulate both inflammation and cell survival (69), the induction of ER chaperones in the brains of Syncytin-1-Tg mice may contribute to enhanced inflammation observed in these animals. Although the expression and function of the protective ER chaperone OASIS have not been elucidated in detail (31), this study indicates that OASIS is induced in MS brain tissue and in astrocytes overexpressing Syncytin-1 with pathogenic effects on oligodendrocytes, possibly mediated by reduced expression of ASCT1.

Diminished expression of ASCT1 in brains of MS patients in conjunction with increased expression of Syncytin-1 prompted the examination of relative levels of ASCT1 and ASCT2 in astrocytes expressing Syncytin-1. Interestingly, cellular differentiation increased ASCT1 receptor expression in macrophages,

FIGURE 10. Model of Syncytin-1-mediated neuropathogenesis. Astrocytes overexpressing Syncytin-1 undergo ER stress, including induction of OASIS. Activation of iNOS by OASIS leads to increased production of NO, which augments Egr1 expression with ensuing suppression of ASCT1, a receptor for Syncytin-1 and an amino acid transporter. Reduced ASCT1 function causes oligodendrocyte injury and death through the regulation of cytotoxic molecule release.



which may have important implications for viral entry. Syncytin-1 has been reported to form infectious pseudotyped viruses with HIV-1, but not MuLV (47). We used a similar pseudotyping strategy to investigate the permissiveness of different neural cells to Syncytin-1-mediated cell entry. Interestingly, Syncytin-1-mediated entry of the pseudotyped virus was restricted to astrocytes and macrophages, although neurons also expressed the putative receptors for Syncytin-1. Given the ubiquity of their expression, it was expected that all cell types were permissive to the Syncytin-1-pseudotyped virus. However, the present negligible infection of human neurons raises the possibility of other (co)receptors mediating viral envelope engagement or perhaps other inhibitory mechanisms including viral interference (70). However, these studies confirmed the functional properties of the present Syncytin-1 clone.

The current report demonstrates that brain cells express ASCT1 and ASCT2, providing the first human *in vivo* description of their expression in the CNS. Furthermore, expression of ASCT2 was low in the adult brain (71) but our observations of ASCT2 immunostaining in human brains reveals its expression in microglia. ASCT1 was chiefly expressed in GFAP-positive astrocytes, but not in neurons, oligodendrocytes, or microglia of mice (72), similar to our observations in human brains. Importantly, there was selective down-regulation of ASCT1 in MS brain white matter. Of interest, ASCT1 was also found to be significantly down-regulated in glial cells treated with 7-keto-cholesterol, which is increased in MS brains and is formed by oxidative stress-damaged myelin (73), supporting the present findings.

To elucidate the mechanism of ASCT1 down-regulation, we hypothesized that Syncytin-1-mediated inflammation and ER stress might contribute to diminished receptor expression. Expression of OASIS in astrocytes resulted in induction of iNOS and suppression of ASCT1. Hence, it was assumed that NO might play a role because NO donors are known to modulate ASCT2 expression (74). The rationale for using NO donors was that Syncytin-1 mediates NO production and the formation of peroxynitrites (12), both of which induce ER stress (75). iNOS expression and overproduction of NO in astrocytes of MS demyelinating lesions also contributes to inflammation and tissue

injury (12, 60). Indeed, SNP, an NO donor, diminished ASCT1 expression in astrocytes, but also induced Egr1, a potential repressor protein of ASCT1 in neural cells (61, 76). Of note, Egr1 also suppresses TNF- α (77), which may have pathogenic consequences in MS due to the protective nature of this proinflammatory cytokine at low concentrations (78). Indeed, Egr1 DNA-binding activity has been associated with oligodendrocyte death (79). Because iNOS and Egr1 are significantly enhanced in brain lesions of MS patients (18) with concurrent down-regulation of ASCT1, we might have also identified a potential role for Egr1 in MS neuropathogenesis. Thus, suppression of ASCT1 was likely brought about by OASIS-mediated iNOS expression through the production of Egr1.

The induction of ER chaperones in Syncytin-1-expressing astrocytes and brain of MS patients might be a mechanism directed to achieving cellular homeostasis; failure to initiate ER stress or protracted ER stress leads to cell death. For example, GADD153/CHOP promotes recovery from ER and oxidative stress by inducing the expression of GADD34 and ER oxidoreductin 1, respectively, but prolonged expression results in release of cytotoxic reactive oxygen species (15). This suggests that the mechanism of oligodendrocyte killing seen in our previous study (12) might be due to OASIS-mediated production of free radicals in astrocytes as OASIS is upstream of GADD153/CHOP. Thus, it appears that OASIS might bind to the promoter of BiP during the early stages of ER stress, as described by others (31) and enhance BiP expression leading to the release of reactive oxygen species and induction of iNOS as described previously (30). Additional ER stress pathways, including phosphorylation of the sensor protein PERK as well as XBP-1 splicing, are potential topics for future experiments. Nevertheless, we have shown that a key ER stress sensor, OASIS, was induced in brains of MS patients and astrocytes expressing Syncytin-1, might be the principal mechanism by which astrocytes expressing Syncytin-1 affect myelin protein expression.

The present results suggest a specific down-regulation of ASCT1 in MS because another astrocytic amino acid transporter, EAAT1 (80), was unaffected by Syncytin-1. A further implication of these findings is that compromised expression of

ASCT1 in the brain, particularly in astrocytes, might affect oligodendrocyte viability and myelin protein expression. ASCT1 is the principal transport system involved in the secretion of L-serine (81), a potent astrocyte-derived neurotrophic factor essential for myelination (82) and neuronal survival (83). In addition, ASCT1 also regulates D-serine and cysteine levels, which exert neurotoxic effects (7). Thus, diminished myelin protein expression observed in our study may be due to withdrawal of trophic amino acids or excess extracellular levels of toxic amino acids. These pathogenic processes require further investigation.

Because the expression of ASCT1 in astrocytes was suppressed by Syncytin-1, a potential mechanism might be its regulation by NO or peroxynitrites, as described for the HIV-1 coreceptors, CXCR4 and CCR5 (84). Alternatively, diminished ASCT1 expression in astrocytes might be a protective host cell response to minimize interaction with viruses and thereby limit immune-mediated pathology (85) or a receptor interference mechanism as in the case of CD4 down-regulation by HIV-1 to prevent superinfection (20). Retrovirus receptor interference and down-regulation proceeds from direct interactions between the virus and the receptor or through indirect (intracellular) mechanisms, possibly involving redox regulation of the receptor (84). Nevertheless, loss of ASCT1 might be compensated by ASCT2 due to the functional redundancy between ASCT1 and ASCT2 (4). This possibility was further emphasized by our observation of increased ASCT2 expression in astrocytes transfected with OASIS (Fig. 4C). Moreover, our observation that inhibition of both ASCT1 and ASCT2 in astrocytes by benzylserine affected myelin protein expression (Fig. 6C) indicated that soluble free radical-induced factors released by astrocytes might be responsible.

Enhanced neuroinflammatory responses in the brains of Syncytin-1-Tg mice as well as recruitment of CD3-positive T cells were evident in our model of MS, suggesting the potential role of Syncytin-1 to chemoattract T cells into the brain and mediate immunopathology in conjunction with neurobehavioral abnormalities. In addition to adenomatous polyposis coli and GSTP1, oligodendrocyte markers that were earlier shown to be affected by Syncytin-1 (12), we now show that CNP, an early marker of myelination and oligodendrocyte viability, was also suppressed in our Tg model compared with MBP, a late marker. Supporting our observation is the finding that CNP, but not MBP, is regulated by redox reactants (86).

Hence, these studies have identified a distinct pathway involved in the pathogenesis of MS, wherein Syncytin-1 induces OASIS in astrocytes, which results in NO production and concurrent suppression of ASCT1 in astrocytes, leading to diminished myelin protein expression (Fig. 10). Moreover, the present mouse model of MS expressing a HERV glycoprotein in astrocytes could be used to dissect the pathogenic mechanisms of MS without the constraints reported for other MS models (87).

Acknowledgments

We thank Robyn Flynn and Neda Shariat for technical assistance, Dr. Farshid Noorbakhsh for useful discussions, and Dr. Iain Campbell (University of Sydney, Sydney, Australia) for the pFGH vector.

Disclosures

The authors have no financial conflict of interest.

References

1. Frohman, E. M., M. K. Racke, and C. S. Raine. 2006. Multiple sclerosis—the plaque and its pathogenesis. *N. Engl. J. Med.* 354: 942–955.
2. Hartung, H. P., and P. Rieckmann. 1997. Pathogenesis of immune-mediated demyelination in the CNS. *J. Neural. Transm.* 50(Suppl.): 173–181.
3. Custer, S. K., G. A. Garden, N. Gill, U. Rueb, R. T. Libby, C. Schultz, S. J. Guyenet, T. Deller, L. E. Westrum, B. L. Sopher, and A. R. La Spada. 2006. Bergmann glia expression of polyglutamine-expanded ataxin-7 produces neurodegeneration by impairing glutamate transport. *Nat. Neurosci.* 9: 1302–1311.
4. Lavillette, D., M. Marin, A. Ruggieri, F. Mallet, F. L. Cosset, and D. Kabat. 2002. The envelope glycoprotein of human endogenous retrovirus type W uses a divergent family of amino acid transporters/cell surface receptors. *J. Virol.* 76: 6442–6452.
5. Dolinska, M., B. Zablocka, U. Sonnewald, and J. Albrecht. 2004. Glutamine uptake and expression of mRNA's of glutamine transporting proteins in mouse cerebellar and cerebral cortical astrocytes and neurons. *Neurochem. Int.* 44: 75–81.
6. Yamamoto, T., I. Nishizaki, T. Nukada, E. Kamegaya, S. Furuya, Y. Hirabayashi, K. Ikeda, H. Hata, H. Kobayashi, I. Sora, and H. Yamamoto. 2004. Functional identification of ASCT1 neutral amino acid transporter as the predominant system for the uptake of L-serine in rat neurons in primary culture. *Neurosci. Res.* 49: 101–111.
7. Weiss, M. D., C. Rossignol, C. Sumners, and K. J. Anderson. 2005. A pH-dependent increase in neuronal glutamate efflux in vitro: possible involvement of ASCT1. *Brain Res.* 1056: 105–112.
8. Blond, J. L., D. Lavillette, V. Cheynet, O. Bouton, G. Oriol, S. Chapel-Fernandes, B. Mandrand, F. Mallet, and F. L. Cosset. 2000. An envelope glycoprotein of the human endogenous retrovirus HERV-W is expressed in the human placenta and fuses cells expressing the type D mammalian retrovirus receptor. *J. Virol.* 74: 3321–3329.
9. Ruprecht, K., K. Obojes, V. Wengel, F. Gronen, K. S. Kim, H. Perron, J. Schneider-Schaulies, and P. Rieckmann. 2006. Regulation of human endogenous retrovirus W protein expression by herpes simplex virus type 1: implications for multiple sclerosis. *J. Neurovirol.* 12: 65–71.
10. Antony, J. M., M. Izad, A. Bar-Or, M. Vodjigani, K. G. Warren, and C. Power. 2006. Quantitative analysis of human endogenous retrovirus-W env in neuroinflammatory diseases. *AIDS Res. Hum. Retroviruses* 22: 1253–1259.
11. Mameli, G., V. Astone, K. Khalili, C. Serra, B. E. Sawaya, and A. Dolci. 2007. Regulation of the syncytin-1 promoter in human astrocytes by multiple sclerosis-related cytokines. *Virology* 362: 120–130.
12. Antony, J. M., G. van Marle, W. Opii, D. A. Butterfield, F. Mallet, V. W. Yong, J. L. Wallace, R. M. Deacon, K. Warren, and C. Power. 2004. Human endogenous retrovirus glycoprotein-mediated induction of redox reactants causes oligodendrocyte death and demyelination. *Nat. Neurosci.* 7: 1088–1095.
13. Sasaki, H., H. Sato, K. Kuriyama-Matsumura, K. Sato, K. Maebara, H. Wang, M. Tamba, K. Itoh, M. Yamamoto, and S. Bannai. 2002. Electrophile response element-mediated induction of the cystine/glutamate exchange transporter gene expression. *J. Biol. Chem.* 277: 44765–44771.
14. Qiang, W., J. M. Cahill, J. Liu, X. Kuang, N. Liu, V. L. Scofield, J. R. Voorhees, A. J. Reid, M. Yan, W. S. Lynn, and P. K. Wong. 2004. Activation of transcription factor Nrf-2 and its downstream targets in response to moloney murine leukemia virus ts1-induced thiol depletion and oxidative stress in astrocytes. *J. Virol.* 78: 11926–11938.
15. Lin, W., A. Kemper, J. L. Dupree, H. P. Harding, D. Ron, and B. Popko. 2006. Interferon- γ inhibits central nervous system remyelination through a process modulated by endoplasmic reticulum stress. *Brain* 129: 1306–1318.
16. Kaufman, R. J. 1999. Stress signaling from the lumen of the endoplasmic reticulum: coordination of gene transcriptional and translational controls. *Genes Dev.* 13: 1211–1213.
17. Rao, R. V., and D. E. Bredesen. 2004. Misfolded proteins, endoplasmic reticulum stress and neurodegeneration. *Curr. Opin. Cell. Biol.* 16: 653–662.
18. Mycko, M. P., R. Papoian, U. Boschert, C. S. Raine, and K. W. Selma. 2004. Microarray gene expression profiling of chronic active and inactive lesions in multiple sclerosis. *Clin. Neurol. Neurosurg.* 106: 223–229.
19. Bauer, J., M. Bradl, M. Klein, M. Leisser, T. L. Deckwerth, H. Wekerle, and H. Lassmann. 2002. Endoplasmic reticulum stress in PLP-overexpressing transgenic rats: gray matter oligodendrocytes are more vulnerable than white matter oligodendrocytes. *J. Neuropathol. Exp. Neurol.* 61: 12–22.
20. Michel, N., I. Allespach, S. Venzke, O. T. Fackler, and O. T. Keppler. 2005. The Nef protein of human immunodeficiency virus establishes superinfection immunity by a dual strategy to downregulate cell-surface CCR5 and CD4. *Curr. Biol.* 15: 714–723.
21. Wang, H., E. Klamo, S. E. Kuhmann, S. L. Kozak, M. P. Kavanaugh, and D. Kabat. 1996. Modulation of ecotropic murine retroviruses by N-linked glycosylation of the cell surface receptor/amino acid transporter. *J. Virol.* 70: 6884–6891.
22. Qiang, W., X. Kuang, J. Liu, N. Liu, V. L. Scofield, A. J. Reid, Y. Jiang, G. Stoica, W. S. Lynn, and P. K. Wong. 2006. Astrocytes survive chronic infection and cytopathic effects of the ts1 mutant of the retrovirus Moloney murine leukemia virus by upregulation of antioxidant defenses. *J. Virol.* 80: 3273–3284.
23. Kim, H. T., K. Waters, G. Stoica, W. Qiang, N. Liu, V. L. Scofield, and P. K. Wong. 2004. Activation of endoplasmic reticulum stress signaling pathway is associated with neuronal degeneration in MoMuLV-ts1-induced spongiform encephalomyelopathy. *Lab. Invest.* 84: 816–827.
24. Dimcheff, D. E., S. Askovic, A. H. Baker, C. Johnson-Fowler, and J. L. Portis. 2003. Endoplasmic reticulum stress is a determinant of retrovirus-induced spongiform neurodegeneration. *J. Virol.* 77: 12617–12629.

25. Dimcheff, D. E., M. A. Faasse, F. J. McAtee, and J. L. Portis. 2004. Endoplasmic reticulum (ER) stress induced by a neurovirulent mouse retrovirus is associated with prolonged BiP binding and retention of a viral protein in the ER. *J. Biol. Chem.* 279: 33782–33790.
26. Clase, A. C., D. E. Dimcheff, C. Favara, D. Dorward, F. J. McAtee, L. E. Parrie, D. Ron, and J. L. Portis. 2006. Oligodendrocytes are a major target of the toxicity of spongiform murine retroviruses. *Am. J. Pathol.* 169: 1026–1038.
27. Johnston, J. B., C. Silva, J. Holden, K. G. Warren, A. W. Clark, and C. Power. 2001. Monocyte activation and differentiation augment human endogenous retrovirus expression: implications for inflammatory brain diseases. *Ann. Neurol.* 50: 434–442.
28. Katsumata, K., H. Ikeda, M. Sato, A. Ishizu, Y. Kawarada, H. Kato, A. Wakisaka, T. Koike, and T. Yoshiki. 1999. Cytokine regulation of env gene expression of human endogenous retrovirus-R in human vascular endothelial cells. *Clin. Immunol.* 93: 75–80.
29. Perron, H., F. Lazarini, K. Rupprecht, C. Pechoux-Longin, D. Seilhean, V. Szadovitch, A. Creange, N. Batail-Poirot, G. Sibai, L. Santoro, et al. 2005. Human endogenous retrovirus (HERV)-W ENV and GAG proteins: physiological expression in human brain and pathophysiological modulation in multiple sclerosis lesions. *J. Neurovirol.* 11: 23–33.
30. Xu, W., L. Liu, J. G. Charles, and S. Moncada. 2004. Nitric oxide induces coupling of mitochondrial signalling with the endoplasmic reticulum stress response. *Nat. Cell Biol.* 6: 1129–1134.
31. Kondo, S., T. Murakami, K. Tatsumi, M. Ogata, S. Kanemoto, K. Otori, K. Iseki, A. Wanaka, and K. Imaizumi. 2005. OASIS, a CREB/ATF-family member, modulates UPR signalling in astrocytes. *Nat. Cell Biol.* 7: 186–194.
32. Tsutsui, S., J. Schnermann, F. Noorbakhsh, S. Henry, V. W. Yong, B. W. Winston, K. Warren, and C. Power. 2004. A1 adenosine receptor upregulation and activation attenuates neuroinflammation and demyelination in a model of multiple sclerosis. *J. Neurosci.* 24: 1521–1529.
33. Power, C., S. Henry, M. R. Del Bigio, P. H. Larsen, D. Corbett, Y. Imai, V. W. Yong, and J. Peeling. 2003. Intracerebral hemorrhage induces macrophage activation and matrix metalloproteinases. *Ann. Neurol.* 53: 731–742.
34. Power, C., P. A. Kong, T. O. Crawford, S. Wesselingh, J. D. Glass, J. C. McArthur, and B. D. Trapp. 1993. Cerebral white matter changes in acquired immunodeficiency syndrome dementia: alterations of the blood-brain barrier. *Ann. Neurol.* 34: 339–350.
35. Power, C., P. A. Kong, and B. D. Trapp. 1996. Major histocompatibility complex class I expression in oligodendrocytes induces hypomyelination in transgenic mice. *J. Neurosci. Res.* 44: 165–173.
36. Yong, V. W., A. J. 1997. Culture of glial cells from human brain biopsies. In *Protocols for Neural Cell Culture*. R. A. Fedoroff, S. ed. Humana, Totowa, pp. 81–96.
37. Riches, D. W., and G. A. Underwood. 1991. Expression of interferon- β during the triggering phase of macrophage cytotoxic activation: evidence for an autocrine/paracrine role in the regulation of this state. *J. Biol. Chem.* 266: 24785–24792.
38. Zhang, K., F. Rana, C. Silva, J. Ethier, K. Wehrly, B. Chesebro, and C. Power. 2003. Human immunodeficiency virus type 1 envelope-mediated neuronal death: uncoupling of viral replication and neurotoxicity. *J. Virol.* 77: 6899–6912.
39. Stalder, A. K., M. J. Carson, A. Pagenstecher, V. C. Asensio, C. Kincaid, M. Benedict, H. C. Powell, E. Masliah, and I. L. Campbell. 1998. Late-onset chronic inflammatory encephalopathy in immune-competent and severe combined immunodeficient (SCID) mice with astrocyte-targeted expression of tumor necrosis factor. *Am. J. Pathol.* 153: 767–783.
40. Cheynet, V., A. Ruggieri, G. Oriol, J. L. Blond, B. Boson, L. Vachot, B. Verrier, F. L. Cosset, and F. Mallet. 2005. Synthesis, assembly, and processing of the Env ERVWE1/syncytin human endogenous retroviral envelope. *J. Virol.* 79: 5585–5593.
41. Guenther, K., R. M. Deacon, V. H. Perry, and J. N. Rawlins. 2001. Early behavioural changes in scrapie-affected mice and the influence of dapsone. *Eur. J. Neurosci.* 14: 401–409.
42. Boston-Howes, W., S. L. Gibb, E. O. Williams, P. Pasinelli, R. H. Brown, Jr., and D. Trotti. 2006. Caspase-3 cleaves and inactivates the glutamate transporter EAAT2. *J. Biol. Chem.* 281: 14076–14084.
43. Rolland, A., E. Jouvin-Marche, C. Viret, M. Faure, H. Perron, and P. N. Marche. 2006. The envelope protein of a human endogenous retrovirus-W family activates innate immunity through CD14/TLR4 and promotes Th1-like responses. *J. Immunol.* 176: 7636–7644.
44. Gegelashvili, M., A. Rodriguez-Kern, I. Pirozhkova, J. Zhang, L. Sung, and G. Gegelashvili. 2006. High-affinity glutamate transporter GLAST/EAAT1 regulates cell surface expression of glutamine/neutral amino acid transporter ASCT2 in human fetal astrocytes. *Neurochem. Int.* 48: 611–615.
45. Chen, C. P., K. G. Wang, C. Y. Chen, C. Yu, H. C. Chuang, and H. Chen. 2006. Altered placental syncytin and its receptor ASCT2 expression in placental development and pre-eclampsia. *BJOG* 113: 152–158.
46. Marin, M., D. Lavillette, S. M. Kelly, and D. Kabat. 2003. N-linked glycosylation and sequence changes in a critical negative control region of the ASCT1 and ASCT2 neutral amino acid transporters determine their retroviral receptor functions. *J. Virol.* 77: 2936–2945.
47. An, D. S., Y. Xie, and I. S. Chen. 2001. Envelope gene of the human endogenous retrovirus HERV-W encodes a functional retrovirus envelope. *J. Virol.* 75: 3488–3489.
48. Lock, C., G. Hermans, R. Pedotti, A. Brendolan, E. Schadt, H. Garren, A. Langer-Gould, S. Strober, B. Cannella, J. Allard, et al. 2002. Gene-microarray analysis of multiple sclerosis lesions yields new targets validated in autoimmune encephalomyelitis. *Nat. Med.* 8: 500–508.
49. Noorbakhsh, F., Q. Tang, S. Liu, C. Silva, G. van Marle, and C. Power. 2006. Lentivirus envelope protein exerts differential neuropathogenic effects depending on the site of expression and target cell. *Virology* 348: 260–276.
50. Mattson, M. P., and D. D. Taub. 2004. Ancient viral protein enrages astrocytes in multiple sclerosis. *Nat. Neurosci.* 7: 1021–1023.
51. Sato, H., M. Tamba, K. Kuriyama-Matsumura, S. Okuno, and S. Bannai. 2000. Molecular cloning and expression of human xCT, the light chain of amino acid transport system xc. *Antioxid. Redox. Signal* 2: 665–671.
52. Kanai, Y., and H. Endou. 2001. Heterodimeric amino acid transporters: molecular biology and pathological and pharmacological relevance. *Curr. Drug Metab.* 2: 339–354.
53. Qin, S., C. Colin, I. Hinners, A. Gervais, C. Cheret, and M. Mallat. 2006. System Xc- and apolipoprotein E expressed by microglia have opposite effects on the neurotoxicity of amyloid- β peptide 1–40. *J. Neurosci.* 26: 3345–3356.
54. Murakami, T., S. Kondo, M. Ogata, S. Kanemoto, A. Saito, A. Wanaka, and K. Imaizumi. 2006. Cleavage of the membrane-bound transcription factor OASIS in response to endoplasmic reticulum stress. *J. Neurochem.* 96: 1090–1100.
55. Bhat, N. R., D. L. Feinstein, Q. Shen, and A. N. Bhat. 2002. p38 MAPK-mediated transcriptional activation of inducible nitric-oxide synthase in glial cells: roles of nuclear factors, nuclear factor κ B, cAMP response element-binding protein, CCAAT/enhancer-binding protein- β , and activating transcription factor-2. *J. Biol. Chem.* 277: 29584–29592.
56. Barnett, M. H., and J. W. Prineas. 2004. Relapsing and remitting multiple sclerosis: pathology of the newly forming lesion. *Ann. Neurol.* 55: 458–468.
57. Kuhlmann, T., C. Lucchinetti, U. K. Zettl, A. Bitsch, H. Lassmann, and W. Bruck. 1999. Bel-2-expressing oligodendrocytes in multiple sclerosis lesions. *Glia* 28: 34–39.
58. Noorbakhsh, F., S. Tsutsui, N. Vergnolle, L. A. Boven, N. Shariat, M. Vojdani, K. G. Warren, P. Andrade-Gordon, M. D. Hollenberg, and C. Power. 2006. Proteinase-activated receptor 2 modulates neuroinflammation in experimental autoimmune encephalomyelitis and multiple sclerosis. *J. Exp. Med.* 203: 425–435.
59. Grever, C., and E. Grabsch. 2004. New inhibitors for the neutral amino acid transporter ASCT2 reveal its Na⁺-dependent anion leak. *J. Physiol.* 557: 747–759.
60. Bo, L., T. M. Dawson, S. Wesselingh, S. Mork, S. Choi, P. A. Kong, D. Hanley, and B. D. Trapp. 1994. Induction of nitric oxide synthase in demyelinating regions of multiple sclerosis brains. *Ann. Neurol.* 36: 778–786.
61. Kanai, Y., and M. A. Hediger. 2004. The glutamate/neutral amino acid transporter family SLC1: molecular, physiological and pharmacological aspects. *Pflügers Arch.* 447: 469–479.
62. Rupprecht, H. D., Y. Akagi, A. Keil, and G. Hofer. 2000. Nitric oxide inhibits growth of glomerular mesangial cells: role of the transcription factor EGR-1. *Kidney Int.* 57: 70–82.
63. Coombs, B. D., A. Best, M. S. Brown, D. E. Miller, J. Corboy, M. Baier, and J. H. Simon. 2004. Multiple sclerosis pathology in the normal and abnormal appearing white matter of the corpus callosum by diffusion tensor imaging. *Mult. Scler.* 10: 392–397.
64. Zhang, L., W. Zhao, B. Li, D. L. Alkon, J. L. Barker, Y. H. Chang, M. Wu, and D. R. Rubinow. 2000. TNF- α induced over-expression of GFAP is associated with MAPKs. *Neuroreport* 11: 409–412.
65. Kawahara, K., S. Oyadomari, T. Gotoh, S. Kohsaka, H. Nakayama, and M. Mori. 2001. Induction of CHOP and apoptosis by nitric oxide in p53-deficient microglial cells. *FEBS Lett.* 506: 135–139.
66. Prat, A., and J. Antel. 2005. Pathogenesis of multiple sclerosis. *Curr. Opin. Neurol.* 18: 225–230.
67. Trapp, B. D. 2004. Pathogenesis of multiple sclerosis: the eyes only see what the mind is prepared to comprehend. *Ann. Neurol.* 55: 455–457.
68. Volterra, A., and J. Meldolesi. 2005. Astrocytes, from brain glue to communication elements: the revolution continues. *Nat. Rev. Neurosci.* 6: 626–640.
69. Zhang, K., X. Shen, J. Wu, K. Sakaki, T. Saunders, D. T. Rutkowski, S. H. Back, and R. J. Kaufman. 2006. Endoplasmic reticulum stress activates cleavage of CREB to induce a systemic inflammatory response. *Cell* 124: 587–599.
70. Ponferrada, V. G., B. S. Mauck, and D. P. Wooley. 2003. The envelope glycoprotein of human endogenous retrovirus HERV-W induces cellular resistance to spleen necrosis virus. *Arch. Virol.* 148: 659–675.
71. Kekuda, R., P. D. Prasad, Y. J. Fei, V. Torres-Zamorano, S. Sinha, T. L. Yang-Feng, F. H. Leibach, and V. Ganapathy. 1996. Cloning of the sodium-dependent, broad-scope, neutral amino acid transporter Bo from a human placental choriocarcinoma cell line. *J. Biol. Chem.* 271: 18657–18661.
72. Sakai, K., H. Shimizu, T. Koike, S. Furuya, and M. Watanabe. 2003. Neutral amino acid transporter ASCT1 is preferentially expressed in L-Ser-synthetic/storing glial cells in the mouse brain with transient expression in developing capillaries. *J. Neurosci.* 23: 550–560.
73. Hackel, D. 2005. Activation of microglia by injured neurons-signal pathways of oxidatively modified lipids. PhD thesis, Otto von Guericke University of Magdeburg, Magdeburg, Magdeburg, p. 169.
74. Uchiyama, T., Y. Matsuda, M. Wada, S. Takahashi, and T. Fujita. 2005. Functional regulation of Na⁺-dependent neutral amino acid transporter ASCT2 by S-nitrosothiols and nitric oxide in Caco-2 cells. *FEBS Lett.* 579: 2499–2506.
75. Dickhout, J. G., G. S. Hossain, L. M. Pozza, J. Zhou, S. Lhotak, and R. C. Austin. 2005. Peroxynitrite causes endoplasmic reticulum stress and apoptosis in human vascular endothelium: implications in atherogenesis. *Arterioscler. Thromb. Vasc. Biol.* 25: 2623–2629.
76. Tatarowicz, W. A., C. E. Martin, A. S. Pekosz, S. L. Madden, F. J. Rauscher, 3rd, S. Y. Chiang, T. A. Beerman, and N. W. Fraser. 1997. Repression of the HSV-1 latency-associated transcript (LAT) promoter by the early growth response

- (EGR) proteins: involvement of a binding site immediately downstream of the TATA box. *J. Neurovirol.* 3: 212–224.
77. Di Battista, J. A., J. Martel-Pelletier, and J. Pelletier. 1999. Suppression of tumor necrosis factor (TNF- α) gene expression by prostaglandin E₂: role of early growth response protein-1 (Egr-1). *Osteoarthritis Cartilage* 7: 395–398.
 78. Korner, H., D. S. Riminton, D. H. Strickland, F. A. Lemckert, J. D. Pollard, and J. D. Sedgwick. 1997. Critical points of tumor necrosis factor action in central nervous system autoimmune inflammation defined by gene targeting. *J. Exp. Med.* 186: 1585–1590.
 79. FitzGerald, U. F., T. Gilbey, S. Brodie, and S. C. Barnett. 2003. Transcription factor expression and cellular redox in immature oligodendrocyte cell death: effect of Bcl-2. *Mol. Cell. Neurosci.* 22: 516–529.
 80. Storck, T., S. Schulte, K. Hofmann, and W. Stoffel. 1992. Structure, expression, and functional analysis of a Na⁺-dependent glutamate/aspartate transporter from rat brain. *Proc. Natl. Acad. Sci. USA* 89: 10955–10959.
 81. Yamamoto, T., I. Nishizaki, S. Furuya, Y. Hirabayashi, K. Takahashi, S. Okuyama, and H. Yamamoto. 2003. Characterization of rapid and high-affinity uptake of L-serine in neurons and astrocytes in primary culture. *FEBS Lett.* 548: 69–73.
 82. Sundaram, K. S., and M. Lev. 1984. Inhibition of sphingolipid synthesis by cycloserine in vitro and in vivo. *J. Neurochem.* 42: 577–581.
 83. Furuya, S., and M. Watanabe. 2003. Novel neuroglial and gliogial relationships mediated by L-serine metabolism. *Arch. Histol. Cytol.* 66: 109–121.
 84. Saccani, A., S. Saccani, S. Orlando, M. Sironi, S. Bernasconi, P. Ghezzi, A. Mantovani, and A. Sica. 2000. Redox regulation of chemokine receptor expression. *Proc. Natl. Acad. Sci. USA* 97: 2761–2766.
 85. Ramakrishna, C., C. C. Bergmann, K. V. Holmes, and S. A. Stohman. 2004. Expression of the mouse hepatitis virus receptor by central nervous system microglia. *J. Virol.* 78: 7828–7832.
 86. Jana, M., and K. Pahan. 2005. Redox regulation of cytokine-mediated inhibition of myelin gene expression in human primary oligodendrocytes. *Free Radic. Biol. Med.* 39: 823–831.
 87. Sriram, S., and I. Steiner. 2005. Experimental allergic encephalomyelitis: a misleading model of multiple sclerosis. *Ann. Neurol.* 58: 939–945.

Impaired Cytotrophoblast Cell–Cell Fusion Is Associated With Reduced Syncytin and Increased Apoptosis in Patients With Placental Dysfunction

MANUELA LANGBEIN,¹ REINER STRICK,^{1*} PAMELA L. STRISSEL,¹ NICOLE VOGT,¹
HANS PARSCH,² MATTHIAS W. BECKMANN,¹ AND RALF L. SCHILD^{1**}

¹Department of Gynaecology and Obstetrics, Laboratory for Molecular Medicine, Erlangen, Germany

²Central-Laboratory, University-Hospital Erlangen at the University of Erlangen-Nuremberg, Erlangen, Germany

ABSTRACT Preeclampsia (PE), Hemolysis Elevated Liver Enzymes and Low Platelets (HELLP)-syndrome, and intrauterine growth restriction (IUGR) are associated with abnormal placentation. In early pregnancy, placental cytotrophoblasts fuse and form multinuclear syncytiotrophoblasts. The envelope gene of the human endogenous retrovirus-W, Syncytin, is a key factor for mediating cell–cell fusion of cytotrophoblasts. This study investigated clinical parameters of PE and HELLP-associated IUGR and analyzed the cell–cell fusion index and β -human chorionic gonadotropin (β -hCG) secretion of cytotrophoblasts isolated and cultured from placentas of these patients. In addition, we performed absolute quantitation of Syncytin and determined the apoptosis rate in both cultured cytotrophoblasts and placental tissues. Cultured cytotrophoblasts from PE and HELLP-associated IUGR correlated with a pronounced lower cell–cell fusion index, 1.8- and 3.6-fold; less nuclei per syncytiotrophoblast, 1.4- and 2.0-fold; a significantly decreased β -hCG secretion, 4.3- and 17.2-fold and a reduction of Syncytin gene expression, 8.1 ($P=0.019$) and 222.7-fold ($P=0.011$) compared with controls, respectively. In contrast, a significantly 2.3-fold higher apoptosis rate was observed in cultured PE/IUGR cytotrophoblasts ($P=0.043$). Importantly, Syncytin gene expression in primary placental tissues of PE/IUGR was 5.4-fold lower ($P=0.047$) and in HELLP/IUGR 10.6-fold lower ($P=0.019$) along with a 1.8- and 1.9-fold significant increase in the apoptosis rate compared with controls, respectively. Low Syncytin expression in both cultured cytotrophoblasts and primary tissues from pathological placentas supports an intrinsic placenta-specific deregulation of cell–cell fusion in the formation of syncytiotrophoblasts leading to increased apoptosis. These processes could contribute to the development and severity of PE and HELLP-associated IUGR. *Mol. Reprod. Dev.*

© 2007 Wiley-Liss, Inc.

Key Words: placentogenesis; cytotrophoblast; cell–cell fusion; preeclampsia; HELLP-syndrome; syncytin

INTRODUCTION

Normal placental morphogenesis occurs through a coordinated interaction between the maternal decidua, myometrium, and fetal trophoblasts (Benirschke and Kaufmann, 2000). This developmental process is essential for a successful pregnancy outcome. Intrauterine growth restriction (IUGR) remains one of the most challenging perinatal problems, which can impact the health of the mother, fetus, or both and also results in increased morbidity and mortality. Preeclampsia (PE), defined as maternal hypertension and increased urinary protein excretion (Wilson et al., 2003) and the Hemolysis Elevated Liver Enzymes and Low Platelets (HELLP)-syndrome both originating from abnormal placental development due to diminished function, can occur alone or in combination with IUGR where the fetus also shows growth restriction (Khong et al., 1986; Roberts et al., 1991; Ness and Roberts, 1996). PE affects nearly 6% of all pregnancies and is the cause of 12% maternal deaths globally and furthermore results up to 13% of stillbirths and 20% of early neonatal deaths in some areas of the world (WHO, 1987; Duley, 1992). Although, much is known about the diagnosis, the molecular etiology of IUGR, PE, and HELLP remains unknown.

In early pregnancy during development of the fetoplacental unit, stem cytotrophoblasts differentiate into villous and extravillous cytotrophoblasts (CT) along two pathways: the fusion and the invasive pathways (Loke and King, 1995; Potgens et al., 2004; James et al., 2005). During cell–cell fusion, mononuclear villous CT fuse

*Correspondence to: Reiner Strick, PhD, Department of Gynaecology and Obstetrics, Laboratory for Molecular Medicine, University-Hospital Erlangen, Universitätsstr. 21-23, D-91054 Erlangen, Germany. E-mail: Reiner.Strick@gyn.imed.uni-erlangen.de

**Correspondence to: Ralf L. Schild, MD, University-Hospital Erlangen, Department of Gynaecology and Obstetrics, Universitätsstr. 21-23, D-91054 Erlangen, Germany.

E-mail: Ralf.Schild@gyn.imed.uni-erlangen.de

Received 6 December 2006; Accepted 24 January 2007

Published online in Wiley InterScience

(www.interscience.wiley.com).

DOI 10.1002/mrd.20729

and form multinuclear syncytiotrophoblasts (SCT), which represent the outer epithelial layer of the chorionic villi and are the primary site for maternal–fetal exchange of nutrients, gas, and waste products (Kingdom et al., 2000). Isolated and cultured CT fuse into SCT after 24–72 hr where SCT differ from CT not only in their morphology, but also in numerous endocrine properties (Kliman et al., 1986; Babalola et al., 1990). For example, it is well established that the secretion of β -human chorionic gonadotropin (β -hCG) correlates with the cell–cell fusion process of CT into multinuclear syncytia (Hoshina et al., 1985; Kliman et al., 1986). Extravillous CT are involved in the invasive differentiation pathway and are important for adequate invasion into uterine tissues and subsequent remodeling of spiral arteries (Pijnenborg et al., 1983; Zhou et al., 1997). Several investigators have demonstrated reduced CT invasiveness in PE (Caniggia et al., 1999; DiFederico et al., 1999; Lim et al., 1997), and which most likely contributes to a reduced placental blood flow and fluctuations in oxygen concentration. One theory has implicated that placental oxidative stress could be a key intermediary element in the development of PE (Redman and Sargent, 2000; Roberts and Hubel, 1999).

Human endogenous retrovirus (HERV) families represent remnants of past retroviral infections of germline cells of human ancestors and encompass 7.7% of the human genome (Bannert and Kurth, 2004). HERV-W is a widely spread, multicopy gene family with sequences on several chromosomes and in general is transcriptionally silent. One functional HERV-W envelope gene, Syncytin, is localized on chromosome 7q21-q22 and is highly expressed in the SCT layer (Mi et al., 2000). Syncytin has evolved as an essential gene in human placentogenesis mediating CT cell–cell fusion and differentiation (Blond et al., 2000; Mi et al., 2000; Frendo et al., 2003). To date, primary PE placental tissues have showed an altered cellular localization of Syncytin (Lee et al., 2001) and a lower Syncytin expression using semi-quantitative Realtime-PCR (Lee et al., 2001; Knerr et al., 2002, 2004). Studies have also identified the sodium-dependent neutral amino acid transporter ASCT2 as a receptor for Syncytin, which is expressed in the basal plasma membrane of SCT (Kudo and Boyd, 1990; Blond et al., 2000). For a successful pregnancy, the coordinated and regulated cell–cell fusion of CT is essential and perturbations in the cell–cell fusion process may be associated with some pregnancy-specific syndromes.

Apoptosis is crucial to the development and homeostasis of human tissues, including the human placenta. The process of apoptosis is highly conserved among multicellular organisms (Vaux and Korsmeyer, 1999) but at present, little is known about the cell type- and stimulus-specific pathways and the control of apoptosis in placental CT. Apoptosis is ongoing in CT of normal placentas with a higher incidence in the third trimester compared to the first trimester (Nelson, 1996; Smith et al., 1997b). Several studies have revealed that

dysregulation of key elements in apoptosis pathways may contribute to the pathology of PE, HELLP, and IUGR, therefore apoptosis is important to study in placentogenesis (Smith et al., 1997b; Ishihara et al., 2002; Levy et al., 2002).

The aim of this study was to analyze an array of clinical parameters associated with PE and HELLP-associated IUGR patients. Importantly, we also investigated the process of cell–cell fusion and apoptosis in cultured placental CT isolated from PE and HELLP-associated IUGR patients as well as confirming our findings in primary pathological placental tissue.

MATERIALS AND METHODS

Patient and Tissue Collective

The diagnosis of IUGR was based on the following constellation of findings: Elevated pulsatility index (PI) in the uterine arteries and/or early diastolic notches in both uterine arteries, elevated PI in umbilical arteries, elevated head/abdomen ratio, reduced amniotic fluid index, and longitudinal measurements of reduced growth of the fetal abdominal circumference (<5 mm/week) and/or cross sectional records of the estimated fetal weight below the 10th centile. PE was defined by the Redman and Jefferies (1988) criteria of hypertension: blood pressure $>140/90$ mmHg on two or more occasions with a rise in diastolic blood pressure >25 mmHg occurring after 20 weeks gestation and proteinuria >0.3 g/24 hr or $>3+$ on dipstick testing where delivery precludes a 24 hr collection. The diagnosis of HELLP followed additional criteria: lactic dehydrogenase >300 U/L, platelets $<100,000$ and liver enzymes twice as high as the upper normal limit.

With the ethical approval of the Ethics Committee at the University of Erlangen-Nuernberg, a total of 23 human placentas were obtained from 7 controls, 8 PE associated with IUGR, and 8 HELLP-associated with IUGR after elective Cesarean section or spontaneous labor. From this patient collective, a sample of patients was chosen for analysis of primary tissue ($n = 12$) and culturing of CT ($n = 10$). For analysis of placental tissue, two specimens from every placenta were dissected from two different regions of the fetal–maternal interface, near the cord and the outer border for comparison. All collected tissues were then snap frozen in liquid nitrogen and stored at -80°C until further use. To obtain additional clinical associations, all patients participated in an extensive questionnaire, personally collected by the attending physicians.

Isolation and Culture of CT

Primary human CT were isolated using the well established trypsin-DNase-dispase/percoll method (Bildirici et al., 2003; Kim et al., 2007; Schaiff et al., 2005) initially described by Kliman et al. (1986) with additional modifications previously described by us (Schild et al., 2006) and in this report. CT were isolated from term (32–40 weeks of gestation) placentas and then cryopreserved in liquid nitrogen. Viability of CT was

assessed after thawing by trypan blue exclusion and showed routinely >85% viability. Briefly, for experiments cells were plated at a density of 300,000 viable cells/cm² in Dulbecco's Modified Eagle's Medium (DMEM) supplemented with 10% fetal calf serum, 20 mM Hepes, 2 mM L-glutamine, penicillin/streptomycin (100 U/ml, 100 µg/ml), and non-essential amino acids in a humidified 5% CO₂ environment at 37°C. Following 4 hr after seeding, the media was changed to remove non-adherent cells and debris and then thereafter changed and collected every 24 hr.

Immunofluorescence of CT

The level of purity from CT isolations was determined using vimentin as a negative marker for CT together with the CT-specific marker Cytokeratin 7 (CK7) (Maldonado-Estrada et al., 2004). After culturing, the CT for 3 days in chamber slides, immunofluorescence was performed using a mouse anti-human vimentin (FITC-conjugated) antibody (1:200 in PBS/3% BSA, Fitzgerald Industries, Concord, MA) and then a mouse anti-human CK7 antibody (1:200 in PBS/3% BSA, Sigma, Taufkirchen, Germany), detected with a texas red conjugated anti-mouse IgG antibody (1:100 in PBS/3% BSA, BioMol GmbH, Hamburg, Germany) according to Maldonado-Estrada et al. (2004) and Strick et al. (2007). Immunofluorescence was examined using a Zeiss Fluorescence Axioscope.

RNA Extraction and Absolute Quantitative Realtime PCR (qPCR)

Total RNA was extracted from 50 to 100 mg of frozen placental tissues by mincing using a Mikro-Dismembrator (Braun Biotech, Sartorius AG, Goettingen, Germany) and purified using Trizol[®] reagent (Invitrogen, Karlsruhe, Germany). From cultured primary human CT, RNA was also isolated and purified using Trizol[®]. RNAs were quantified by absorbance at 260 nm. For Syncytin analysis, RNA was first pretreated with DNase I (Sigma-Aldrich, Taufkirchen, Germany) and cDNA was generated with the High Capacity cDNA Kit (Applied Biosystems, Darmstadt, Germany) in a thermal cycler 2720 (ABI) for 2 hr at 37°C. For qPCR of Syncytin, a QuantiTect Multiplex Assay (Qiagen, Hilden, Germany) was designed according to Strick et al. (2007). Primer 1 (CCCTATGACCATCTACAC) and 2 (GCACTCCTGCTCCTATAACAAA) with FAM-labeled probe (ATCTAAGCCCCGCAAC) including a 18s-rRNA control. Cloned Syncytin DNA with known copy numbers was used as an external standard, to generate a standard curve with the C_T value against the log of amount of standard. The C_T of Syncytin was calculated according to the standard curve.

Assessment of SCT by May-Gruenwald-Giemsa Staining and β-hCG Measurements

CT were cultured in LabTek slides (Nunc, Wiesbaden, Germany) or in 6-well plates (BD Biosciences, Heidelberg, Germany) and analyzed for cell-cell fusions at day 3 using May-gruenwald-Giemsa (Sigma-Aldrich) stain-

ing, which is a well established method for visualizing SCT and determining the fusion index (Cheynet et al., 2005; Dupressoir et al., 2005; Yagi et al., 2005). For each patient group, four different fields from CT cultures were assayed for the fusion index as well as for the average of nuclei present in SCT by two independent researchers. The fusion index expressed in percent was calculated as follows: $[(N - S)/T] \times 100$, where N equals the number of nuclei in SCT, S equals the number of SCT, and T equals the total number of nuclei counted. In addition, secreted β-hCG was used as a specific biochemical fusion marker (Hoshina et al., 1985; Kliman et al., 1986). Therefore, as represented for normal CT, supernatants from cultured CT were collected at day 3 when cell-cell fusion peaked, stored at -80°C, and then assayed in duplicates for β-hCG by an Immulite2000 (DPC).

Apoptosis Measurements

Primary viable CT were plated at a density of 300,000 cells/cm² in 96-well dishes in DMEM media at 37°C and 5% CO₂. At day 3, cells were lysed and apoptosis was measured directly and quantitatively by an ELISA Assay (Roche, Mannheim, Germany) using monoclonal antibodies against DNA and histones, which specifically determined amounts of mono- and oligonucleosomes in the cytoplasmatic fraction of cell lysates. For CT cultures, the apoptosis rate was defined as the amount of apoptosis per 20,000 cells in arbitrary units (a.U.). From frozen placentas, 20–30 mg tissues were first incubated with cell lysis buffer, then the total amount of proteins in the cell lysates was determined according to Bradford's method (Sigma) using BSA as a standard. Cell lysates were then analyzed for apoptosis also using the ELISA assay. The rate of apoptosis was defined as amount of apoptosis per 10 mg/ml of total protein (a.U.).

Statistical Analysis

All data were expressed as mean ± standard error of the mean (SEM). Differences were assessed using the independent-sample *t* test using SPSS 13.0 (SPSS, Inc). A *P*-value of less than 0.05 was considered statistically significant. The graphs were performed using SPSS 13.0.

RESULTS

Table 1 summarizes the clinical characteristics and statistical associations of 23 patients including PE/IUGR and HELLP/IUGR women compared to controls. Table 2 summarizes all clinical characteristics of newborns in this investigation.

Due to the pivotal role of CT for placentogenesis and development of the fetus, we established the culturing of pathological CT to study the process of cell-cell fusion. To compare differences in cell-cell fusion, the cell-cell fusion index and β-hCG measurements were determined. In addition, we quantitated the absolute Syncytin copy number per ng total RNA (Strick et al., 2007) and determined the apoptosis rate in cultured CT compared with placental tissues. Therefore, this study

TABLE 1. Clinical Characteristics of 23 Patients

	Control (n = 7)	PE/IUGR (n = 8)	P-value	HELLP/IUGR (n = 8)	P-value
Maternal age [years]	30 ± 3	29 ± 2	0.741	32 ± 2	0.494
Gestational age [days]	270.86 ± 3.01	251.13 ± 8.73	0.065	228.38 ± 11.46	0.005*
BMI	26.7 ± 1.2	28.0 ± 1.8	0.566	26.2 ± 1.3	0.821
Max systolic blood pressure [mmHg]	123 ± 4	167 ± 4	<0.0001*	170 ± 4	<0.0001*
Max diastolic blood pressure [mmHg]	73 ± 4	104 ± 4	<0.0001*	106 ± 3	<0.0001*
Min. platelet count [$\times 10^3/\mu\text{l}$]	210 ± 23	205 ± 24	0.881	94 ± 9	<0.0001*
Creatinine [mg/dl]	n.d.	1.19 ± 0.35	n.d.	0.72 ± 0.04	n.d.
GOT [U/L]	17 ± 3	61 ± 19	0.03*	239 ± 73	0.009*
GPT [U/L]	21 ± 8	47 ± 20	0.218	189 ± 58	0.012*
LDH [U/L]	177 ± 30	395 ± 90	0.3	582 ± 92	0.001*
Protein [mg/24 hr]	n.d.	6189 ± 2983	n.d.	5196 ± 596	n.d.
Hemoglobin [g/dl]	11.85 ± 0.75	12.46 ± 0.86	0.745	11.79 ± 0.52	0.957
Hematocrit [%]	35.2 ± 3.1	36.5 ± 2.5	0.820	33 ± 1.3	0.487
Gravidity	1.86 ± 0.26	1.38 ± 0.18	0.147	1.62 ± 0.49	0.699
Parity	0.29 ± 0.18	0.37 ± 0.18	0.738	0.37 ± 0.26	0.791
Prior miscarriages [%]	42	12.6	n.d.	25	n.d.
Allergies [%]	42	62.5	n.d.	50	n.d.
Recurrent PE/HELLP [%]	0	25	n.d.	0	n.d.
Clinical family history [%]	28.6 hypertension, 14.3 diabetes, 14.3 hypertension and diabetes	25 hypertension, 12.5 hypertension and diabetes	n.d.	12.5 hypertension, 12.5 diabetes, 25 hypertension and diabetes	n.d.

P-values were performed using Student's *t*-test. Significant P-values are indicated (*). n.d = not done.

represents a comprehensive analysis of various parameters involved in the development of normal and pathological placentas.

A Decreased Cell-Cell Fusion Index Correlated With Reduced β -hCG, Syncytin Expression, and an Enhanced Rate of Apoptosis in Cultured CT From Women With PE/IUGR and HELLP/IUGR

Primary human CT were isolated from 10 different placentas (control *n* = 4; PE/IUGR *n* = 4; HELLP/IUGR *n* = 2) from our patient collective and fractionated cells were cultured. Over 95% of cells in primary cultures stained positive for the CT marker CK7, but negative for vimentin, a marker for mesenchymal cells including fibroblasts, endothelial cells, and leukocytes (data not shown).

To investigate the process of cell–cell fusion, CT from control (*n* = 4), PE/IUGR (*n* = 4), and HELLP/IUGR (*n* = 2) cultures were analyzed microscopically at day 3 to quantitate the fusion index and the average number of nuclei per SCT (Fig. 1). Interestingly, a 1.8-fold lower

fusion index in PE/IUGR (37.6%) and a 3.6-fold lower fusion index in HELLP/IUGR (18.9%) were observed as compared to controls (68.9%). In addition, the average amount of nuclei in SCT from pathological CT was also lower compared to controls. For example, for controls, the average nuclei number was 6.5, whereas for PE/IUGR and HELLP/IUGR, 4.6 and 3.2 nuclei were found per SCT, respectively. Therefore, pathological CT not only showed a lower number of cell–cell fusions but also a 1.4-fold (PE/IUGR) or 2-fold (HELLP/IUGR) lower average of nuclei per SCT.

A quantitative analysis of β -hCG secretion from cultured CT of control (*n* = 4), PE/IUGR (*n* = 4), and HELLP/IUGR (*n* = 2) women was performed. Results showed that at day 3, the amount of secreted β -hCG was reduced from $2,630.5 \pm 466.9$ mIU/ml in control CT to 615.0 ± 361.6 mIU/ml (*P* = 0.014) in the PE/IUGR group (Fig. 2A). A further reduction to 153.0 ± 22.0 mIU/ml (*P* = 0.038) was observed in HELLP/IUGR. Thus, cultivated CT showed a 4.3-fold and 17.2-fold β -hCG reduction in PE/IUGR and HELLP/IUGR, respectively

TABLE 2. Characteristics of Newborns

	Control (n=7)	PE/IUGR (n=8)	P-value	HELLP/IUGR (n=8)	P-value
Fetal birthweight [g]	3071 ± 171	2256 ± 389	0.091	1463 ± 248	<0.0001*
Ponderal index	29.8 ± 0.6	29.0 ± 0.22	0.223	28.3 ± 0.30	0.038*
Length [cm]	48.8 ± 1.1	44.0 ± 2.7	0.138	39.1 ± 2.4	0.003*
Head size [cm]	34.5 ± 0.6	31.0 ± 1.6	0.066	28.1 ± 1.3	0.001*
Gender [%]	87.5 male, 14.3 female	62.5 male, 37.5 female	n.d.	37.5 male, 62.5 female	n.d.

P-values were performed using Student's *t*-test. Significant P-values are indicated (*). n.d = not done.

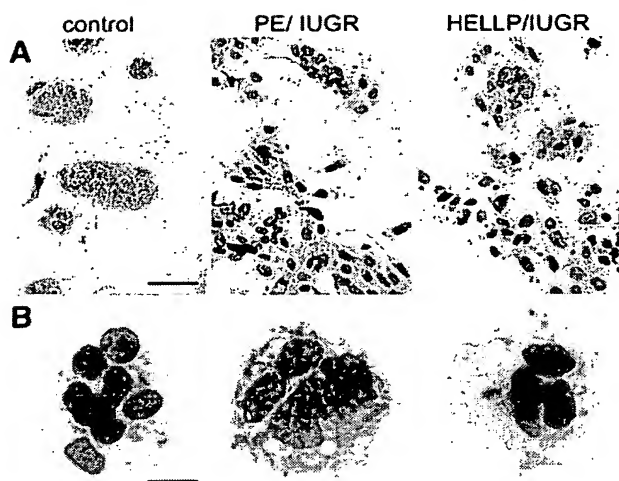


Fig. 1. Light microscopy of cultured CT (3 days) isolated from control, PE/IUGR, and HELLP/IUGR patients and stained with May-Gruenwald-Giemsa. A: Overview of CT and cell-cell fusion events. Scale bar: 50 µm. B: Single multinucleated SCT.

as compared to controls. This finding supports a reduction in cell-cell fusion as demonstrated above for pathological CT.

Syncytin was quantified using absolute qPCR at day 3 in CT cultivated from control ($n = 4$), PE/IUGR ($n = 4$), and HELLP/IUGR ($n = 2$) placentas. Results showed that Syncytin copy number per ng RNA was significantly reduced both in the PE/IUGR (73.80 ± 26.99 ; $P = 0.019$) and the HELLP/IUGR (2.68 ± 0.99 ; $P = 0.011$) groups in comparison to controls (601.3 ± 164.1) (Fig. 2B). Therefore, the decrease of Syncytin expression compared to controls was 8.1-fold lower in the PE/IUGR group and even more reduced to 222.7-fold in placentas with HELLP/IUGR.

In addition to analyzing differences regarding cell-cell fusion, the rate of apoptosis was determined in cultured CT from PE/IUGR placentas ($n = 4$) in comparison to controls ($n = 4$). At day 3, a significantly higher rate of apoptosis was observed in the PE/IUGR group ($P = 0.043$) compared to controls (1.767 ± 0.33 vs.

0.784 ± 0.195 , Fig. 2C). Thus, pathological CT showed a 2.3-fold higher apoptosis rate than controls.

Primary Pathological Placental Tissues Were Similar to Cultured CT With Reduced Syncytin Expression and a Higher Apoptosis Rate

To compare the above findings of cultured pathological CT, primary placentas from control ($n = 4$), PE/IUGR ($n = 4$), and HELLP/IUGR ($n = 4$) patients, including two different samples from each placenta, were analyzed for the expression of Syncytin using absolute qPCR to obtain copy number per ng total RNA (Fig. 3A). A comparison of Syncytin mRNA copy numbers between the two different specimens from one placenta showed no significant differences. The analysis between the patient groups demonstrated a statistically significant lower level of Syncytin mRNA copy number in both the PE/IUGR ($P = 0.047$) and the HELLP/IUGR groups ($P = 0.019$) as compared to controls. A 5.4-fold lower copy number of Syncytin/ng total RNA was found in PE/IUGR (29.2 ± 19.0 copies Syncytin/ng total RNA) than in controls (158.27 ± 28.02 copies Syncytin/ng total RNA) and was even further reduced 10.6-fold in placentas from HELLP/IUGR patients (14.95 ± 9.10 copies Syncytin/ng total RNA). There was no significant Syncytin reduction comparing HELLP/IUGR with PE/IUGR.

To determine, whether primary tissue from patients with PE and HELLP-associated IUGR (each $n = 4$) also demonstrated an increase in placental apoptosis, placenta samples from our collectives were analyzed in comparison to controls ($n = 4$). Results indicated that a statistically significant higher apoptosis rate occurred in both the PE/IUGR and the HELLP/IUGR group (Fig. 3B). In detail, a 1.8-fold higher apoptosis rate was observed in the PE/IUGR group (0.655 ± 0.130 a.U., $P = 0.04$) and a 1.9-fold higher rate was found in HELLP/IUGR placentas (0.676 ± 0.088 a.U., $P = 0.008$) compared to controls (0.349 ± 0.056 a.U.). These results showed that in patients with PE and HELLP-associated IUGR placental apoptosis is enhanced along with a significant reduction of Syncytin expression.

In summary, these data indicated that a lower Syncytin expression and higher apoptosis rate in pathological primary tissue were similar to cultured

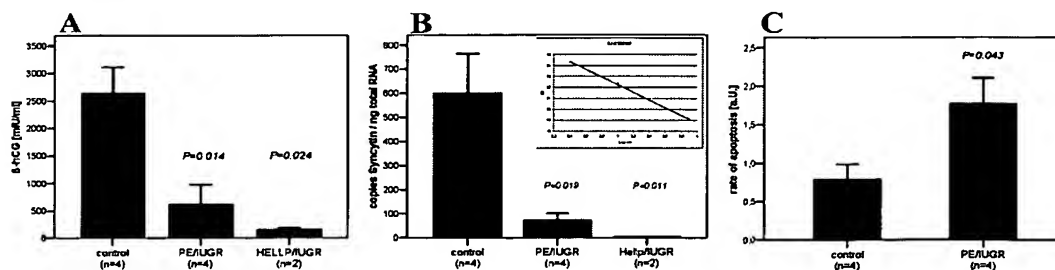


Fig. 2. A: β -hCG secretion from cultured CT (3 days) from patients with PE/IUGR and HELLP/IUGR in comparison to controls. The β -hCG analyses were performed in duplicates. B: Absolute qPCR gene expression analyses of Syncytin in cultured CT (3 days) isolated from patients with PE/IUGR and HELLP/IUGR in comparison to controls. C: Rate of apoptosis assayed by ELISA in CT isolated from control placentas in comparison to PE/IUGR CT at day 3.

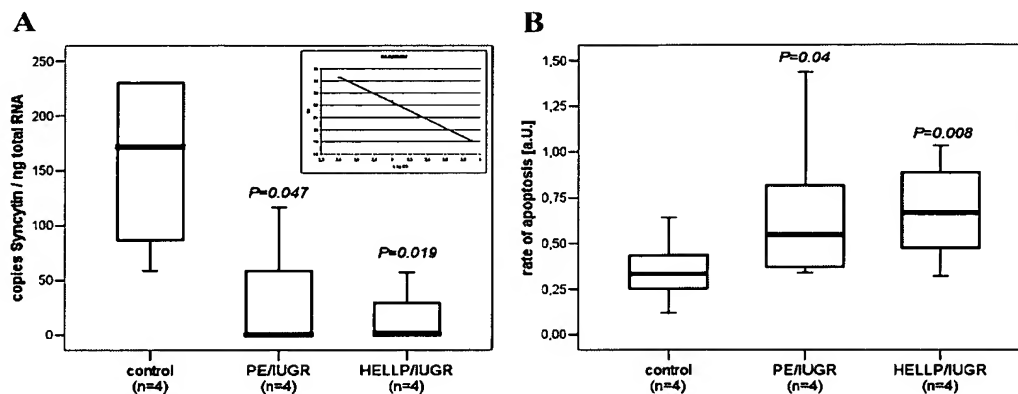


Fig. 3. A: Absolute quantitative Realtime PCR gene expression analyses of Syncytin in placental primary tissue from patients with PE/IUGR ($n=4$) and HELLP/IUGR ($n=4$) compared with control patients ($n=4$). B: Rate of apoptosis assayed by ELISA in placental tissue from patients with PE/IUGR ($n=4$) and HELLP/IUGR ($n=4$) compared with control patients ($n=4$).

CT from patients with PE and HELLP-associated IUGR. Therefore, cultivated pathological CT mimic the same deregulations as found in primary tissues (summarized in Table 3).

DISCUSSION

Our comparative in vitro growth analysis of both normal and pathological CT presents a new opportunity to study the cell biological/molecular properties of placental disorders. This investigation demonstrated that cultured pathological PE and HELLP-associated IUGR CT had an intrinsic impaired ability of cells to fuse. Furthermore, the lower cell–cell fusion ability supports a link with reduced Syncytin levels in PE/IUGR and HELLP/IUGR.

Importantly, microscopic analysis of cultivated pathological CT at day 3 showed deregulation in cell–cell fusion process with both a lower fusion index and a lower average number of nuclei per SCT (fusion index PE/IUGR = 37.6%, 4.6 nuclei/SCT; fusion index HELLP/IUGR = 18.9%, 3.2 nuclei/SCT) in comparison to controls (fusion index control = 68.9%, 6.5 nuclei/SCT) indicating reduced cell–cell fusion activity (Table 3, Fig. 1). The correlation of a reduced cell–cell fusion index with a decreased fold expression of Syncytin was

not only significantly lower in cultivated CT from patients with PE/IUGR (8.1-fold, $P=0.019$) and HELLP/IUGR (222.7-fold, $P=0.011$) but the Syncytin copy number was also statistically significantly lower in primary placental tissues from patients with PE (5.4-fold, $P=0.047$) and HELLP (10.6-fold, $P=0.019$)-associated IUGR compared with controls (Figs. 2B, 3A). Furthermore, Syncytin copy number correlated with disease severity, for example, Syncytin expression was consistently lower in HELLP/IUGR (14.95 ± 9.10 copies Syncytin/ng total RNA) compared to PE/IUGR (29.2 ± 19.0 copies Syncytin/ng total RNA) placentas (Fig. 3A).

In the literature, a 25-fold lower Syncytin hybridization signal was detected at the mRNA level in PE placental specimens when compared with controls and a lower Syncytin/ β -actin mRNA ratio was shown in women with PE (0.59 vs. 0.97) by semi-quantitative Realtime PCR (Knerr et al., 2002; Lee et al., 2001). In addition, Syncytin was also shown to be reduced in PE placentas approximately 50% at the protein level using immunoblots (Chen et al., 2006). All these studies have demonstrated decreased Syncytin expression in primary pathological tissues, but an absolute Syncytin quantification of RNA copy number in primary tissue

TABLE 3. Summary of Data From Placental Primary Tissue and Cultured Trophoblasts

	Control	PE/IUGR	HELLP/IUGR
	$n=4$	$n=4$	$n=2$
Cultured trophoblasts			
Fusion index	68.9%	37.6%	18.9%
Nuclei/SCT	6.5	4.6	3.2
β -hCG [U/ml]	$2630 \pm 466.9^*$	$615 \pm 361.6^*$	$153.0 \pm 22.0^*$
Syncytin [copies/ng RNA total]	$601.3 \pm 164.1^*$	$73.8 \pm 26.9^*$	$2.7 \pm 0.5^*$
Apoptosis [a.u.]	$0.784 \pm 0.19^*$	$1.767 \pm 0.33^*$	n.d.
Placental tissue	$n=4$	$n=4$	$n=4$
Syncytin [copies/ng RNA total]	$158.3 \pm 28.02^*$	$29.2 \pm 19.0^*$	$14.9 \pm 9.1^*$
Apoptosis [a.u.]	$0.349 \pm 0.05^*$	$0.655 \pm 0.13^*$	$0.676 \pm 0.08^*$

P-values were performed using Student's *t*-test. Significant *P*-values ($P < 0.05$) are indicated as a *; for details see text. Values represent mean \pm SEM. n.d. = not done.

and especially in cultivated CT from PE and HELLP-associated IUGR patients to our knowledge has not been performed until now. In placental development, a strict regulation of Syncytin occurs up to day 12 after implantation during SCT establishment (de novo fusion) and also until birth in the maintenance of the SCT layer where CT fuse into the existing SCT (Potgens et al., 2004). The finding of lower Syncytin expression in PE/IUGR and HELLP/IUGR placentas analyzed at birth and especially the Syncytin downregulation in cultivated CT reflects a severe perturbation in the de novo and maintenance cell–cell fusion activities and supports an intrinsic impaired ability of CT to fuse in pathological placentas.

Besides analysis of Syncytin expression as a key protein for cell–cell fusion events and visualizing SCT in cultured CT, β -hCG levels were analyzed as a biochemical fusion marker. It is well known that CT produce low β -hCG, whereas SCT express high levels of β -hCG (Hoshina et al., 1985; Shi et al., 1993). Therefore, a higher percentage of non-fused single CT in pathological cultured CT would predict a lower β -hCG secretion. Our results showed that day 3, CT cultures from PE/IUGR placentas had a 4.3-fold lower and from HELLP/IUGR placentas a 17.2-fold lower β -hCG level (Fig. 2A). In addition, β -hCG levels correlated with the severity of the diseases, with the lowest values detected in CT supernatants from HELLP/IUGR placentas.

Different factors regulate Syncytin-mediated cell–cell fusion during human placentogenesis. The receptor for Syncytin, ASCT2 has been implicated in the fusion process, but was not found downregulated in PE placentas (Chen et al., 2006). The placental-specific transcription factor glial cell missing gene GCM1 (also called GCMa), was demonstrated as a transactivator for Syncytin expression (Anson-Cartwright et al., 2000; Schreiber et al., 2000). In the 5' flanking region of Syncytin at chromosome 7q21, GCM1 bound two GCM1 elements and upregulated Syncytin expression in CT (Yu et al., 2002). In addition, both GCM1-induced Syncytin expression and Syncytin-mediated cell–cell fusion were demonstrated in two choriocarcinoma trophoblastic cell lines BeWo and JEG-3 (Yu et al., 2002). Importantly, GCM1 was significantly downregulated both at RNA as well as at protein level in placentas from women with PE (Chen et al., 2004). Therefore, it is highly possible that lowered Syncytin expression in PE and HELLP-associated IUGR correlates with GCM1 reduction and should be further investigated.

Besides abnormalities in the process of syncytial fusion, a dysregulation of the apoptotic process in placental tissue may also be contributing to the development of PE and HELLP-associated or non-associated IUGR. A statistically significant higher apoptosis rate (1.8-fold in PE/IUGR ($P = 0.04$) and 1.9-fold in HELLP/IUGR ($P = 0.008$) occurred in pathological placental tissues and also in cultured PE/IUGR CT (2.3-fold) (Figs. 2C, 3B). These results support earlier studies, which demonstrated that placental sections showed a higher level of apoptosis in pregnancies complicated by

IUGR (Miller et al., 1996; Smith et al., 1997a) and PE (DiFederico et al., 1999; Leung et al., 2001). Additionally, a 3.7-fold higher incidence of apoptosis was observed in PE placentas in comparison to controls (Allaire et al., 2000) or a 2.3-fold increased apoptotic index was observed in PE/IUGR placentas using light and electron microscopy (Leung et al., 2001) or the TUNEL assay (Ishihara et al., 2002).

Recently, a new link between Syncytin and apoptosis was postulated where Syncytin showed anti-apoptotic effects (Knerr et al., 2007). This would predict that in pathological placentas due to a lower Syncytin expression and reduced cell–cell fusion a higher incidence of apoptosis and deregulation in the pathway could pursue. For example, upregulation of effector caspases and p53 or a lower expression of the anti-apoptotic Bcl-2 protein could occur. Molecular support of this could be the following: (1) p53 was shown to be upregulated in villous tissue from IUGR placentas (Levy et al., 2002); (2) Decreased Bcl-2 expression was shown in SCT from primary PE and IUGR placental tissue (Ishihara et al., 2002), and (3) *bcl-2* deletion in mice resulted in fetuses with growth retardation, confirming a role for this protein in placental development (Veis et al., 1993).

Some known risk factors for developing PE include chronic hypertension, diabetes mellitus, previous PE, and multiple pregnancies (Albrecht and Tomich, 1996; O'Brien et al., 2003; Villar et al., 2006). The clinical findings in our collective showed that 25% of PE/IUGR patients had recurrent PE or HELLP pregnancies (Table 1), supporting a possible predisposition in some patients. Two present theories have been described for the pathogenesis of PE (Smith and Kenny, 2006). In the "two-stage process," abnormal placentation leads to a poorly perfused placenta. This results in the release of circulating factors that causes endothelial cell damage leading to a multisystemic disorder affecting both the fetus and the mother. A response to a poorly perfused placenta may be a fetal adaptive response. The second so called "continuum theory" proposes that a poorly perfused placenta releases higher amounts of debris leading to an inflammatory reaction and endothelial cell dysfunction (Smith and Kenny, 2006).

We propose that during PE/IUGR and HELLP/IUGR-associated pregnancies, lower levels of Syncytin expression could result in a deregulation of the de novo and maintenance cell–cell fusion pathways leading to an accumulation of non-fused CT. Higher amounts of non-fused CT blocked in their programmed developmental pathway become more susceptible to apoptosis and lead to a higher apoptosis rate. This higher rate of apoptosis may be contributing to an inflammatory response and/or result in a diminished exchange of nutrients or cellular by-products between mother and fetus over the SCTs.

ACKNOWLEDGMENTS

The authors are especially grateful to the patients who participated in this study and to the Dept. of Gynaecology and Obstetrics, Erlangen. The authors

wish to thank Mrs. Staerker and Mrs. Toborek for β -hCG determinations. This work was supported by the DFG (SCHI 552/2-2).

REFERENCES

- Albrecht JL, Tomich PG. 1996. The maternal and neonatal outcome of triplet gestations. *Am J Obstet Gynecol* 174:1551–1556.
- Allaire AD, Ballenger KA, Wells SR, McMahon MJ, Lessey BA. 2000. Placental apoptosis in preeclampsia. *Obstet Gynecol* 96: 271–276.
- Anson-Cartwright L, Dawson K, Holmyard D, Fisher SJ, Lazzarini RA, Cross JC. 2000. The glial cells missing-1 protein is essential for branching morphogenesis in the chorioallantoic placenta. *Nat Genet* 25:311–314.
- Babalola GO, Coutifaris C, Soto EA, Kliman HJ, Shuman H, Strauss JF 3rd. 1990. Aggregation of dispersed human cytotrophoblastic cells: Lessons relevant to the morphogenesis of the placenta. *Dev Biol* 137:100–108.
- Bannert N, Kurth R. 2004. Retroelements and the human genome: New perspectives on an old relation. *Proc Natl Acad Sci U S A* 101:14572–14579.
- Benirschke K, Kaufmann P. 2000. Characterization of the developmental stages. In: Benirschke K, Kaufmann P, editors. *Pathology of the Human Placenta*, 4th edn. New York: Springer-Verlag. pp 155–170.
- Bildirici I, Roh CR, Schaiff WT, Lewkowski BM, Nelson DM, Sadovsky Y. 2003. The lipid droplet-associated protein adipophilin is expressed in human trophoblasts and is regulated by peroxisomal proliferator-activated receptor- γ /retinoid X receptor. *J Clin Endocrinol Metab* 88:6056–6062.
- Blond JL, Lavielle D, Cheynet V, Bouton O, Oriol G, Chapel-Fernandes S, Mandrand B, Mallet F, Cosset FL. 2000. An envelope glycoprotein of the human endogenous retrovirus HERV-W is expressed in the human placenta and fuses cells expressing the type D mammalian retrovirus receptor. *J Virol* 74:3321–3329.
- Caniggia I, Grisaru-Gravnosky S, Kuliszewsky M, Post M, Lye SJ. 1999. Inhibition of TGF- β 3 restores the invasive capability of extravillous trophoblasts in preeclamptic pregnancies. *J Clin Invest* 103:1641–1650.
- Chen CP, Chen CY, Yang YC, Su TH, Chen H. 2004. Decreased placental GCM1 (glial cells missing) gene expression in preeclampsia. *Placenta* 25:413–421.
- Chen CP, Wang KG, Chen CY, Yu C, Chuang HC, Chen H. 2006. Altered placental syncytin and its receptor ASCT2 expression in placental development and pre-eclampsia. *Bjog* 113:152–158.
- Cheyne V, Ruggieri A, Oriol G, Blond JL, Boson B, Vachot L, Verrier B, Cosset FL, Mallet F. 2005. Synthesis, assembly, and processing of the Env ERVWE1/syncytin human endogenous retroviral envelope. *J Virol* 79:5585–5593.
- DiFederico E, Genbacev O, Fisher SJ. 1999. Preeclampsia is associated with widespread apoptosis of placental cytotrophoblasts within the uterine wall. *Am J Pathol* 155:293–301.
- Duley L. 1992. Maternal mortality associated with hypertensive disorders of pregnancy in Africa, Asia, Latin America and the Caribbean. *Br J Obstet Gynaecol* 99:547–553.
- Dupressoir A, Marceau G, Vernochet C, Benit L, Kanellopoulos C, Sapin V, Heidmann T. 2005. Syncytin-A and syncytin-B, two fusogenic placenta-specific murine envelope genes of retroviral origin conserved in Muridae. *Proc Natl Acad Sci U S A* 102:725–730.
- Frendo JL, Olivier D, Cheynet V, Blond JL, Bouton O, Vidaud M, Rabreau M, Evain-Brion D, Mallet F. 2003. Direct involvement of HERV-W Env glycoprotein in human trophoblast cell fusion and differentiation. *Mol Cell Biol* 23:3566–3574.
- Hoshina M, Boothby M, Hussa R, Pattillo R, Camel HM, Boime I. 1985. Linkage of human chorionic gonadotrophin and placental lactogen biosynthesis to trophoblast differentiation and tumorigenesis. *Placenta* 6:163–172.
- Ishihara N, Matsuo H, Murakoshi H, Laoag-Fernandez JB, Samoto T, Maruo T. 2002. Increased apoptosis in the syncytiotrophoblast in human term placentas complicated by either preeclampsia or intrauterine growth retardation. *Am J Obstet Gynecol* 186:158–166.
- James JL, Stone PR, Chamley LW. 2005. Cytotrophoblast differentiation in the first trimester of pregnancy: Evidence for separate progenitors of extravillous trophoblasts and syncytiotrophoblast. *Reproduction* 130:95–103.
- Khong TY, De Wolf F, Robertson WB, Brosens I. 1986. Inadequate maternal vascular response to placentation in pregnancies complicated by pre-eclampsia and by small-for-gestational age infants. *Br J Obstet Gynaecol* 93:1049–1059.
- Kim HS, Roh CR, Chen B, Tycko B, Nelson DM, Sadovsky Y. 2007. Hypoxia regulates the expression of PHLDA2 in primary term human trophoblasts. *Placenta* 28:77–84.
- Kingdom J, Jauniaux E, O'Brien P. 2000. *The Placenta: Basic Science and Clinical practice*. Royal College of Obstetricians and Gynaecologists. 1 ed.
- Kliman HJ, Nestler JE, Sermasi E, Sanger JM, Strauss JF 3rd. 1986. Purification, characterization, and in vitro differentiation of cytotrophoblasts from human term placentae. *Endocrinology* 118:1567–1582.
- Knerr I, Beinder E, Rascher W. 2002. Syncytin, a novel human endogenous retroviral gene in human placenta: Evidence for its dysregulation in preeclampsia and HELLP syndrome. *Am J Obstet Gynecol* 186:210–213.
- Knerr I, Huppertz B, Weigel C, Dotsch J, Wich C, Schild RL, Beckmann MW, Rascher W. 2004. Endogenous retroviral syncytin: Compilation of experimental research on syncytin and its possible role in normal and disturbed human placentogenesis. *Mol Hum Reprod* 10:581–588.
- Knerr I, Schnare M, Hermann K, Kausler S, Lehner M, Vogler T, Rascher W, Meissner U. 2007. Fusogenic endogenous-retroviral syncytin-1 exerts anti-apoptotic functions in staurosporine-challenged CHO cells. *Apoptosis* 12:37–43.
- Kudo Y, Boyd CA. 1990. Characterization of amino acid transport systems in human placental basal membrane vesicles. *Biochim Biophys Acta* 1021:169–174.
- Lee X, Keith JC Jr, Stumm N, Moutsatsos I, McCoy JM, Crum CP, Genest D, Chin D, Ehrenfels C, Pijnenborg R, van Assche FA, Mi S. 2001. Downregulation of placental syncytin expression and abnormal protein localization in pre-eclampsia. *Placenta* 22:808–812.
- Leung DN, Smith SC, To KF, Sahota DS, Baker PN. 2001. Increased placental apoptosis in pregnancies complicated by preeclampsia. *Am J Obstet Gynecol* 184:1249–1250.
- Levy R, Smith SD, Yusuf K, Huettner PC, Kraus FT, Sadovsky Y, Nelson DM. 2002. Trophoblast apoptosis from pregnancies complicated by fetal growth restriction is associated with enhanced p53 expression. *Am J Obstet Gynecol* 186:1056–1061.
- Lim KH, Zhou Y, Janatpour M, McMaster M, Bass K, Chun SH, Fisher KH. 1997. Human cytotrophoblast differentiation/invasion is abnormal in pre-eclampsia. *Am J Pathol* 151:1809–1818.
- Loke Y, King A. 1995. *Human implantation. Cell biology and immunology*. Cambridge, UK: Cambridge University Press. pp 1–313.
- Maldonado-Estrada J, Menu E, Roques P, Barre-Sinoussi F, Chaouat G. 2004. Evaluation of Cytokeratin 7 as an accurate intracellular marker with which to assess the purity of human placental villous trophoblast cells by flow cytometry. *J Immunol Methods* 286: 21–34.
- Mi S, Lee X, Li X, Veldman GM, Finnerty H, Racie L, LaVallie E, Tang XY, Edouard P, Howes S, Keith JC Jr, McCoy JM. 2000. Syncytin is a captive retroviral envelope protein involved in human placental morphogenesis. *Nature* 403:785–789.
- Miller MJ, Voelker CA, Olister S, Thompson JH, Zhang XJ, Rivera D, Eloby-Childress S, Liu X, Clark DA, Pierce MR. 1996. Fetal growth retardation in rats may result from apoptosis: Role of peroxynitrite. *Free Radic Biol Med* 21:619–629.
- Nelson DM. 1996. Apoptotic changes occur in syncytiotrophoblast of human placental villi where fibrin type fibrinoid is deposited at discontinuities in the villous trophoblast. *Placenta* 17:387–391.
- Ness RB, Roberts JM. 1996. Heterogeneous causes constituting the single syndrome of preeclampsia: A hypothesis and its implications. *Am J Obstet Gynecol* 175:1365–1370.
- O'Brien TE, Ray JG, Chan WS. 2003. Maternal body mass index and the risk of preeclampsia: A systematic overview. *Epidemiology* 14:368–374.

- Pijnenborg R, Bland JM, Robertson WB, Brosens I. 1983. Uteroplacental arterial changes related to interstitial trophoblast migration in early human pregnancy. *Placenta* 4:397–413.
- Potgens AJ, Drewlo S, Kokozidou M, Kaufmann P. 2004. Syncytin: The major regulator of trophoblast fusion? Recent developments and hypotheses on its action. *Hum Reprod Update* 10:487–496.
- Redman CW, Jefferies M. 1988. Revised definition of pre-eclampsia. *Lancet* 1:809–812.
- Redman CW, Sargent IL. 2000. Placental debris, oxidative stress and pre-eclampsia. *Placenta* 21:597–602.
- Roberts JM, Hubel CA. 1999. Is oxidative stress the link in the two-stage model of pre-eclampsia? *Lancet* 354:788–789.
- Roberts JM, Taylor RN, Goldfien A. 1991. Clinical and biochemical evidence of endothelial cell dysfunction in the pregnancy syndrome preeclampsia. *Am J Hypertens* 4:700–708.
- Schaiff WT, Bildirici I, Cheong M, Chern PL, Nelson DM, Sadovsky Y. 2005. Peroxisome proliferator-activated receptor-gamma and retinoid X receptor signaling regulate fatty acid uptake by primary human placental trophoblasts. *J Clin Endocrinol Metab* 90:4267–4275.
- Schild RL, Sonnenberg-Hirche CM, Schaiff WT, Bildirici I, Nelson DM, Sadovsky Y. 2006. The kinase p38 regulates peroxisome proliferator activated receptor-gamma in human trophoblasts. *Placenta* 27:191–199.
- Schreiber J, Riethmacher-Sonnenberg E, Riethmacher D, Tuerk EE, Enderich J, Bosl MR, Wegner M. 2000. Placental failure in mice lacking the mammalian homolog of glial cells missing, GCMa. *Mol Cell Biol* 20:2466–2474.
- Shi QJ, Lei ZM, Rao CV, Lin J. 1993. Novel role of human chorionic gonadotropin in differentiation of human cytotrophoblasts. *Endocrinology* 132:1387–1395.
- Smith RA, Kenny LC. 2006. Current thoughts on the pathogenesis of pre-eclampsia. *Obstet Gynaecol* 8:7–13.
- Smith SC, Baker PN, Symonds EM. 1997a. Increased placental apoptosis in intrauterine growth restriction. *Am J Obstet Gynecol* 177:1395–1401.
- Smith SC, Baker PN, Symonds EM. 1997b. Placental apoptosis in normal human pregnancy. *Am J Obstet Gynecol* 177:57–65.
- Strick R, Ackermann S, Langbein M, Swiatek J, Schubert SW, Hashemolhosseini S, Koscheck T, Fasching PA, Schild RL, Beckmann MW, Strissel PL. 2007. Proliferation and cell-cell fusion of endometrial carcinoma are induced by the human endogenous retroviral Syncytin-1 and regulated by TGF-beta. *J Mol Med* 85:23–38.
- Vaux DL, Korsmeyer SJ. 1999. Cell death in development. *Cell* 96:245–254.
- Veis DJ, Sorenson CM, Shutter JR, Korsmeyer SJ. 1993. Bcl-2-deficient mice demonstrate fulminant lymphoid apoptosis, polycystic kidneys, and hypopigmented hair. *Cell* 75:229–240.
- Villar J, Carroli G, Wojdyla D, Abalos E, Giordano D, Ba'aqeel H, Farnot U, Bergsjö P, Bakketeig L, Lumbiganon P, Campodonico L, Al-Mazrou Y, Lindheimer M, Kramer M. 2006. Preeclampsia, gestational hypertension and intrauterine growth restriction, related or independent conditions? *Am J Obstet Gynecol* 194:921–931.
- WHO. 1987. The hypertensive disorders of pregnancy World Health Organ Tech Rep Ser WHO study group. pp 1–114.
- Wilson ML, Goodwin TM, Pan VL, Ingles SA. 2003. Molecular epidemiology of preeclampsia. *Obstet Gynecol Surv* 58:39–66.
- Yagi M, Miyamoto T, Sawatani Y, Iwamoto K, Hosogane N, Fujita N, Morita K, Ninomiya K, Suzuki T, Miyamoto K, Oike Y, Takeya M, Toyama Y, Suda T. 2005. DC-STAMP is essential for cell-cell fusion in osteoclasts and foreign body giant cells. *J Exp Med* 202:345–351.
- Yu C, Shen K, Lin M, Chen P, Lin C, Chang GD, Chen H. 2002. GCMa regulates the syncytin-mediated trophoblastic fusion. *J Biol Chem* 277:50062–50068.
- Zhou Y, Damsky CH, Fisher SJ. 1997. Preeclampsia is associated with failure of human cytotrophoblasts to mimic a vascular adhesion phenotype. One cause of defective endovascular invasion in this syndrome? *J Clin Invest* 99:2152–2164.